Determining the Role of Prostanoids in the Pathogenesis of Pulmonary Fibrosis

Alysia Kern Lovgren

A dissertation submitted to the faculty of the University of North Carolina at Chapel Hill in partial fulfillment of the requirements for the degree of Doctor of Philosophy in the Curriculum of Genetics and Molecular Biology

Chapel Hill
2007

Approved By:

Advisor: Beverly Koller, PhD
Committee: Cam Patterson, MD
Richard Rippe, PhD
Steve Tilley, MD
David Threadgill, PhD
Jeff Sekelsky, PhD

ABSTRACT

Alysia Kern Lovgren

Determining the Role of Prostanoids in the Pathogenesis of Pulmonary Fibrosis

(Under the direction of Dr. Beverly H. Koller, PhD)

Idiopathic pulmonary fibrosis is a relentless, fatal disease characterized by alveolar epithelial cell injury, proliferation of mesenchymal cell populations, and extracellular matrix deposition. Unknown microinjuries to the lung initiate an aberrant repair process in susceptible individuals which ultimately alters lung architecture and leads to progressive loss of pulmonary function. Lipid mediators called prostanoids have been implicated in both inflammatory and fibrotic signaling pathways. It has been postulated that the COX-2 metabolite prostaglandin E_2 (PGE_2) is responsible for protection against pulmonary fibrosis. To study this lipid mediator, we first generated a mouse line deficient in the putative cytosolic PGE_2 synthase, cPGES/p23. These mice died at birth due to respiratory failure, and our data shows that cPGES/p23 is a co-chaperone that is important for both DNA-binding-dependent and -independent mechanisms of the glucocorticoid receptor. However, characterization of primary embryonic fibroblasts derived from the cPGES/p23-deficient mice, as well as embryonic tissues, demonstrated that cPGES/p23 is not required for the direct production of PGE_2 from COX-derived PGH_2. We, therefore, went on to demonstrate that upregulation of PGE_2 after bleomycin administration was dependent on the microsomal PGE_2 synthase, mPGES1. However, neither loss of PGE_2 synthesis nor signaling through the G_s-coupled EP2 and EP4 receptors had an effect on the development of fibrotic lung disease.

Interestingly, we show that COX-2-dependent production of prostacyclin plays an important role in the development of disease, limiting both the development of fibrosis and the consequential alterations in lung mechanics. Our studies reveal an important role for the COX-2-prostacyclin synthetic pathway in protection from bleomycin-induced pulmonary fibrosis.

To my Grandmother, Joyce Busch, who passed away due to pulmonary fibrosis and associated complications caused by scleroderma, memories of her helped me through the tough times and reminded me why biomedical research is so important

ACKNOWLEDGEMENTS

I would like to acknowledge the following individuals for their continued support both professional and personally:

My advisor, Beverly Koller, without whom this work would not be possible. She taught me how to be a more critical researcher and has inspired me with her excitement and vast knowledge in science. I greatly appreciate her guidance and expertise throughout my graduate career. Being mentored by such a brilliant and well-respected scientist has truly been an honor.

The members of my dissertation committee were essential to my graduate training and career progression. I would like to thank Cam Patterson, Richard Rippe, Steve Tilley, Jeff Sekelsky, and David Threadgill for their encouragement, guidance, and confidence in my abilities as a scientist. Their advice and helpful suggestions have guided me both professionally and personally.

The members of the Koller lab, past and present, who have supported me throughout this work. I would particularly like to thank: John Hartney for helpful scientific discussions and technical expertise regarding airway physiology; Leigh Jania for her substantial technical assistance and her friendship and support through tough times; Coy Allen for helpful scientific and career discussions, for technical expertise regarding airway physiology, for his friendship and laughter, and for always being there for me and answering all my questions whether he truly knew the answer or not; Julie Ledford for her friendship, encouragement,

and making my time in lab more enjoyable; Anne Latour for assisting with genotyping, sharing her tissue culture expertise, and helping with the production of mouse embryonic fibroblasts which will haunt her forever; Kelly Parsons for her assistance with mastering the dangerous hydroxyproline assay; MyTrang Nguyen for her amazing technical expertise; Soo Kim for assisting with genotyping, Artiom Gruzdev for moral support; Martina Kovarova for assistance with flow cytometry and overall helpfulness and encouragment; Subhashini Chandrasekharan for scientific discussions, critical review of manuscripts, and making days in lab a little brighter; Jay Snouwaert for help and advice with cloning and designing my Southern probe; and Amy Pace for helpful scientific and career discussions and computer technical assistance.

I would also like to acknowledge Bob Bagnell and Vicki Madden for substantial assistance with both light and electron microscopy and Mitsuo Yamauchi's lab members for assistance with the hydroxyproline assay.

I'd also like to thank my friends and classmates, especially Jen Knies, Folami Ideraabdullah, Mark Schliekelman, Coy Allen, and Josh Uronis, who got me through some of the most difficult times in graduate school. Their support, encouragement, and friendship made this journey more bearable.

Lastly, I'd like to thank my family. My parents have always encouraged and supported me to excel in all aspects of my life. I really can't thank them enough for all the opportunites that they have provided. My sisters have pushed me to try new things and be the best that I can be.

And most importantly, my husband Jimmy, who has finally earned his honorary PhD for patiently listening to every experiment and every trial and tribulation that I have gone

through. I'm glad that you are the one by my side through it all. Thank you for understanding and providing me with the strength, and most importantly, the happiness necessary to complete this. You're everything.

TABLE OF CONTENTS

LIST OF TABLES

LIST OF FIGURES

LIST OF ABBREVIATIONS AND SYMBOLS

AA	arachidonic acid
AEC	alveolar epithelial cells
ANOVA	analysis of variance
ATP	adenosine triphosphate
BALF	bronchoalveolar lavage fluid
cAMP	cyclic adenosine monophosphate
cDNA	complementary DNA
Ca^{2+}	intracellular calcium
COPD	chronic obstructive pulmonary disease
COX	Cyclooxygenase
cPGES	cytosolic Prostaglandin E synthase
$cPLA_2$	cytosolic phospholipase A_2
C_{st}	static compliance
CTGF	connective tissue growth factor
DMEM	Dulbecco modified Eagles medium
DNA	deoxyribonucleic acid
E	embryonic day
ENaCγ	epithelial sodium channel subunit γ
EP	prostanglandin E receptor
G6pc	glucose-6-phosphatase
G	tissue damping
GM-CSF	granulocyte-macrophage colony stimulating factor

GR	glucocorticoid receptor
GRE	glucocorticoid response element
H	tissue elastance
H & E	hematoxylin and eosin
Hsp	heat shock protein
ILD	interstitial lung disease
IP	prostacyclin receptor
IPF	idiopathic pulmonary fibrosis
LO	lipoxygenase
LT	leukotriene
LPS	bacterial lipopolysaccharide
MK	midkine
MMP	matrix metalloproteinase
mPGES1	microsomal Prostaglandin E synthase 1
mPGES2	microsomal Prostaglandin E synthase 2
NSAID	non-steriodal antiinflammatory drug
PAS	periodic acid-schiff reaction
PCR	polymerase chain reaction
PEEP	positive end expiratory pressure
PG	prostaglandin
PGDH	15-hydroxyprostaglandin dehydrogenase
PGE_2	prostaglandin E_2
PGH_2	prostaglandin endoperoxide

PGI_2	prostacyclin
Sds	serine dehydratase
SEM	standard error of the mean
SP	surfactant protein
TGF-β	transforming growth factor beta
TNF-α	tumor necrosis factor alpha
TP	thromboxane receptor
TX	thromboxane
V_2O_5	vanadium pentoxide
wt	wild type

CHAPTER 1

INTRODUCTION

The Significance, Histopathology, and Classification of Idiopathic Pulmonary Fibrosis

Idiopathic pulmonary fibrosis (IPF) is a chronic progressive lung disease of the distal airways which leads to excessive scarring and decreased lung function. Symptoms include dyspnea and nonproductive cough, and most patients display symptoms for over six months before visiting a physician. Onset is usually in the later stages of life; however, once diagnosed, the median survival is only 2-3 years and ultimately results in respiratory failure. Currently, no therapies exist to increase life expectancy or improve quality of life.

IPF is the most common interstitial lung disease among older adults, and it is more prevalent in men than in women. The disease etiology is unknown. Although some risk factors have been suggested, such as cigarette smoking and environmental hazards, there is little evidence indicating any predisposing or etiological factors (59). Familial IPF has been reported in about .5-2.2% of cases and, aside from earlier onset of disease, are indistinguishable from non-familial cases (38). Mutations in various cytokines, structural proteins, and even telomerase have been linked to familial IPF in different pedigrees (68).

IPF is characterized by patchy subpleural parenchymal fibrosis due to excess extracellular matrix deposition and failure of alveolar re-epithelialization after injury. The hallmark characteristics of idiopathic pulmonary fibrosis are temporal heterogeneity and myofibroblast foci. Temporal heterogeneity means that different areas of the lung are alternating with healthy lung and various stages of disease: honeycombing and scarring (chronic), fibroblastic foci and interstitial fibrosis (subacute), and alveolar epithelial cell apoptosis and possibly inflammation (acute). The honeycomb structure is due to distended alveolar septa adjacent to areas of excessive collagen deposition. Fibroblast foci are dense areas of proliferating and transforming fibroblasts. Fibroblasts recruited to the injury

transform into myofibroblasts, which express alpha smooth muscle actin and change the lung architecture. These fibroblasts produce excess collagen and fibronectin that cause the thickening of the septal walls. This thickening leads to an inability to transport oxygen from the alveolar spaces into the capillaries.

Several acute and chronic lung diseases characterized by variable degrees of inflammation and fibrosis are classified as interstitial lung diseases (ILD). Collagen vascular diseases, inhalation of environmental/occupational hazards, drug-induced lung disease, connective tissue diseases (such as scleroderma), and granulomatous lung diseases are some of the known causes of ILD. Idiopathic pulmonary fibrosis is a subgroup of the ILDs of unknown etiology. Accurate diagnosis of disease is important for appropriate therapeutic options and prognosis to be determined. The American Thoracic Society/European Respiratory Society classification system recognizes seven groups: idiopathic pulmonary fibrosis (IPF)/usual interstitial pneumonia (UIP), nonspecific interstitial pneumonia (NSIP), acute interstitial pneumonitis (AIP), respiratory bronchiolitis-associated ILD, desquamative interstitial pneumonia, cryptogenic organizing pneumonia (COP), and lymphocyte interstitial pneumonia (1). Compared to IPF/UIP, the majority of the other ILDs have a definitive inflammatory stage and tend to improve with corticosteroid therapy and have a better prognosis. The unique combination of histopathological entities and its inevitable progression to death demonstrate a huge need to study new therapies.

Pathophysiology

Idiopathic pulmonary fibrosis begins from unknown repeated insults or microinjuries to the lung epithelia. These microinjuries lead to dysregulated repair and an epithelial-

fibroblastic disorder. Activated epithelial cells and possibly inflammatory cells, including neutrophils, macrophages, and lymphocytes, induce activation of fibroblasts. This activation includes migration to the injured site, proliferation, and transformation into myofibroblasts. Dense extracellular matrix and collagen are deposited in the interstitial spaces. In IPF, the mechanisms necessary for proper re-epithelialization are impaired, such as epithelial cell migration, proliferation, and differentiation (59). Myofibroblasts disrupt the basement membrane and may enhance epithelial cell apoptosis. A loss of signals to reduce fibroblast migration and proliferation and increase myofibroblast apoptosis along with continuous epithelial cell apoptosis leads to impaired re-epithelialization and aberrant wound healing (60).

The key morphological alteration linked with the progression of fibrosis is the number of fibroblastic foci. Fibroblasts and myofibroblasts form distinct clusters within the alveolar septa. Fibroblastic foci represent the areas of acute lung injury where the alveolar epithelia is disorganized and the basement membrane denuded (34). In an attempt to repair this, fibroblasts assume three general phenotypes: migratory, proliferative, and profibrotic. Myofibroblasts, which express α-smooth muscle actin, have been demonstrated to align parallel to one another to change the contractile abilities and architecture of the lung parenchyma. They secrete matrix proteins and are the premier source of increased collagen production, and their proliferation correlates with a decrease in lung compliance (42, 78, 80). Myofibroblasts also secrete profibrotic mediators like TGF-β and matrix metalloproteinases, enzymes that can disrupt the basement membrane (79).

An imbalance of growth factors, cytokines, and enzymes contributes to abnormal wound healing and an enhanced fibrotic response. Activated fibroblasts, epithelial cells, and

possibly inflammatory cells can release these mediators to alter disease development. Improper signaling leads to dysregulated repair through altered collagen metabolism, apoptotic pathways, and chemotactic gradients. Profibrotic mediators include TGF-β, IL-8, fibroblast growth factor, platelet derived growth factor, thromboxane A_2, monocyte chemoattractant protein-1, leukotrienes, and tumor necrosis factor α. Antifibrotic mediators include prostaglandin E_2, IFN-γ, IL-10, and granulocyte-macrophage colony stimulating factor (GM-CSF). The matrix metalloproteinases and tissue inhibitors of metalloproteinases are important enzymes in regulating extracellular matrix turnover, and recent evidence suggests that the expression of these is altered in IPF patients (23). Understanding the role of all of these factors is important for unraveling the mystery of this epithelial-fibroblastic disorder.

Historical Perspectives and Current Therapies

Idiopathic pulmonary fibrosis was originally described by Hamman and Rich in 1935 at Johns Hopkins Hospital. The original cases are now classified as acute interstitial pneumonia instead of usual interstitial pneumonia. However, the Hamman-Rich syndrome was considered the definition of idiopathic pulmonary fibrosis for many decades. In the 1960s, the Liebow classifications started the modern era for interstitial lung diseases by describing five histopathological subgroups highlighting the importance of the histological patterns. In the 1980s, the inflammation hypothesis for the pathogenesis of IPF was generated by a number of leaders in the pulmonary field (52). This hypothesis has fallen under much scrutiny in recent years; however, these early studies made huge contributions to the understanding of many other inflammatory lung diseases. Another observation from the

1980s was the importance of growth factors in the pathogenesis of IPF. This paved the way for the paradigm shift away from inflammation and towards abnormal wound healing. The emergence in recent years of the epithelial-mesenchymal disorder has highlighted the importance of re-epithelialization and unregulated proliferation and collagen deposition by fibroblasts. The current understanding of the pathogenesis of pulmonary fibrosis is a conglomeration of epithelial and fibroblastic issues, cytokine and growth factor imbalances, and inflammation. The hypothesis will continue to evolve as new studies shed light on this complex disease.

Chronic inflammation was once believed to be the cause and perpetuating factor in idiopathic pulmonary fibrosis. Although the role of the infiltration of inflammatory cells and their secretion of various cytokines is now controversial, anti-inflammatory treatment with corticosteroids was the main treatment protocol for many years. The clinical features of dyspnea and a restrictive pulmonary test overlap other interstitial lung diseases, and the lack of a well-defined disease made diagnosis difficult over the years. About 15-30% of patients were once believed to benefit from anti-inflammatory therapy due to inflated numbers from inaccurate diagnosis and inclusion of other ILDs in this statistic (21). As better technology has emerged so has the definition and classification schemes to aid in more accurate diagnosis. Now it is believed that corticosteroid treatment alone is ineffective at treating IPF. In addition, the negative side effects far outweigh any negligible improvement. For this reason, corticosteroids alone are not recommended as standard therapy (73).

Currently, corticosteroids along with cytotoxic agents are widely prescribed; however, this treatment approach is not recommended due to unproven benefits and enhanced morbidity (73). Currently, no specific drug treatment is recommended. Patients

should be evaluated for lung transplant suitability, and doctors should have end-of-life discussions with their patients. Recently, the most promising novel therapies have been the antioxidant N-acetylcysteine and the TGF-β inhibitor pirfenidone; however, additional trials are necessary to determine efficacy for these new compounds. These drugs and current research into new therapies are targeting the mechanisms and pathways behind the aberrant tissue remodeling.

Eicosanoids and Pulmonary Fibrosis

Overview of Eicosanoid Metabolism

The eicosanoids are bioactive lipids that are produced by almost all cells to act as autocrine and paracrine mediators. The term eicosanoid comes from the greek "eicosa" which means twenty. The eicosanoids are lipids produced from the 20 carbon fatty acid, arachidonic acid. The activation of the phospholipase enzymes, such as cytosolic phospholipase A2 (cPLA2), causes the release of arachidonic acid from the cell membrane phospholipids. The metabolism of arachidonic acid yields leukotrienes through the 5-lipoxygenase (5-LO) pathway or the prostanoids through the cyclooxygenase pathway (COX-1 or COX-2). The COX enzymes exist in two specific isoforms, the inducible COX-2 isoform and the constitutively expressed COX-1 isoform. The COX enzymes have two different functions for converting arachidonic acid into the intermediate prostaglandin endoperoxide (PGH_2). First, the cyclooxygenase activity of COX-1 and COX-2 converts arachadonic acid into prostaglandin G_2 (PGG_2). Second, the peroxidase activity converts PGG_2 into prostaglandin endoperoxide, PGH_2, which is then metabolized to the various prostanoids by their corresponding terminal synthases. The type of prostanoid released from

a given tissue depends on the synthases expressed. The prostanoids include prostacyclin (PGI_2), thromboxane A_2 (TxA_2), prostaglandin D_2 (PGD_2), prostaglandin F (PGF), and prostaglandin E_2 (PGE_2). Figure 1 shows the arachidonic acid pathway and includes relevant enzymes, metabolites, and receptors.

Prostanoids mediate their biological actions through binding to specific G-protein-associated receptors which initiate signal transduction events. A single receptor binds thromboxane and prostacyclin, TP and IP, respectively. PGE_2 has affinity for four receptors (EP1-EP4) with different expression patterns and coupling to intracellular signaling pathways. Activation of EP1 increases second messenger Ca^{2+} levels. EP2 and EP4 are coupled to G_s and increase cAMP levels. Similar responses have been described for the IP receptor. EP3 can couple to either $G_{i,s,or\ q}$ proteins thus can increase and decrease cAMP levels and increase Ca^{2+}. The expression profile of the receptors is different on given cell types to enhance the diversity of action of these mediators.

Leukotrienes and Prostanoids in Pulmonary Fibrosis

Eicosanoids are well-known for their role in platelet aggregation, pain, smooth muscle contraction, and inflammation and have been linked with diseases such as rheumatoid arthritis, cardiovascular disease, and asthma. However, studies have begun to shed light on even more roles for eicosanoids in immune responses, proliferation, and apoptosis. Numerous studies have suggested a delicate balance between the profibrotic leukotrienes and the antifibrotic prostaglandins in the pathophysiology of pulmonary fibrosis. Leukotrienes, especially cysteinyl leukotrienes, are best known for their involvement in the pathogenesis of asthma. In the 1980s, leukotrienes were demonstrated to have an effect on fibroblast

Figure 1.1

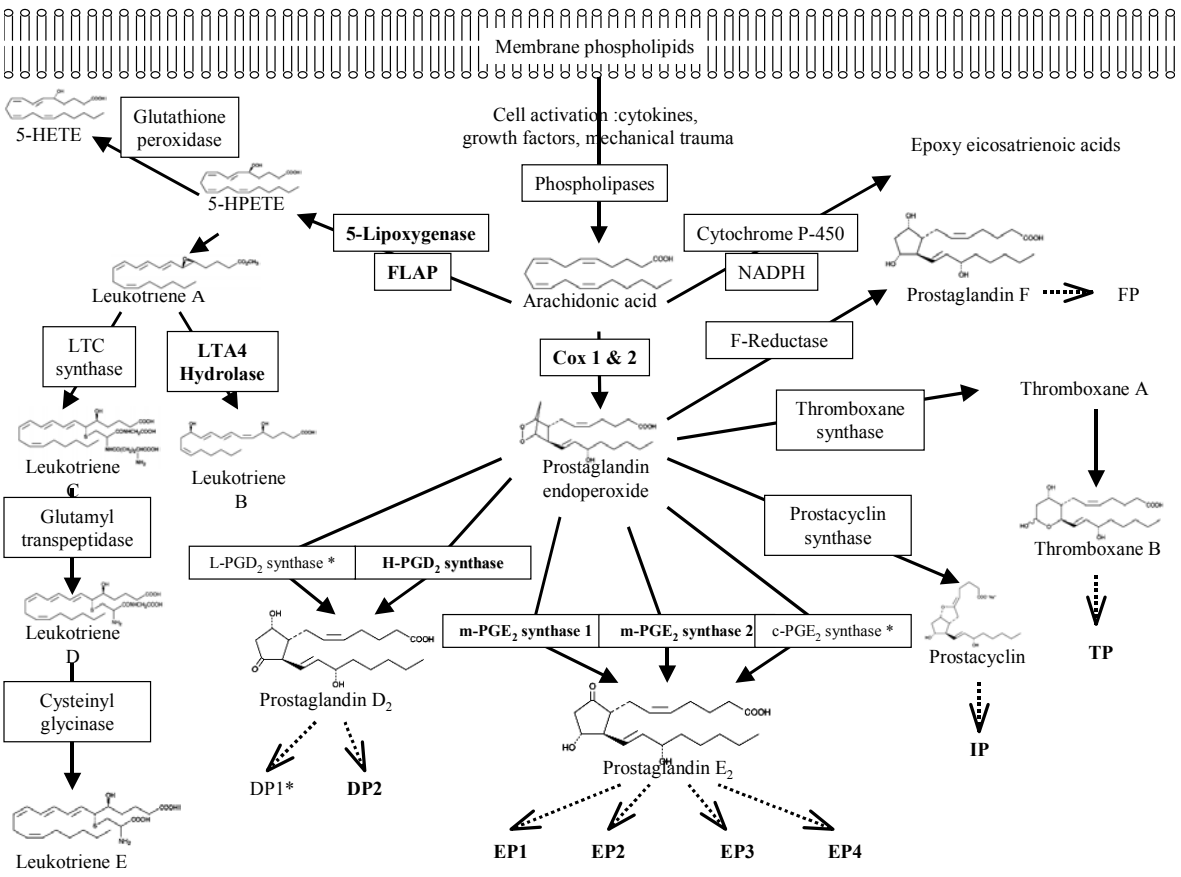

Figure 1.1. The Arachidonic Acid Cascade. Solid arrows designate path from substrate to product. Boxes designate genes whose products catalyze the conversion from substrate to product. Dashed arrows designate path from ligand to receptor.

migration and proliferation (4, 41). Also, elevated levels of leukotrienes were measured in bronchoalveolar lavage fluid from patients with pulmonoary fibrosis (74). In 1996, Wilborn et al. demonstrated that patients with pulmonary fibrosis had increased levels of leukotrienes in lung homogenates from biopsy samples (76). Continuing their investigations, this group demonstrated that leukotriene-deficient mice were protected from bleomycin-induced pulmonary fibrosis (54). This suggested that leukotrienes play a causal role in the development of pulmonary fibrosis. Leukotriene-deficient mice had a decrease in the initial inflammatory response and an increase in anti-fibrotic cytokines that may have contributed to their protection from disease. Currently, 5-LO inhibitors are being investigated as a novel therapeutic.

COX-2, the inducible cyclooxygenase enzyme, produces prostanoids during pathological conditions and has been studied in numerous inflammatory diseases. COX-2 expression has also been shown to be reduced in lung fibroblasts isolated from patients with pulmonary fibrosis (77). Originally, COX-2-deficient mice were demonstrated to be more susceptible to both vanadium pentoxide and bleomycin-induced pulmonary fibrosis (8, 30). However, another study by one of the original groups contradicted these finding and claimed that only the COX-2 heterozygous mice had an increased susceptibility to disease (25). Despite the slightly contradictory reports, these studies demonstrate the importance of COX-2 metabolites in the pathogenesis of pulmonary fibrosis.

The most well-studied of the prostanoids in pulmonary fibrosis is PGE_2. Numerous studies have identified this COX-2 metabolite to be responsible for protection against pulmonary fibrosis due to its anti-inflammatory and anti-fibrotic actions. IPF patients have a decrease of PGE_2 in bronchoalveolar fluid, and fibroblasts taken from these patients are

defective in PGE_2 synthesis (9, 77). It is therefore possible that the increased disease in these patients is partly due to their inability to produce sufficient PGE_2. A possible mechanism for PGE_2 is suggested by numerous *ex vivo* reports. PGE_2 was shown to suppress fibroblast proliferation and suppress collagen synthesis of lung fibroblasts (7, 18, 19, 39). PGE_2 has also been shown to inhibit fibroblast migration and fibroblast to myofibroblast transition (32, 33). Thus, an increased number of myofibroblasts in the absence of PGE_2 is likely to contribute to the morphological changes as well as the contractile changes of lung parenchyma characteristic of IPF.

The ability of PGE_2 to alter activity and gene expression of fibroblasts has been attributed to engagement of G_s-coupled receptors, particularily EP2, and cAMP release. Early studies demonstrated in human embryo lung fibroblasts (IMR90 cells) that PGE_2 reduced collagen mRNA levels (10). They demonstrated that an EP2/EP4 agonist and a cAMP activator, but not an EP3/EP1 agonist, had a similar effect on collagen expression. More recently, a similar study was done specifically in adult lung parenchymal fibroblasts with identical results (26). In addition, they used a more specific EP2 agonist, instead of an EP2/EP4 agonist, and were able to identify PKA as the major cAMP effector. Other studies have also demonstrated that PGE_2 inhibits fibroblasts migration and myofibroblast differentiation through an EP2-mediated pathway (33, 75).

PGE_2 Synthases

Three different genes have been reported to encode proteins capable of generating PGE_2 from the COX-derived metabolite PGH_2 *in vitro*. These include microsomal prostaglandin E synthase 1 (mPGES1), microsomal prostaglandin E synthase 2 (mPGES2),

and cytosolic prostaglandin E synthase (cPGES). Each synthase has a unique expression profile and has been demonstrated to produce PGE_2 under varying conditions. Since PGE_2 plays a critical role in inflammation and proliferation, understanding the synthases responsible for its production becomes crucial for determining new targets and potential therapeutics for many chronic diseases.

The biosynthesis of PGE_2 by mPGES1 has been well-established. mPGES1 is a member of the MAPEG (membrane-associated proteins involved in eicosanoid and glutathione metabolism) protein superfamily, and both *in vitro* studies and analysis of mice lacking mPGES1 support an important role for this enzyme in PGE_2 synthesis, especially during inflammatory responses. The expression of mPGES1 increases rapidly in many tissues and cells after exposure to proinflammatory cytokines and lipopolysaccharide (LPS) (27, 45). Specifically, mPGES1 coordinated with COX-2 in the production of PGE_2 from macrophages after exposure to lipopolysaccharide (LPS) (45). Also, by using mPGES1-deficient macrophages, this enzyme was demonstrated to be essential for LPS-induced PGE_2 production (69). Not surprisingly, *in vivo* studies of mice lacking this gene indicate that this enzyme is responsible for the increased levels of PGE_2 measured during inflammatory responses. Uematsu et al. demonstrated that mPGES1-deficient mice were unable to upregulate PGE_2 after LPS exposure compared to wild-type controls (69). Since PGE_2 is an important mediator of pain and leukocyte recruitment, analyzing the mPGES1-deficient mice in models of acute and chronic inflammation was important for understanding how this synthase contributes to disease pathogenesis. The mPGES1-deficient mice displayed impaired inflammatory pain perception and a reduction in severity and incidence in an experimental model of human rheumatoid arthritis, a chronic inflammatory disease (67).

This indicates an important contribution of mPGES1 to both PGE_2-dependent models of inflammatory pain and chronic inflammation. This evidence for mPGES1 as an inducible synthase responsible for elevating PGE_2 levels during inflammation demonstrates its importance during pathophysiological states.

A number of lines of evidence suggest that other means for production of PGE_2 *in vivo* are possible. PGE_2 production can still be detected in the mPGES1-deficient animals. Also, the mPGES1-deficient mice do not recapitulate all of the phenotypes of the mice deficient in the PGE_2 EP receptors, such as patent ductus arteriosus in the EP4-deficient mice and the fertilization defect observed in the EP2-deficient mice (51, 66). A possible explanation could be basal production of PGE_2 from the other identified PGE_2 synthases, mPGES2 and cPGES, which have been shown to increase PGE_2 production when over-expressed in various cell lines (44) (64).

Similar to mPGES1, mPGES2 is a microsomal protein. However, the expression of this gene is not induced by LPS treatment and increased levels are not observed in inflamed tissues (44). This enzyme has been demonstrated to couple with both COX-1 and COX-2 in PGE_2 production. Since expression of mPGES2 is ubiquitous and constitutive, it has been suggested that this synthase contributes primarily to maintenance of basal PGE_2 levels. However, determining the role of this protein *in vivo* is important to establish whether it truly has synthase capabilities and how it contributes to PGE_2 production in both homeostatic and pathological conditions.

The third protein capable of *in vitro* PGE_2 production was termed cPGES reflecting the fact that, unlike the other two synthases, this protein was purified from rat brain cytosolic extracts. Similar to mPGES1, this synthase was shown to have glutathione-dependent PGE_2

synthase activity (64). cPGES is expressed in many cell lines and in a wide range of tissues. Similar to mPGES2, expression of the gene is generally not sensitive to inflammatory stimuli with one notable exception. Tanioka *et al.* demonstrated that LPS treatment increased levels of cPGES three-fold in the brain (64). Co-transfection of human cPGES cDNA with COX-1, but not with COX-2, resulted in a large increase in PGE_2 production. These findings led to the suggestion that in most cells COX-1 collaborates with cPGES in basal PGE_2 production. This same research group has also shown that cPGES is regulated by serine phosphorylation (31). Casein kinase II (CKII) mediates this phosphorylation by forming a tertiary complex with the molecular chaperone Hsp90 and cPGES. In vitro experiments demonstrated that phosphorylation correlates with increased cPGES activity and Hsp90 association, and Hsp90 association stimulates phosphorylation by CKII. This phosphorylation and activation were abrogated following treatment with CKII and Hsp90 inhibitors. This data suggested a unique regulation of an enzyme in the eicosanoid biosynthetic pathway; however, the contribution of this enzyme to PGE_2 production *in vivo* has yet to been defined.

cPGES was determined by peptide microsequencing to be identical to a previously identified small acidic protein named p23 (64). p23 was originally co-purified with the inactive avian progesterone receptor/hsp90 complex from cell lysates (61). Toft and colleagues demonstrated p23 to be expressed in many tissues, highly conserved in numerous species, and an important co-chaperone of the hsp90 complex that aids in the progesterone receptor complex formation (28).

p23 and the Hsp90 Chaperone System

Hsp90 is a ubiquitous and essential chaperone protein for nearly 100 different client proteins including transcription factors, protein kinases, and growth and hormone receptors involved in signal transduction. This highly conserved and abundant stress protein forms a multiprotein chaperone system that is critical for the conformational change of the client protein to a state that is ready to respond to signal transduction. In steroid receptors, Hsp90 is responsible for the conformational change that opens the binding cleft for the steroid substrate.

The association of steroid receptors, especially the glucocorticoid receptor (GR), and the hsp90 chaperone system has been used extensively to study this model. The chaperone system consists of five proteins including hsp90, hsp70, Hop, hsp40, and p23. In an ATP-dependent fashion, hsp70 and hsp40 bind to the receptor to prepare the receptor for the conformational change. Then, in another ATP-dependent reaction, Hsp90 and Hop, bind to the primed GR/Hsp70 complex. Dittmar et al. demonstrated that only Hsp90, hsp70, and Hop were necessary to carry out the folding change that converts the hormone binding domain to a steroid binding conformation (15). After Hsp90 binding, another ATP-dependent step leads to opening of the hydrophobic binding cleft. p23 can now bind directly to Hsp90 in its ATP-dependent conformation (15). p23 appears to protect Hsp90/GR heterocomplexes against disassembly while increasing steroid binding activity in reticulocyte lysate. The rate of heterocomplex formation does not seem to be altered by p23 (15). This finding was strengthened by a study demonstrating that p23 was a limiting component responsible for stabilizing the Hsp90/client protein complex in Sf9 cells (43). At the point of p23 binding, Hop dissociates from the heterocomplex to allow immunophilins to bind to the

steroid receptor/Hsp90 heterocomplex and assist in trafficking. Specifically, TPR (tetratricopeptide repeat) domain immunophilins have been shown to link Hsp90 to a dynein motor protein through direct binding of the peptidylprolyl isomerase domain to aid in GR translocation to the nucleus (20). The complicated functions of p23 and the Hsp90 chaperone system in the maturation and stability of the GR still remain to be elucidated in vivo.

The Biological Functions of Glucocorticoids and the Glucocorticoid Receptor

Glucocorticoids are a class of steroid hormones that mediate many important biological functions. The adrenal cortex synthesizes and secretes glucocorticoids. The term glucocorticoid came from early studies that demonstrated a role for glucocorticoids in glucose metabolism. Glucocorticoids have since been shown to have a multitude of biological functions including roles in inflammation and lung development. The GR is a ligand-activated transcription factor that mediates the biological effects of glucocorticoids. GR is primarily in the cytoplasm sequestered by a multi-protein complex as described above. Upon hormone binding to the ligand binding domain, a conformational change occurs in GR and the multi-protein complex is released. GR can now translocate to the nucleus and regulate gene expression by both DNA-binding-dependent and –independent mechanisms. GR can bind to glucocorticoid response elements (GREs) upstream of specific target genes to induce transcription. GR has been shown to modify chromatin structure to allow for binding of cofactor complexes to stimulate gene transcription (24). Also, GR can bind to other transcription factors via direct protein-protein interactions, or tethering, to inhibit transcription of their target genes.

Glucocorticoids in Glucose Metabolism

Glucose is essential for animals as both a fuel and as a precursor for other carbohydrates. Intricate mechanisms exist to ensure that proper blood glucose levels are maintained. Glucose is primarily stored in the liver in the form of glycogen. The amount of glycogen stored in the liver is only enough to supply glucose to the brain for half a day, and glucose is the primary energy source for the brain. Thus, the intricate mechanisms, gluconeogenesis and glycogenolysis, become extremely important metabolic processes during times of limited food intake. Glycogenolysis is the catabolism of glycogen into glucose-1-phosphate, which can then be used to release free glucose into the bloodstream. Gluconeogenesis is the production of glucose from noncarbohydrate precursors. Again, the goal is to release free glucose into the blood to maintain homeostasis. Glucose-6-phosphatase is the final enzyme in both the gluconeogenic and glycogenolytic pathways. The glucose-6-phosphatase promoter has a glucocorticoid response element, and glucocorticoids have been demonstrated to stimulate its expression as well as other genes involved in gluconeogenesis, such as tyrosine aminotransferase (TAT) (11, 70). GR-deficient mice show reduced expression of enzymes involved in gluconeogenesis confirming their role in this process.

The role of glucocorticoids in metabolism was first noted over 60 years ago. Adrenalectomized animals could not maintain blood glucose levels or liver glycogen stores, and these defects could be corrected by treatment with glucocorticoids (13, 37). In 1970, adrenal corticosteroids were demonstrated to increase glycogen in fetal rat livers (22). Shortly thereafter, studies demonstrated that glycogen synthase, the final enzyme responsible for glycogen production, is stimulated by glucocorticoids (17, 71).

Glucocorticoids in Lung Development

Lung development is an intricate process involving growth and differentiation factors as well as circulating hormones that are temporally and spacially regulated. Glucocorticoids are important hormones that regulate the expression of genes necessary for proper lung maturation. During the final stages of lung development, glucocorticoids are important for epithelial cell differentiation and terminal saccule development (36, 62). Thinning of the mesenchyme is important to form the epithelial-endothelial junction necessary for efficient gas exchange. Glucocorticoids decrease the interstitial tissues in numerous animal species, and this is most likely through regulation of glucocorticoid-sensitive growth factors such as TNF-α, epithelial growth factor, and fibrocyte-pneumocyte factor (5, 55).

Administration of glucocorticoids is widely used to accelerate lung maturation and increase lung surfactant production in preterm infants (62). Lung surfactant is a lipoprotein that is synthesized by type II alveolar epithelial cells. Surfactants form a thin film on the alveolar surface that promotes lung compliance and prevents alveolar collapse. Lung surfactant contains four associated proteins SP-A, SP-B, SP-C, and SP-D, and numerous studies have demonstrated that glucocorticoids stimulate the expression of the surfactant protein genes (40). Glucocorticoids also regulates gene expression of the epithelial sodium channel (ENaC) which is essential for clearance of lung liquid at birth to improve compliance and gas exchange (72).

To further study the role of glucocorticoids in fetal lung development, mice lacking a functional glucocorticoid receptor were generated. These mice died at birth due to improper lung maturation (12). Surfactant protein expression was reduced in these mice, and the lungs were hypercellular and had reduced septal thinning. Ultrastructural analysis demonstrated a

reduction in type I alveolar epithelial cells, and this observation was confirmed by Northern analysis demonstrating reduced mRNA expression of type I AEC markers, T1α and aquaporin-5. Type I alveolar epithelial cells are flat cells with long cytoplasmic extensions that cover 90% of the alveolar space. These cytoplasmic extensions form thin boundaries with the endothelial cells to allow oxygen diffusion into the capillary bed. Thus, loss of these type I cells and lack of mesenchymal thinning can lead to a condensed lung architecture and respiratory insufficiency. The phenotypes of the glucocorticoid-deficient mice emphasize the importance of glucocorticoids in lung development and epithelial cell differentiation.

Glucocorticoids in Inflammation

Inflammation plays a key role in many chronic diseases, such as asthma, COPD, and rheumatoid arthritis. Sophisticated molecular mechanisms exist that involve the interaction of cytokines, chemokines, and lipid mediators in perpetuating disease pathology. Glucocorticoids have the ability to alter expression of these numerous inflammatory mediators and thus have been widely used for the treatment of inflammatory diseases. As discussed earlier, for many years, glucocorticoids have also been the primary treatment for pulmonary fibrosis although they have not demonstrated to improve life expectancy or quality of life. Three different mechanisms can account for the anti-inflammatory capabilites of glucocorticoids. GR can bind to GREs upstream of target genes to induce transcription of anti-inflammatory mediators. Glucocorticoids can also inhibit the expression of multiple proinflammatory genes through direct protein-protein interactions with transcription factors. Lastly, protein production and mRNA stability has also been shown to be affected by glucocorticoids (3, 46).

The most notable is the ability of glucocorticoids to inhibit the expression of many genes including those encoding cytokines, enzymes, receptors, and adhesion molecules that regulate inflammatory responses. Many of these genes do not have typical GRE sites to modify gene expression. Instead, GR tethers other transcription factors in a direct protein-protein interaction independent of DNA binding. This phenomenon was first described for the collagenase gene which is induced by activator protein-1 (AP-1) (29). Phorbol esters and tumor necrosis factor α (TNF-α) activate AP-1 which induces the collagenase gene. However, glucocorticoids inhibit this induction of the collagenase gene by forming a protein-protein complex with AP-1. Adcock et al. demonstrated that, in human lung, phorbol ester increased AP-1 binding to DNA, and glucocorticoids reversed the effect (2). This phenomenon has also been described for NF-κB, which is important in regulating expression of numerous inflammatory genes.

GR can also induce the transcription of anti-inflammatory mediators. For example, lipocortin-1 expression is induced by glucocorticoids. Lipocortin-1 inhibits phospholipase A2, which is important for release of AA and eicosanoid metabolism (14). This decreases the production of inflammatory lipid mediators. Glucocorticoids can also induce the transcription of Iκ-B-α, the inhibitor of NF-κB (58). The concentration of glucocorticoids necessary to stimulate gene transcription is much higher than necessary to inhibit expression by binding other transcription factors, and the induction of these genes is relatively slow (24-48hrs) compared to the more rapid anti-inflammatory effects observed after glucocorticoid treatment. Thus, the transactivation of anti-inflammatory genes is probably secondary to the ability of glucocorticoids to inhibit proinflammatory genes. The negative side effects from effecting metabolic processes is the more prominent effect from transactivation by GR (3).

Lastly, glucocorticoids have post-transcriptional and translational control of gene expression. Glucocorticoids have been shown to reduce protein production by decreasing mRNA stability, and it has been suggested that this is due to the induction of mRNA-degrading ribonucleases (53). These enzymes target AU-rich sequences located within the 3' untranslated region of many cytokines, growth factors, and inflammatory genes such as GM-CSF and COX-2 (6). These regions play an important role in mRNA stabilization and translational blockage.

Interestingly, COX-2 has been shown to be regulated by glucocorticoids by all three of the mechanisms described here: induction of transcription by transactivation, inhibition of transcription by tethering mechanisms, and post-transcriptional/translational control. Glucocorticoids can induce the expression of lipocortin-1 which indirectly regulates COX-2, as described above. Also, potential GRE elements have been defined in the COX-2 promoter regions which may play a role in the induction of gene transcription (65). Interestingly, the ability of glucocorticoids to stimulate production of prostanoids in specific cell types has been reported, particularily in primary amniotic fibroblasts (16, 63). These studies show that dexamethasone increases expression of COX-2 in these cells. In the majority of cell types, however, glucocorticoids are better known for their inhibition of COX-2 expression to reduce inflammation. Glucocorticoids have been shown to reduce COX-2 activity in cells by decreasing COX-2 transcription via tethering of transcription factors, such as NF-κB, essential for induction of this gene during inflammation (47, 48). In addition, post-transcriptional and translational regulation of COX-2 activity have been reported (35, 49, 50). For example, glucocorticoids have been shown to inhibit mitogen-activated protein kinase p38 which results in COX-2 mRNA destabilization (35). The numerous regulatory

mechanisms of COX-2 illustrates the complex interactions that are possible for mediating the anti-inflammatory effects of glucocorticoids.

DNA-binding-dependent versus –independent mechanisms of the glucocorticoid receptor

To elucidate the mechanism for glucocorticoid regulation of metabolic genes and other biological functions, a mouse line was generated in which GR could not homodimerize and bind DNA (56). This offered the unique opportunity to determine which biological effects of glucocorticoids were dependent on DNA binding to GREs to induce transcription or independent of DNA binding and involved tethering of other transcription factors. These mice, named GR^{dim}, survived to adulthood and had normal lung development. This suggests that lung development is a DNA-binding-independent process. In contrast, these mice did not induce genes involved in gluconeogenesis. Thus, metabolic processes require the DNA-binding ability of the GR to alter gene expression. In addition, glucocorticoids repressed both local and systemic inflammatory responses effectively in these mice (57). This study also demonstrated the appropriate repression of an NF-κB reporter gene by glucocorticoids in CD4+ splenocytes from these mice. This data supports that the tethering mechanism of GR with other transcription factors is the crucial mechanism for altering inflammatory responses especially in the case of human diseases. These mice provide in vivo evidence to confirm the in vitro studies that had separated the DNA-binding-dependent and –independent functions of GR.

Summary and Organization of Dissertation

The overall aim of this dissertation was to determine the role of prostanoids in the pathogenesis of pulmonary fibrosis. We first chose to analyze the role of PGE_2 in the development of disease due to its anti-fibrotic and anti-inflammatory properties in the lung. The work presented in Chapter 2 examines the in vivo role of the putative PGE_2 synthase, cPGES/p23, to elucidate the involvement of this protein in prostanoid metabolism and thus its subsequent value in fibrosis studies. This chapter also includes a detailed assessment of cPGES/p23 as a co-chaperone necessary for glucocorticoid receptor function. Chapter 3 discusses the use of the well-established bleomycin-induced pulmonary fibrosis model to investigate the pathogenesis of disease in mouse lines deficient in synthases or receptors that alter prostanoid signaling. Bleomycin-induced fibrosis has both pathological and biochemical similarities to human idiopathic pulmonary fibrosis and has been used extensively to model aspects of disease pathogenesis. Chapter 4 discusses possible mechanisms for the enhanced disease susceptibility of mice deficient in prostacyclin signaling.

REFERENCES

1. American Thoracic Society/European Respiratory Society International Multidisciplinary Consensus Classification of the Idiopathic Interstitial Pneumonias. This joint statement of the American Thoracic Society (ATS), and the European Respiratory Society (ERS) was adopted by the ATS board of directors, June 2001 and by the ERS Executive Committee, June 2001. *Am J Respir Crit Care Med* 165: 277-304, 2002.

2. Adcock IM, Shirasaki H, Gelder CM, Peters MJ, Brown CR, and Barnes PJ. The effects of glucocorticoids on phorbol ester and cytokine stimulated transcription factor activation in human lung. *Life Sci* 55: 1147-1153, 1994.

3. Barnes PJ. Anti-inflammatory actions of glucocorticoids: molecular mechanisms. *Clin Sci (Lond)* 94: 557-572, 1998.

4. Baud L, Perez J, Denis M, and Ardaillou R. Modulation of fibroblast proliferation by sulfidopeptide leukotrienes: effect of indomethacin. *J Immunol* 138: 1190-1195, 1987.

5. Beck JC, Mitzner W, Johnson JW, Hutchins GM, Foidart JM, London WT, Palmer AE, and Scott R. Betamethasone and the rhesus fetus: effect on lung morphometry and connective tissue. *Pediatr Res* 15: 235-240, 1981.

6. Bickel M, Iwai Y, Pluznik DH, and Cohen RB. Binding of sequence-specific proteins to the adenosine- plus uridine-rich sequences of the murine granulocyte/macrophage colony-stimulating factor mRNA. *Proc Natl Acad Sci U S A* 89: 10001-10005, 1992.

7. Bitterman PB, Wewers MD, Rennard SI, Adelberg S, and Crystal RG. Modulation of alveolar macrophage-driven fibroblast proliferation by alternative macrophage mediators. *J Clin Invest* 77: 700-708, 1986.

8. Bonner JC, Rice AB, Ingram JL, Moomaw CR, Nyska A, Bradbury A, Sessoms AR, Chulada PC, Morgan DL, Zeldin DC, and Langenbach R. Susceptibility of cyclooxygenase-2-deficient mice to pulmonary fibrogenesis. *Am J Pathol* 161: 459-470, 2002.

9. Borok Z, Gillissen A, Buhl R, Hoyt RF, Hubbard RC, Ozaki T, Rennard SI, and Crystal RG. Augmentation of functional prostaglandin E levels on the respiratory epithelial surface by aerosol administration of prostaglandin E. *Am Rev Respir Dis* 144: 1080-1084, 1991.

10. Choung J, Taylor L, Thomas K, Zhou X, Kagan H, Yang X, and Polgar P. Role of EP2 receptors and cAMP in prostaglandin E2 regulated expression of type I collagen alpha1, lysyl oxidase, and cyclooxygenase-1 genes in human embryo lung fibroblasts. *J Cell Biochem* 71: 254-263, 1998.

11. Cole TJ, Blendy JA, Schmid W, Strahle U, and Schutz G. Expression of the mouse glucocorticoid receptor and its role during development. *J Steroid Biochem Mol Biol* 47: 49-53, 1993.

12. Cole TJ, Solomon NM, Van Driel R, Monk JA, Bird D, Richardson SJ, Dilley RJ, and Hooper SB. Altered epithelial cell proportions in the fetal lung of glucocorticoid receptor null mice. *Am J Respir Cell Mol Biol* 30: 613-619, 2004.

13. Cori C and Cori G. Fate of sugar in animal body: carbohydrate metabolism of adrenalectomized rats and mice. *Journal of Biological Chemistry* 74: 473, 1927.

14. Croxtall JD, Choudhury Q, Tokumoto H, and Flower RJ. Lipocortin-1 and the control of arachidonic acid release in cell signalling. Glucocorticoids (changed from glucorticoids) inhibit G protein-dependent activation of cPLA2 activity. *Biochem Pharmacol* 50: 465-474, 1995.

15. Dittmar KD, Demady DR, Stancato LF, Krishna P, and Pratt WB. Folding of the glucocorticoid receptor by the heat shock protein (hsp) 90-based chaperone machinery. The role of p23 is to stabilize receptor.hsp90 heterocomplexes formed by hsp90.p60.hsp70. *J Biol Chem* 272: 21213-21220, 1997.

16. Economopoulos P, Sun M, Purgina B, and Gibb W. Glucocorticoids stimulate prostaglandin H synthase type-2 (PGHS-2) in the fibroblast cells in human amnion cultures. *Mol Cell Endocrinol* 117: 141-147, 1996.

17. Eisen HJ, Goldfine ID, and Glinsmann WH. Regulation of hepatic glycogen synthesis during fetal development: roles of hydrocortisone, insulin, and insulin receptors. *Proc Natl Acad Sci U S A* 70: 3454-3457, 1973.

18. Elias JA, Rossman MD, Zurier RB, and Daniele RP. Human alveolar macrophage inhibition of lung fibroblast growth. A prostaglandin-dependent process. *Am Rev Respir Dis* 131: 94-99, 1985.

19. Fine A, Poliks CF, Donahue LP, Smith BD, and Goldstein RH. The differential effect of prostaglandin E2 on transforming growth factor-beta and insulin-induced collagen formation in lung fibroblasts. *J Biol Chem* 264: 16988-16991, 1989.

20. Galigniana MD, Harrell JM, Murphy PJ, Chinkers M, Radanyi C, Renoir JM, Zhang M, and Pratt WB. Binding of hsp90-associated immunophilins to cytoplasmic dynein: direct binding and in vivo evidence that the peptidylprolyl isomerase domain is a dynein interaction domain. *Biochemistry* 41: 13602-13610, 2002.

21. Gay SE, Kazerooni EA, Toews GB, Lynch JP, 3rd, Gross BH, Cascade PN, Spizarny DL, Flint A, Schork MA, Whyte RI, Popovich J, Hyzy R, and Martinez FJ. Idiopathic pulmonary fibrosis: predicting response to therapy and survival. *Am J Respir Crit Care Med* 157: 1063-1072, 1998.

22. Greengard O and Dewey HK. The premature deposition or lysis of glycogen in livers of fetal rats injected with hydrocortisone or glucagon. *Dev Biol* 21: 452-461, 1970.

23. Hayashi T, Stetler-Stevenson WG, Fleming MV, Fishback N, Koss MN, Liotta LA, Ferrans VJ, and Travis WD. Immunohistochemical study of metalloproteinases and their tissue inhibitors in the lungs of patients with diffuse alveolar damage and idiopathic pulmonary fibrosis. *Am J Pathol* 149: 1241-1256, 1996.

24. Hebbar PB and Archer TK. Chromatin remodeling by nuclear receptors. *Chromosoma* 111: 495-504, 2003.

25. Hodges RJ, Jenkins RG, Wheeler-Jones CP, Copeman DM, Bottoms SE, Bellingan GJ, Nanthakumar CB, Laurent GJ, Hart SL, Foster ML, and McAnulty RJ. Severity of lung injury in cyclooxygenase-2-deficient mice is dependent on reduced prostaglandin E(2) production. *Am J Pathol* 165: 1663-1676, 2004.

26. Huang S, Wettlaufer SH, Hogaboam C, Aronoff DM, and Peters-Golden M. Prostaglandin E(2) inhibits collagen expression and proliferation in patient-derived normal lung fibroblasts via E prostanoid 2 receptor and cAMP signaling. *Am J Physiol Lung Cell Mol Physiol* 292: L405-413, 2007.

27. Jakobsson PJ, Thoren S, Morgenstern R, and Samuelsson B. Identification of human prostaglandin E synthase: a microsomal, glutathione-dependent, inducible enzyme, constituting a potential novel drug target. *Proc Natl Acad Sci U S A* 96: 7220-7225, 1999.

28. Johnson JL, Beito TG, Krco CJ, and Toft DO. Characterization of a novel 23-kilodalton protein of unactive progesterone receptor complexes. *Mol Cell Biol* 14: 1956-1963, 1994.

29. Jonat C, Rahmsdorf HJ, Park KK, Cato AC, Gebel S, Ponta H, and Herrlich P. Antitumor promotion and antiinflammation: down-modulation of AP-1 (Fos/Jun) activity by glucocorticoid hormone. *Cell* 62: 1189-1204, 1990.

30. Keerthisingam CB, Jenkins RG, Harrison NK, Hernandez-Rodriguez NA, Booth H, Laurent GJ, Hart SL, Foster ML, and McAnulty RJ. Cyclooxygenase-2 deficiency results in a loss of the anti-proliferative response to transforming growth factor-beta in human fibrotic lung fibroblasts and promotes bleomycin-induced pulmonary fibrosis in mice. *Am J Pathol* 158: 1411-1422, 2001.

31. Kobayashi T, Nakatani Y, Tanioka T, Tsujimoto M, Nakajo S, Nakaya K, Murakami M, and Kudo I. Regulation of cytosolic prostaglandin E synthase by phosphorylation. *Biochem J* 381: 59-69, 2004.

32. Kohyama T, Ertl RF, Valenti V, Spurzem J, Kawamoto M, Nakamura Y, Veys T, Allegra L, Romberger D, and Rennard SI. Prostaglandin E(2) inhibits fibroblast chemotaxis. *Am J Physiol Lung Cell Mol Physiol* 281: L1257-1263, 2001.

33. Kolodsick JE, Peters-Golden M, Larios J, Toews GB, Thannickal VJ, and Moore BB. Prostaglandin E2 inhibits fibroblast to myofibroblast transition via E. prostanoid receptor 2 signaling and cyclic adenosine monophosphate elevation. *Am J Respir Cell Mol Biol* 29: 537-544, 2003.

34. Kuhn C and McDonald JA. The roles of the myofibroblast in idiopathic pulmonary fibrosis. Ultrastructural and immunohistochemical features of sites of active extracellular matrix synthesis. *Am J Pathol* 138: 1257-1265, 1991.

35. Lasa M, Brook M, Saklatvala J, and Clark AR. Dexamethasone destabilizes cyclooxygenase 2 mRNA by inhibiting mitogen-activated protein kinase p38. *Mol Cell Biol* 21: 771-780, 2001.

36. Liggins GC. Premature delivery of foetal lambs infused with glucocorticoids. *J Endocrinol* 45: 515-523, 1969.

37. Long C, Katzin B, and Fry E. The adrenal cortex and carbohydrate metabolism. *Endocrinology* 26: 309, 1940.

38. Marshall RP, Puddicombe A, Cookson WO, and Laurent GJ. Adult familial cryptogenic fibrosing alveolitis in the United Kingdom. *Thorax* 55: 143-146, 2000.

39. McAnulty RJ, Hernandez-Rodriguez NA, Mutsaers SE, Coker RK, and Laurent GJ. Indomethacin suppresses the anti-proliferative effects of transforming growth factor-beta isoforms on fibroblast cell cultures. *Biochem J* 321 (Pt 3): 639-643, 1997.

40. Mendelson CR. Role of transcription factors in fetal lung development and surfactant protein gene expression. *Annu Rev Physiol* 62: 875-915, 2000.

41. Mensing H and Czarnetzki BM. Leukotriene B4 induces in vitro fibroblast chemotaxis. *J Invest Dermatol* 82: 9-12, 1984.

42. Mitchell J, Woodcock-Mitchell J, Reynolds S, Low R, Leslie K, Adler K, Gabbiani G, and Skalli O. Alpha-smooth muscle actin in parenchymal cells of bleomycin-injured rat lung. *Lab Invest* 60: 643-650, 1989.

43. Morishima Y, Kanelakis KC, Murphy PJ, Lowe ER, Jenkins GJ, Osawa Y, Sunahara RK, and Pratt WB. The hsp90 cochaperone p23 is the limiting component of the multiprotein hsp90/hsp70-based chaperone system in vivo where it acts to stabilize the client protein: hsp90 complex. *J Biol Chem* 278: 48754-48763, 2003.

44. Murakami M, Nakashima K, Kamei D, Masuda S, Ishikawa Y, Ishii T, Ohmiya Y, Watanabe K, and Kudo I. Cellular prostaglandin E2 production by membrane-bound prostaglandin E synthase-2 via both cyclooxygenases-1 and -2. *J Biol Chem* 278: 37937-37947, 2003.

45. Murakami M, Naraba H, Tanioka T, Semmyo N, Nakatani Y, Kojima F, Ikeda T, Fueki M, Ueno A, Oh S, and Kudo I. Regulation of prostaglandin E2 biosynthesis by inducible membrane-associated prostaglandin E2 synthase that acts in concert with cyclooxygenase-2. *J Biol Chem* 275: 32783-32792, 2000.

46. Newton R. Molecular mechanisms of glucocorticoid action: what is important? *Thorax* 55: 603-613, 2000.

47. Newton R, Kuitert LM, Bergmann M, Adcock IM, and Barnes PJ. Evidence for involvement of NF-kappaB in the transcriptional control of COX-2 gene expression by IL-1beta. *Biochem Biophys Res Commun* 237: 28-32, 1997.

48. Newton R, Kuitert LM, Slater DM, Adcock IM, and Barnes PJ. Cytokine induction of cytosolic phospholipase A2 and cyclooxygenase-2 mRNA is suppressed by glucocorticoids in human epithelial cells. *Life Sci* 60: 67-78, 1997.

49. Newton R, Seybold J, Kuitert LM, Bergmann M, and Barnes PJ. Repression of cyclooxygenase-2 and prostaglandin E2 release by dexamethasone occurs by transcriptional and post-transcriptional mechanisms involving loss of polyadenylated mRNA. *J Biol Chem* 273: 32312-32321, 1998.

50. Newton R, Seybold J, Liu SF, and Barnes PJ. Alternate COX-2 transcripts are differentially regulated: implications for post-transcriptional control. *Biochem Biophys Res Commun* 234: 85-89, 1997.

51. Nguyen M, Camenisch T, Snouwaert JN, Hicks E, Coffman TM, Anderson PA, Malouf NN, and Koller BH. The prostaglandin receptor EP4 triggers remodelling of the cardiovascular system at birth. *Nature* 390: 78-81, 1997.

52. Noble PW and Homer RJ. Back to the future: historical perspective on the pathogenesis of idiopathic pulmonary fibrosis. *Am J Respir Cell Mol Biol* 33: 113-120, 2005.

53. Peppel K, Vinci JM, and Baglioni C. The AU-rich sequences in the 3' untranslated region mediate the increased turnover of interferon mRNA induced by glucocorticoids. *J Exp Med* 173: 349-355, 1991.

54. Peters-Golden M, Bailie M, Marshall T, Wilke C, Phan SH, Toews GB, and Moore BB. Protection from pulmonary fibrosis in leukotriene-deficient mice. *Am J Respir Crit Care Med* 165: 229-235, 2002.

55. Pinkerton KE, Willet KE, Peake JL, Sly PD, Jobe AH, and Ikegami M. Prenatal glucocorticoid and T4 effects on lung morphology in preterm lambs. *Am J Respir Crit Care Med* 156: 624-630, 1997.

56. Reichardt HM, Kaestner KH, Tuckermann J, Kretz O, Wessely O, Bock R, Gass P, Schmid W, Herrlich P, Angel P, and Schutz G. DNA binding of the glucocorticoid receptor is not essential for survival. *Cell* 93: 531-541, 1998.

57. Reichardt HM, Tuckermann JP, Gottlicher M, Vujic M, Weih F, Angel P, Herrlich P, and Schutz G. Repression of inflammatory responses in the absence of DNA binding by the glucocorticoid receptor. *Embo J* 20: 7168-7173, 2001.

58. Scheinman RI, Cogswell PC, Lofquist AK, and Baldwin AS, Jr. Role of transcriptional activation of I kappa B alpha in mediation of immunosuppression by glucocorticoids. *Science* 270: 283-286, 1995.

59. Selman M, King TE, and Pardo A. Idiopathic pulmonary fibrosis: prevailing and evolving hypotheses about its pathogenesis and implications for therapy. *Ann Intern Med* 134: 136-151, 2001.

60. Selman M and Pardo A. Idiopathic pulmonary fibrosis: an epithelial/fibroblastic cross-talk disorder. *Respir Res* 3: 3, 2002.

61. Smith DF, Faber LE, and Toft DO. Purification of unactivated progesterone receptor and identification of novel receptor-associated proteins. *J Biol Chem* 265: 3996-4003, 1990.

62. Snyder JM, Rodgers HF, O'Brien JA, Mahli N, Magliato SA, and Durham PL. Glucocorticoid effects on rabbit fetal lung maturation in vivo: an ultrastructural morphometric study. *Anat Rec* 232: 133-140, 1992.

63. Sun K, Ma R, Cui X, Campos B, Webster R, Brockman D, and Myatt L. Glucocorticoids induce cytosolic phospholipase A2 and prostaglandin H synthase type 2 but not microsomal prostaglandin E synthase (PGES) and cytosolic PGES expression in cultured primary human amnion cells. *J Clin Endocrinol Metab* 88: 5564-5571, 2003.

64. Tanioka T, Nakatani Y, Semmyo N, Murakami M, and Kudo I. Molecular identification of cytosolic prostaglandin E2 synthase that is functionally coupled with cyclooxygenase-1 in immediate prostaglandin E2 biosynthesis. *J Biol Chem* 275: 32775-32782, 2000.

65. Tazawa R, Xu XM, Wu KK, and Wang LH. Characterization of the genomic structure, chromosomal location and promoter of human prostaglandin H synthase-2 gene. *Biochem Biophys Res Commun* 203: 190-199, 1994.

66. Tilley SL, Audoly LP, Hicks EH, Kim HS, Flannery PJ, Coffman TM, and Koller BH. Reproductive failure and reduced blood pressure in mice lacking the EP2 prostaglandin E2 receptor. *J Clin Invest* 103: 1539-1545, 1999.

67. Trebino CE, Stock JL, Gibbons CP, Naiman BM, Wachtmann TS, Umland JP, Pandher K, Lapointe JM, Saha S, Roach ML, Carter D, Thomas NA, Durtschi BA, McNeish

JD, Hambor JE, Jakobsson PJ, Carty TJ, Perez JR, and Audoly LP. Impaired inflammatory and pain responses in mice lacking an inducible prostaglandin E synthase. *Proc Natl Acad Sci U S A* 100: 9044-9049, 2003.

68. Tsakiri KD, Cronkhite JT, Kuan PJ, Xing C, Raghu G, Weissler JC, Rosenblatt RL, Shay JW, and Garcia CK. Adult-onset pulmonary fibrosis caused by mutations in telomerase. *Proc Natl Acad Sci U S A* 104: 7552-7557, 2007.

69. Uematsu S, Matsumoto M, Takeda K, and Akira S. Lipopolysaccharide-dependent prostaglandin E(2) production is regulated by the glutathione-dependent prostaglandin E(2) synthase gene induced by the Toll-like receptor 4/MyD88/NF-IL6 pathway. *J Immunol* 168: 5811-5816, 2002.

70. Vander Kooi BT, Onuma H, Oeser JK, Svitek CA, Allen SR, Vander Kooi CW, Chazin WJ, and O'Brien RM. The glucose-6-phosphatase catalytic subunit gene promoter contains both positive and negative glucocorticoid response elements. *Mol Endocrinol* 19: 3001-3022, 2005.

71. Vanstapel F, Dopere F, and Stalmans W. The role of glycogen synthase phosphatase in the glucocorticoid-induced deposition of glycogen in foetal rat liver. *Biochem J* 192: 607-612, 1980.

72. Wallace MJ, Hooper SB, and Harding R. Effects of elevated fetal cortisol concentrations on the volume, secretion, and reabsorption of lung liquid. *Am J Physiol* 269: R881-887, 1995.

73. Walter N, Collard HR, and King TE, Jr. Current perspectives on the treatment of idiopathic pulmonary fibrosis. *Proc Am Thorac Soc* 3: 330-338, 2006.

74. Wardlaw AJ, Hay H, Cromwell O, Collins JV, and Kay AB. Leukotrienes, LTC4 and LTB4, in bronchoalveolar lavage in bronchial asthma and other respiratory diseases. *J Allergy Clin Immunol* 84: 19-26, 1989.

75. White ES, Atrasz RG, Dickie EG, Aronoff DM, Stambolic V, Mak TW, Moore BB, and Peters-Golden M. Prostaglandin E(2) inhibits fibroblast migration by E-prostanoid 2 receptor-mediated increase in PTEN activity. *Am J Respir Cell Mol Biol* 32: 135-141, 2005.

76. Wilborn J, Bailie M, Coffey M, Burdick M, Strieter R, and Peters-Golden M. Constitutive activation of 5-lipoxygenase in the lungs of patients with idiopathic pulmonary fibrosis. *J Clin Invest* 97: 1827-1836, 1996.

77. Wilborn J, Crofford LJ, Burdick MD, Kunkel SL, Strieter RM, and Peters-Golden M. Cultured lung fibroblasts isolated from patients with idiopathic pulmonary fibrosis have a diminished capacity to synthesize prostaglandin E2 and to express cyclooxygenase-2. *J Clin Invest* 95: 1861-1868, 1995.

78. Zhang HY, Gharaee-Kermani M, Zhang K, Karmiol S, and Phan SH. Lung fibroblast alpha-smooth muscle actin expression and contractile phenotype in bleomycin-induced pulmonary fibrosis. *Am J Pathol* 148: 527-537, 1996.

79. Zhang K, Flanders KC, and Phan SH. Cellular localization of transforming growth factor-beta expression in bleomycin-induced pulmonary fibrosis. *Am J Pathol* 147: 352-361, 1995.

80. Zhang K, Rekhter MD, Gordon D, and Phan SH. Myofibroblasts and their role in lung collagen gene expression during pulmonary fibrosis. A combined immunohistochemical and in situ hybridization study. *Am J Pathol* 145: 114-125, 1994.

CHAPTER 2

cPGES/p23 is required for glucocorticoid receptor function and embryonic growth but not PGE_2 synthesis

cPGES/p23 is required for glucocorticoid receptor function and embryonic growth but not PGE_2 synthesis

Alysia Kern Lovgren, Martina Kovarova, Beverly H. Koller*

Department of Genetics, University of North Carolina at Chapel Hill, Chapel Hill, North Carolina 27599-7248.

This chapter has been published in the June 2007 issue of Molecular and Cellular Biology. I would like to thank the contributing authors: Martina Kovarova for help with the translocation experiments and flow cytometry for the proliferation assay and Bev Koller for her guidance and support.

ABSTRACT

A number of studies have identified cPGES/p23 as a cytoplasmic protein capable of the metabolism of prostaglandin E_2 (PGE_2) from the cyclooxygenase metabolite prostaglandin endoperoxide (PGH_2). However, this protein has also been implicated in a number of other pathways, including the stabilization of the glucocorticoid receptor (GR) complex. To define the importance of the functions assigned to this protein, mice lacking detectible cPGES/p23 expression were generated. cPGES/p23$^{-/-}$ pups die during the perinatal period and display retarded lung development reminiscent of the phenotype of GR-deficient neonates. Furthermore, GR-sensitive gluconeogenic enzymes are not induced in the prenatal period. However, unlike GR-deficient embryos, cPGES/p23$^{-/-}$ embryos are small in size, and a proliferation defect is observed in cPGES/p23$^{-/-}$ fibroblasts. Analysis of arachidonic acid metabolites in embryonic tissues and primary fibroblasts failed to support a function for this protein in PGE_2 biosynthesis. Thus, while the growth retardation of the cPGES/p23$^{-/-}$ pups and decreased proliferation of primary fibroblasts identifies functions for this protein in addition to GR stabilization, it is unlikely that these functions include metabolism of PGH_2 to PGE_2.

INTRODUCTION

Prostaglandin E_2 (PGE_2) is a lipid mediator involved in a wide range of normal biological functions as well as pathological processes such as chronic inflammation. Biosynthesis begins with the metabolism of arachidonic acid into prostaglandin endoperoxide (PGH_2) by cyclooxygenase enzymes (COX-1 or COX-2). Three terminal synthase enzymes, capable of producing PGE_2 from COX-derived PGH_2 *in vitro*, have been reported. These include microsomal PGE_2 synthase 1 (mPGES1), microsomal PGE_2 synthase 2 (mPGES2), and the cytosolic PGE_2 synthase (cPGES) (24, 59, 60). mPGES1 is a member of the MAPEG (membrane-associated proteins involved in eicosanoid and glutathione metabolism) protein superfamily and its expression increases rapidly in many cells after exposure to proinflammatory cytokines and lipopolysaccharide (LPS) (24, 62, 65). Not surprisingly, *in vivo* studies of mice lacking this gene indicate that this enzyme is responsible for the increased levels of PGE_2 measured in many inflammatory responses (62). However, PGE_2 production can still be detected in the mPGES1-deficient animals, supporting the contention that additional pathways are present that, at least under some circumstances, can produce PGE_2. One candidate is mPGES2. Similar to mPGES1, mPGES2 is a microsomal protein. However, as the expression of this gene is not induced by LPS treatment and increased levels are not observed in inflamed tissues, it has been suggested that this synthase contributes primarily to maintenance of basal PGE_2 levels (38).

The third protein capable of *in vitro* PGE_2 production was termed cPGES reflecting the fact that, unlike the other two synthases, this protein was purified from rat brain cytosolic extracts. Similar to mPGES1, this synthase was shown to have glutathione-dependent PGE_2 synthase activity (60). cPGES is expressed in many cell lines and in a wide range of tissues.

Similar to mPGES2, expression of the gene is generally not sensitive to inflammatory stimuli with one notable exception. Tanioka *et al.* demonstrated that LPS treatment increased levels of cPGES three-fold in the brain (60). Co-transfection of human cPGES cDNA with COX-1, but not with COX-2, resulted in a large increase in PGE_2 production (60). These findings led to the suggestion that in most cells COX-1 collaborates with cPGES in basal PGE_2 production.

Peptide mapping demonstrated that cPGES was identical to human p23, a highly conserved protein that functions as a co-chaperone for Hsp90 (25, 55, 60). The Hsp90 chaperone system has been shown to be critical for the function of a variety of hormone and growth factor receptors, including glucocorticoid receptor (GR), mineralocorticoid receptor , androgen receptor, epidermal growth factor receptor, and platelet-derived growth factor receptor (48). Steroid receptors, particularily GR, are used extensively to model the interactions of p23 with Hsp90 chaperone system and its client proteins. An important function of the Hsp90 complex is to facilitate folding of the hormone binding domain to a conformation capable of binding substrate. GR forms a heterocomplex with Hsp90, Hsp70, and p60, which are sufficient to carry out this folding change. p23 has been reported to increase the stability and hormone binding activity of the GR/Hsp90 complex (12). p23 binds directly to Hsp90 with bound ATP to stabilize the GR/Hsp90 complex from inactivation and disassembly.

GR is a ligand-activated transcription factor that mediates the biological effects of glucocorticoids. Upon steroid binding, GR translocates into the nucleus, dimerizes, and binds to glucocorticoid response elements (GREs) upstream of specific target genes. GR has also been shown to have DNA-binding-independent mechanisms of gene regulation through

direct protein-protein interactions, or tethering, of transcription factors, such as AP-1 and NF-κB (40). Many of these glucocorticoid-regulated genes, such as the epithelial sodium channel subunit γ (ENaCγ) and the surfactant proteins (SP-A, SP-B, SP-C), are important in the final stages of mouse lung development. These genes are responsible for the production of lung surfactant which increases alveolar stability by decreasing surface tension and the clearance of lung liquid to improve lung tissue compliance and gas exchange upon birth (33, 70). Glucocorticoids are also known to promote the differentiation of alveolar epithelial cells and development of terminal alveoli required for the transition to air breathing (30, 56).

A multifunctional role has been proposed for cPGES/p23, as both a terminal PGE_2 synthase and a co-chaperone for the GR/Hsp90 complex. In addition, many other functions linked to its association with Hsp90 have been assigned to this protein. To date, the role of cPGES/p23 in these processes has been primarily characterized *in vitro*, so the *in vivo* role of cPGES/p23 remains unclear. We have generated a mouse line deficient in cPGES/p23 to better characterize this protein and elucidate its role *in vivo*. The cPGES/p23-deficiency causes perinatal lethality due to improper lung maturation. We demonstrate that cPGES/p23 is required for both DNA-binding-dependent and -independent GR functions. However, additional phenotypes of this animal suggest GR-independent functions for this protein in development. Characterization of primary embryonic fibroblasts derived from the cPGES/p23-deficient mice, as well as embryonic tissues, demonstrates that cPGES/p23 is not required for PGE_2 synthesis.

MATERIALS AND METHODS

Experimental Animals

All studies were conducted in accordance with the National Institutes of Health Guide for the Care and Use of Laboratory Animals as well as the Institutional Animal Care and Use Committee guidelines of the University of North Carolina at Chapel Hill.

Generation of cPGES/p23-deficient mice

A mouse ES cell line (RST271) containing an insertional mutation in *cPGES/p23* was obtained from BayGenomics, a gene-trapping resource (57). A gene-trap vector, pGTOTMpfs, was used that contained a splice-acceptor sequence upstream of a reporter gene, β-geo (a fusion of β-galactosidase and neomycin phosphotransferase II). This vector inserted into the first intron of *cPGES/p23* creating a fusion transcript containing sequences from the first exon joined to the β-geo marker. 5' rapid amplification of cDNA ends (5' RACE) followed by automated DNA sequencing was used to determine the identity of the trapped gene as *cPGES/p23*. Male chimeras generated from this ES cell line were bred to B6/D2 females to generate mice heterozygous for the mutated allele. These heterozygotes were intercrossed to produce mice homozygous for the mutation. Pregnant heterozygous females were euthanized with CO_2, and embryos were removed by cesarean section. The genotypes of the offspring were determined by Southern blot analysis. A specific probe was designed 3' of exon 2 and used to screen genomic DNA digested with PvuII. Insertion of the vector in the first intron results in a reduced fragment size for the mutant allele compared to the endogenous wild-type allele.

Northern Blot Analysis

Total RNA was isolated from embryonic day (E) 18.5 embryos with RNA-Bee (Tel-Test Inc) according to manufacturer's instructions. Total RNA (20μg) was separated by gel electrophoresis on a 1.2% agarose/formaldehyde gel and transferred to a nitrocellulose (Immobilon NC, Amersham Biosciences) membrane overnight. Northern blots were hybridized with a [^{32}P]dCTP (Amersham Biosciences)-labeled cPGES cDNA probe prepared with a random primed labeling kit (Roche Diagnostics). The cPGES cDNA probe was generated from commercially available EST clones (Invitrogen Laboratories). Membranes were hybridized with a β-actin cDNA probe to verify similar RNA loading.

Prostanoid Measurements in Whole Embryos and Embryo lungs

Tissues were flash frozen in liquid nitrogen and stored in the -80°C freezer until use. Samples were pulverized and then homogenized in 1x PBS with 1mM EDTA pH 7.4 and 10 mM indomethacin and sonicated. Lipids were purified through an Amprep Octadecyl C18 mini column (Amersham Biosciences), and prostanoid content was determined by using enzyme immunoassay kits (Assay Designs) according to manufacturer's instructions.

Generation of MEFs

E13.5 embryos were used to generate MEFs. The embryos were washed with sterile PBS, finely minced, and trypsinized twice for 30 minutes in a 37° H_2O bath. Tissue debris was discarded, and the fibroblasts were cultured in Dulbecco modified Eagles medium (DMEM) with 10% fetal bovine serum and supplemented with 100 μg/ml streptomycin sulfate and 100 units/ml penicillin G sodium at 37° C with 5% CO_2.

Prostanoid Measurements in MEFs

MEFs were seeded in nickel-well plates (10^5 cells/well) and grown to 80% confluence. Fibroblasts were washed and cultured in 1.5 ml serum-free media for 1 hour. Supernatant was collected, and the cells were trypsinized and pelleted for total protein determination by the BCA method (Pierce). Enzyme immunoassay kits (Assay Designs) were used to determine the amount of PGE_2 and thromboxane B_2 (TxB_2) in the supernatants. All assays were performed in triplicate, and cells treated with indomethacin were used as a negative control.

Proliferation Assay

Carboxyfluorescein diacetate succinimidyl ester (CFSE, CellTrace Cell Proliferation kit, Invitrogen) was used to stain primary fibroblasts to monitor cell proliferation. Primary fibroblasts were plated in a 6-well plate, and 16 hours later, the cells were stained with 5 μM CFSE according to manufacturer's instructions. Cells were harvested, counted, and analyzed by FACScalibur flow cytometer (Becton Dickinson) and CellQuest software at the indicated time points. The doubling time has been calculated by using the equation:

$Y_t = Y_{(o)} * 2^{nt}$. $Y_{(t)}$ = number of cells at time (t); $Y_{(o)}$ = initial number of cells; n = cell cycles/hour.

Light Microscopy and Histological Analysis

Tissues were removed from embryos, fixed overnight in 10% formalin, and embedded in paraffin. Sections of lung and liver tissues were stained with hematoxylin/eosin for routine

histology. Liver sections were also stained with periodic acid-Schiff (PAS) for glycogen content. Sections were observed using a light microscope (Nikon FXA).

Transmission Electron Microscopy

Lungs were dissected from E18.5 embryos and fixed in 2% paraformaldehyde/2.5% glutaraldehyde in .15M sodium phosphate pH 7.4. Following three rinses with phosphate buffer, the samples were post-fixed for 1 hour in 1% osmium tetroxide/1.25% potassium ferrocyanide in sodium phosphate buffer. The tissues were rinsed in deionized water and dehydrated through increasing concentrations of ethanol (30%, 50%, 75%, 100%, 100%, 10 minutes each) and put through two changes of propylene oxide (15 minutes each). Tissue samples were infiltrated with a 1:1 mixture of propylene oxide: Polybed 812 epoxy resin (1A:2B formulation, Polysciences, Inc.,Warrington, PA) for 3 hours followed by an overnight infiltration in 100% resin. The tissue pieces were embedded in fresh epoxy resin and polymerized for 24 hours at 60˚C. The blocks were trimmed, and 1 micrometer sections of the tissue were mounted on glass slides and stained with 1% toluidine blue O in 1% sodium borate. Representative areas were selected by light microscopy, and 70nm ultrathin sections were cut using a diamond knife. Ultrathin sections were collected on 200 mesh copper grids and stained with 4% aqueous uranyl acetate for 15 minutes, followed by Reynolds' lead citrate for 7 minutes. Sections were observed using a LEO EM910 transmission electron microscope at 80kV (LEO Electron Microscopy, Thornwood, NY) and photographed using a Gatan Bioscan Digital Camera (Gatan, Inc., Pleasanton, CA).

Isolation of RNA and Quantitative Real-Time PCR

Lung tissue was removed from E18.5 embryos, and total RNA was isolated by RNA-Bee (Tel-Test Inc) according to manufacturer's instructions. RNA concentration was determined by absorbance at 260 nm. RNA was purified using the RNeasy mini kit (Qiagen), and 5μg was used to generate cDNA with the High-Capacity cDNA Archive kit (Applied Biosystems). cDNA (2.5 ng) was used in amplification reactions with Taqman PCR Universal Mastermix and commercially available primer and probe sets (Applied Biosystems) on an ABI Prism 7900 Thermocycler. Expression levels were normalized to an endogenous control, β-actin. Quantification of samples was performed using the comparative Ct (ΔΔCt) method, as described in the Assays-on-Demand Users Manual (Applied Biosystems). Relative gene expression was determined by the formula $x = 2^{-\Delta\Delta Ct}$. Results were expressed as fold change relative to wild-type expression levels.

Western Blot Analysis

Total protein was isolated from tissue by homogenizing frozen tissue in lysis buffer (50 mM HEPES, .15M NaCl, 1.5mM $MgCl_2$, 1% Triton-X 100, 10% glycerol, 10μg/ml leupeptin, 500μM Na_3VO_4, .1M PMSF, and Roche Complete mini protease inhibitor tablet). Homogenates were centrifuged at 14,000 rpm for 5 minutes at 4°C, and protein content of the supernatant was measured using BCA assay (Pierce). A quantity of 75 μg of protein per sample was separated by SDS-PAGE and electrophoretically transferred onto polyvinylidene difluoride membranes (Hybond-P, Amersham Biosciences). Membranes were blocked in 5% nonfat milk in 1x TBST (Tris-buffered saline and .05% Tween 20) for 1 hr at room temp. Immunoblots were probed with primary antibody to GR (abcam, ab3579, dilution 2.5 μg/ml, incubated at 4°C overnight),

cPGES/p23 (Cayman, dilution 1:500, incubated at room temp for 1 hr), and ß-actin (Sigma, dilution 1:5,000, incubation at room temp for 1 hr) followed by goat anti-rabbit or goat anti-mouse secondary antibody (dilution 1:5000 and 1:10000 respectively) for 45 minutes at room temp. Membranes were incubated with ECL reagent and signal was detected by autoradiography after exposure to Hyperfilm (Amersham Biosciences).

For the nuclear localization analysis, 1.5 $x10^6$ fibroblasts were starved from serum for 24 hr and activated with 10nM dexamethasone for 0, 30, and 60 min. Cell pellet was resuspended in 200 µl of lysis buffer (HBSS buffer, 1.26 mM calcium, 1 mM magnesium, 0.1% NP-40, 200 nM PMSF and Roche Complete mini protease inhibitor tablet) and kept on ice for 20 min before centrifugation at 700xg for 20 min at 4°C. Nuclear pellet was washed in 200 µl lysis buffer, centrifuged at 700xg for 20 min at 4°C, resuspended in protein sample buffer, and processed for Western blot. Cytoplasmic supernatant was recentrifuged at 12,000xg for 20 min, and the supernatant was mixed with 80µl of protein sample buffer and processed for Western blot. GR was detected on Western blot by M20 antibody (Santa Cruz Biotechnology). The blots were reprobed with antibodies to α- tubulin (Sigma) and histone H1 (Santa Cruz Biotechnology).

Transfection Assay

Primary fibroblasts were immortalized by transfection with pSV3-neo (ATCC), a plasmid expressing SV40 large T antigen. Transformed fibroblasts (~2 x 10^5 cells) were seeded in a 6-well plate, and after 24 hours, fibroblasts were transfected with either 3 µg of pGRE-luc (Clontech) and .05 µg of pCMVβ (Applied Biosystems) or 3 µg of pTAL-luc (Clontech) and .05 µg pCMVβ using Lipofectamine PLUS reagent (Invitrogen) according to manufacturer's instructions. After transfection, the fibroblasts were incubated with dexamethasone (10nM) for

24 hours. Cell lysates were collected and analyzed for luciferase and β-galactosidase expression using the Dual-Light Luciferase/β-galactosidase Reporter Gene Assay kit (Applied Biosystems). Luciferase activity was normalized to β-galactosidase activity. Negative control values from the transformed fibroblasts transfected with pTAL-luc were subtracted from the experimental values.

Immunofluorescence Staining of Transformed MEFs for GR

Coverslips (number 1; 12 mm circle, thickness range, 0.13–0.17 mm; Fisher Scientific, Pittsburgh, PA) were coated with 0.1% gelatin. Cells were resuspended in growth medium at a final concentration of 4×10^4 cells/ml. 500 or 1000 μl of suspension was applied to a coverslip in 24-well plate, and the cells were allowed to adhere for 3 hr at 37˚C. Cultivation medium was replaced by medium without serum and cells were starved for 16 hr. Cells were activated by 10nM dexamethasone for 0, 30, and 60 min in medium without serum. Activation was stopped by ice cold PBS and cells were immediately fixed by methanol for 20 min at -20˚C and permeabilized for 1 min by acetone at -20˚C. Cells were blocked in blocking buffer (20% FBS, 5% BSA, 0.05% gelatin) for 30 min at room temperature and incubated with GR antibody (M-20, Santa Cruz Biotechnnology Inc., Santa Cruz, CA) diluted 1:150 in TBST buffer (10 mM Tris, 150 mM NaCl, 0.1% Tween) overnight at 4˚C. Coverslips were washed 3 times in TBST buffer and incubated with FITC-conjugated anti-rabbit antibody (Jackson ImmunoResearch, West Grove, PA) diluted 1:100 at room temperature for 1 hr. Coverslips were washed 3 times with TBST buffer and 2 times with PBS, dried and mounted on slides (SuperFrost Plus Microscope Slides; Fisher Scientific) in mounting solution and visualized with Nikon Microphot FXA Upright fluorescence

microscope (Nikon Inc.,Garden City, NY) using a x60 objective. ImageJ software (NIH) was used to measure the mean pixel density in the nucleus.

Statistical Analysis

Values are presented as mean +/- standard error of the mean and are analyzed by Student's two-tailed t-test (Mann-Whitney or Tukey-Kramer test for multiple comparisons where indicated). A p-value less than 0.05 is considered statistically significant.

RESULTS

Generation of cPGES/p23$^{-/-}$ mice

Mouse ES cells with a gene-trap inserted in the first intron of *cPGES/p23* were obtained from BayGenomics (57). The gene-trap contains splice acceptors, which direct anomalous splicing of the primary transcript, resulting in loss of cPGES/p23 expression. Male chimeras generated from this ES cell line were bred to B6/D2 females to generate mice heterozygous for the mutated allele. No pups homozygous for the mutant allele were identified at weaning in litters obtained by intercross of these heterozygous animals. In contrast, Southern blot analysis of E18.5 embryos demonstrated the presence of homozygous fetuses at normal Mendelian frequency (Figure 1a). Examination and monitoring of neonates indicated that at least some cPGES/p23$^{-/-}$ pups were alive at birth, but these died shortly thereafter, after taking several agonal breaths.

To verify that the insertion of the gene-trap into intron 1 of the *cPGES/p23* gene resulted in loss of expression, RNA was prepared from cPGES/p23$^{-/-}$ and cPGES/p23$^{+/+}$ embryos and expression of cPGES/p23 determined by Northern blot analysis. No cPGES/p23 transcript was detected by this method (Figure 1b). Similarly, cPGES/p23 could not be detected by Western blot analysis of protein extracts prepared from the livers and primary fibroblasts of cPGES/p23$^{-/-}$ embryos (Figure 1c).

Mice lacking COX-2, as well as mice lacking the PGE_2 EP4 receptor, die in the perinatal period due to a patent ductus arteriosus (31, 45). The majority of mice lacking both COX-1 and COX-2 die within 30 minutes of delivery. We therefore examined the possibility that cPGES/p23 was required for the PGE_2 production essential for maturation of the vessel. Similar to mice lacking EP4 and COX-2, the ductus failed to close in the cPGES/p23-deficient mice;

however, in contrast to the EP4$^{-/-}$ and COX-2$^{-/-}$ mice, death of the cPGES/p23-deficient neonates preceded the inflation of the lungs. Although this early death of the cPGES/p23-deficient mice excludes the assessment of this protein in PGE_2 production under various physiological stress in the mature animal, survival of these embryos to full-term allowed us to assess prostanoid production both in fetal tissues and in cell lines derived from the cPGES/p23-deficient embryos.

Analysis of prostaglandin production in cPGES/p23$^{-/-}$ embryos

To identify a role for cPGES/p23 in PGE_2 production, we determined PGE_2 levels in full-term embryos and E18.5 lungs. Consistent with the PGE_2 synthase function assigned to this protein, PGE_2 levels were reduced in the cPGES/p23$^{-/-}$ embryos and embryonic lungs compared to the wild-type tissues. However, a similar decrease in the level of other COX-dependent metabolites, thromboxane (TxB_2) and prostacyclin, in these tissues was also observed (Figure 2a). This finding was not consistent with loss of expression of a PGE_2 synthase, but rather suggested cPGES/p23 might have a pleotropic function in prostaglandin synthesis.

The first step in the synthesis of prostanoids is the release of arachidonic acid from the plasma membrane by $cPLA_2$. A small decrease in the expression of this enzyme was detected by quantitative RT-PCR of RNA prepared from cPGES/p23$^{-/-}$ E18.5 lungs (Figure 2b). However, this change did not achieve statistical significance. COX-1 and COX-2 are essential for the production of PGH_2, the common substrate for all prostanoids. We, therefore, next determined whether loss of cPGES/p23 resulted in altered expression of these two enzymes. A 50% reduction in COX-2 and a 30% reduction in COX-1 transcripts were observed in RNA prepared from the cPGES/p23$^{-/-}$ lungs (Figure 2b).

Increased basal PGE_2 and TxB_2 levels in Mouse Embryonic Fibroblasts (MEFs)

To further examine the impact of decreased expression of cPGES/p23 on prostanoid biosynthesis, we examined the production of PGE_2 in MEFs derived from E13.5 embryos. Since MEFs produce high levels of PGE_2, even in the absence of stimuli (14), we measured constitutive production of PGE_2 in cultures of cPGES/$p23^{-/-}$ and cPGES/$p23^{+/+}$ fibroblasts. Equal numbers of cells were seeded and grown to confluence in 24-well plates. The cells were cultured in serum-free DMEM for 1 hour, and the PGE_2 released into the medium during this time period was measured. Surprisingly, basal levels of PGE_2 were higher in the cPGES/$p23^{-/-}$ fibroblasts compared to the wild-type fibroblasts, which again is not consistent with loss of a PGE_2 synthase (Figure 3). Parallel cultures treated with indomethacin, which inhibits the enzymatic activity of both COX-1 and COX-2, served as a negative control in this assay. Compared to these negative control indomethacin-treated cells, thromboxane levels were below the detectable limit in the wild-type fibroblasts. However, thromboxane was easily measured in the supernatant collected from the cPGES/$p23^{-/-}$ cells (Figure 3), thus, similar to the *in vivo* measurements, the change in PGH_2 metabolites was not limited to PGE_2.

Growth retardation of the cPGES/p23-deficient embryos

Our failure to define a role for cPGES/p23 in the direct regulation of PGE_2 levels makes it unlikely that this previously assigned function contributes to the perinatal lethality of these mice. Further analysis of the mutant animals was carried out to determine whether the phenotype of the cPGES/$p23^{-/-}$ embryos would support other functions assigned to this protein. Embryos were removed at E15.5 and E18.5, and each embryo was weighed and the crown-rump length determined. The weight and length of the E15.5 cPGES/p23-deficient pups tended to be less

than that of the wild-type littermates, but this difference did not achieve statistical significance with this small group of animals. However, later in gestation, a significant decrease in both the weight and crown-rump length of the mice lacking cPGES/p23 became apparent (Figure 4a).

To determine whether the smaller size of the cPGES/p23 embryos reflected a role for cPGES/p23 in proliferation, embryonic fibroblast cultures were established from control and mutant E13.5 embryos. After isolation of these cells and establishment of the primary cultures, equal numbers of wild-type and cPGES/p23$^{-/-}$ cells were seeded and the growth monitored daily. Attached viable cells, as well as the dead cells present in the culture media, were counted at twenty-four, forty-eight, and seventy-two hours after plating. As can be seen in Figure 4b, the growth of the cPGES/p23-deficient cells lagged behind that of the wild-type. This did not appear to represent a loss of cells due to cell death as no difference was observed in the number of dead cells present in the media. The average doubling time for the two wild-type primary cell cultures, derived from two different embryos, was calculated to be 18.3 hours while the average doubling time for two cPGES/p23$^{-/-}$ cell cultures was 25.4 hours. An additional two cultures of each genotype were examined, and the average doubling times were 17.0 hours and 33.1 hours for the wild-type and cPGES/p23$^{-/-}$ cell cultures, respectively. To further examine this point, cells were labeled with CFSE. This dye is retained in the cells but diminishes in intensity with each round of proliferation. Cells were stained 24 hours after plating, and flow cytometric analysis was performed to determine proliferation rate at 24 and 48 hours after staining. As shown in Figure 4c, the cPGES/p23$^{-/-}$ fibroblasts were not proliferating as rapidly as the wild-type to produce the next generations at both 24 and 48 hours after addition of the dye. Overall, this supports a role of cPGES/p23 either directly or indirectly in cell cycle progression of primary fibroblasts.

cPGES/p23$^{-/-}$ mice have abnormal lung development

The small decrease in growth of the cPGES/p23$^{-/-}$ pups alone is unlikely to account for the perinatal lethality of this mutation. As discussed above, necropsy of the pups indicated minimal inflation of the cPGES/p23$^{-/-}$ lungs after birth. In contrast to the impact of cPGES/p23 on the overall growth of the pup, the size of the cPGES/p23$^{-/-}$ lungs did not differ from that of wild-type embryos, and, in fact, measurement of total RNA content indicated an increase in the cellularity of the lungs at E18.5 (Figure 5a). We, therefore, compared the architecture of the cPGES/p23$^{-/-}$ and wild-type lungs at various stages of development. Lung development can be divided into four stages (9). The embryonic stage is marked by the initial branching of the lung from the primitive foregut and the development of the broncho-pulmonary segments. During the pseudoglandular stage (E12.5-E16.0) there is further branching of the duct system generating the conducting portion of the respiratory system including the terminal bronchioles. These early developmental events were not altered in the mice lacking cPGES/p23. As shown in Figure 5b, no apparent differences are observed between the E15.5 wild-type and cPGES/p23$^{-/-}$ lung. During the next two stages of development, the canalicular phase (E16.0-17.5) and the saccular/alveolar phase (E17.5 to postnatal day 5), the terminal bronchioles undergo further branching to form the respiratory bronchioles. This is followed by the formation of terminal sacs and thinning of the stroma that separated these saccules from the developing vascular bed, thus forming the thin diffusible interface between the airways and the pulmonary circulation required after birth. It is during the canalicular stage that differences in the development of the cPGES/p23$^{-/-}$ lungs become apparent. At E18.5, the cPGES/p23$^{-/-}$ lungs still display morphology similar to the wild-type lungs early in the canalicular stage (Figure 5b). Terminal sac development appears

absent in the cPGES/p23$^{-/-}$ embryos resulting in a more condensed lung architecture. Thus, the development of the cPGES/p23$^{-/-}$ lungs appears arrested in the canalicular stage (E16.0-E17.5).

Transmission electron microscopy was used to compare the epithelial cell profile as well as other ultrastructural features of the lungs from cPGES/p23$^{-/-}$ and wild-type full-term embryos. In the wild-type embryonic lung, type II alveolar epithelial cells (type II AECs), progenitors of type I alveolar epithelial cells (type I AECs), can easily be distinguished within each saccule by their cuboidal shape, apical microvilli, and the presence of the lamellar bodies, structures essential for the intracellular storage of surfactant. The saccules are largely lined by type I AECs (Figure 6a). The thin cytoplasmic extensions of this cell type reduces the air-capillary interface. Thus, the differentiation of these cells from their type II AEC precursors is essential for survival. Marked differences are observed in the ultrastructure of the distal lungs obtained from cPGES/p23$^{-/-}$ embryos. Most notably, no type I AECs were observed in the cPGES/p23$^{-/-}$ lungs (Figure 6b). Type II AECs could, however, be identified based on their unique apical microvilli and lamellar bodies. Consistent with differentiation of this cell type, surfactant can be identified in the airways of the cPGES/p23$^{-/-}$ lung. The distal airway of the cPGES/p23$^{-/-}$ embryos also contains a large number of cuboidal cells which cannot be classified, based on morphological characteristics. It is likely that these represent precursors of type II AECs.

To further examine the developmental changes in the cPGES/p23$^{-/-}$ lungs, we prepared RNA from E18.5 embryo lungs and quantitated the expression of genes which are commonly used as cell-specific markers for airway epithelia, type I AECs, and type II AECs. In the lung, especially in the neonatal period, the airway epithelia expresses high levels of the

Na^+-K^+-$2Cl^-$ cotransporter (NKCC1) (53). The thyroid transcription factor (TTF-1) is expressed in both type II AECs and in Clara epithelial cells and has been used previously as a specific marker of lung epithelial cell demarcation (76, 79). No difference in expression of these two genes was observed between wild-type and cPGES/p23$^{-/-}$ animals indicating normal proximal-distal epithelial cell patterning (Figure 6c).

To quantitate the loss of type I AECs, quantitative RT-PCR was used to compare expression of type I cell-specific markers, T1α and aquaporin 5, in RNA prepared from wild-type and E18.5 cPGES/p23$^{-/-}$ lungs (72). A dramatic decrease in expression of T1α and aquaporin 5 is observed in the cPGES/p23$^{-/-}$ lungs, consistent with our failure to identify type I cells in these lung (Figure 6c).

Analysis of a type II cell-specific marker, dendritic-cell lysosomal-associated membrane protein (DC-LAMP) (54), showed a significant decrease in the cPGES/p23$^{-/-}$ lungs (Figure 6c). Similarly, a dramatic decrease in the expression of surfactant genes (SP-A, SP-B, SP-C) was observed (Figure 6c). The remarkable changes in the expression of these genes were greater than predicted given our ability to identify type II AECs and surfactant in cPGES/p23-deficient lungs.

Expression of GR-sensitive genes in the cPGES/p23$^{-/-}$ lungs

The severe lung phenotype of the cPGES/p23-deficient mice is similar to the lung phenotype of the GR-deficient mice (5, 8). We, therefore, next determined whether expression of GR-sensitive genes was altered in the cPGES/p23$^{-/-}$ lungs. The best studied of these genes are those encoding the surfactants. As described above, we observed a significant decrease in mRNA levels for these genes in the cPGES/p23$^{-/-}$ embryos. The expression of DC-LAMP

has also been shown to be sensitive to glucocorticoids (32). Again, a significant decrease in the expression of this gene was observed in the mutant lungs. However, interpretation of these differences is complicated since these genes are expressed almost exclusively by type II AECs, and thus the paucity of mRNA may reflect both decreased numbers of mature type II AECs and regulation of these genes by GR. We therefore also examined the expression of ENaCγ, whose expression has also been shown to be sensitive to glucocorticoids (53, 68). mRNA levels of ENACγ were analyzed by quantitative RT-PCR, and a significant decrease in expression was measured in the cPGES/p23$^{-/-}$ lungs (Figure 7a).

Recently, glucocorticoids have been shown to be important in regulating the growth factor midkine (MK). From E16.5 to E17.5, a significant decrease in the expression of this gene is observed in wild-type mice but not embryos lacking GR. Thus, in these mutant animals, levels at birth are 3-fold higher that wild-type littermates (27). We reasoned that if cPGES/p23 is essential for GR function, we would expect a similar pattern of expression in cPGES/p23$^{-/-}$ lungs. Consistent with this, MK expression is 3-fold higher in the cPGES/p23-deficient mice compared to the wild-type mice (Figure 7a). Taken together, the decreased expression of ENACγ and the increased expression of MK indicated that cPGES/p23 is essential in the regulation of glucocorticoid-sensitive genes in the mouse lung. To determine whether this loss of GR function was the result of decreased levels of GR, protein extracts were prepared from wild-type and cPGES/p23$^{-/-}$ fetal lungs. No significant difference in the level of the steroid receptor was observed, suggesting that loss of cPGES/p23 primarily altered the activity of the receptor (Figure 7b).

cPGES/p23 is necessary for the induction of gluconeogenic enzymes

The analysis of expression of glucocorticoid-regulated genes in the lung is complicated by the dramatic alterations in the development of this organ in the cPGES/p23$^{-/-}$ animals. To further verify the relationship between cPGES/p23 and expression of GR-sensitive transcripts, we examined the expression of genes required for gluconeogenesis in the liver of the E18.5 wild-type and cPGES/p23$^{-/-}$ embryos. While gluconeogenesis in the mouse does not occur until after birth, the induction of some of the enzymes, including glucose-6-phosphatase and serine dehydratase, is observed late in gestation (2, 18). The final step of both gluconeogenic and glycogenolytic pathways is carried out by glucose-6-phosphatase and contribution of glucocorticoids to the regulation of the expression of this gene has been noted (66). The promoter contains a number of GRE elements and the binding of GR together with other accessory factors form the glucocorticoid response unit which regulates gene expression. Expression of both glucose-6-phosphatase and serine dehydratase were significantly decreased in the cPGES/p23$^{-/-}$ livers (Figure 8a). A similar decrease has been reported for these genes in GR-deficient mice (7). To further examine the role of cPGES/p23 in maturation of the liver, we examined the accumulation of glycogen which normally begins to accumulate late in gestation. Previous studies have suggested a role for glucocorticoids in this induction (67). The cPGES/p23-deficient mice have abnormal liver morphology compared to the wild-type mice at E17.5 (Figure 8b,c). Analysis of the livers by PAS staining confirmed the failure of glycogen to accumulate in the cPGES/p23$^{-/-}$ livers (Figure 8d,e)

Delayed maturation of the skin in cPGES/p23$^{-/-}$ embryos

Upon external examination, the skin of the cPGES/p23$^{-/-}$ mice appeared more translucent than that of their littermates. Histological examination of the dorsal stratified epithelium from one pair of E17.5 wild-type and cPGES/p23$^{-/-}$ embryos and three pairs of genetically-matched E18.5 embryos showed that loss of cPGES/p23 had indeed altered the development of this organ. As expected, all of the structures of the skin were apparent on examination of the sections obtained from the E17.5 wild-type fetus (Figure 9). A single basal layer of proliferating cells and the suprabasal layers of terminally differentiating cells transitioning as they move towards the surface of the skin are observed. Transcriptionally active spinous and granular cells, as well as several layers of stratum corneum, consisting of metabolically inert enucleated cells are apparent at this embryonic stage. Similar to the wild-type pups, the basal epithelia cells were easily identified in the cPGES/p23$^{-/-}$ animals. A well-defined stratum spinosum was also observed. However, remarkable differences were noted in the terminal differentiation of the kerotinocytes. A well-defined stratum granulosum, characterized by darkly stained keratohyaline granules, was not present in the cPGES/p23$^{-/-}$ skin, although a few cells with some keratohyalin granules could be identified. A dramatic deficit in the stratum corneum was also observed. By E18.5 the stratum granulosum was more apparent in the mutant fetuses, although the development of this layer and the degree of granulation varied between the mutant pups. However, in all three animals, the lamellar organization of the granulocytic layer, the flattening of the cells, and the discarding of the nucleus had not progressed to the same degree as in the skin of the control animals. In fact, in many instances, numerous nucleated cells with some keratohyalin granules were present at the

epithelia surface. In all the cPGES/p23 mutant animals, deficiencies in the development of the stratum corneum were apparent.

Loss of GR transactivation and tethering mechanisms in cPGES/p23$^{-/-}$ fibroblasts

As normal levels of GR protein were measured in the cPGES/p23$^{-/-}$ fetal tissue, we next examined directly the ability of these receptors to activate gene transcription in cells lacking cPGES/p23. Transformed embryonic fibroblasts were transiently transfected with pGRE-luc, a reporter plasmid with three GRE enhancer elements. Binding of ligand-bound GR to the GREs drives luciferase expression. The fibroblasts were co-transfected with pCMVβ, and β-galactosidase expression was used to normalize for transfection efficiency. pTAL-luc, a reporter plasmid with no GRE enhancer elements, was independently transfected as a negative control, and these baseline expression values were subtracted from the experimental values. Upon incubation with dexamethasone, a synthetic glucocorticoid, the wild-type fibroblasts had a significant increase in luciferase expression. The cPGES/p23-deficient fibroblasts had a significantly lower luciferase expression compared to the wild-type suggesting that loss of cPGES/p23 reduces GR transactivation (Figure 10a).

GR has been shown to inhibit gene transcription through direct protein-protein interaction, or tethering, with transcription factors, such as AP-1. This interaction was first established for the AP-1-regulated gene, collagenase-3 (47). Relative expression of collagenase-3 was determined after activating AP-1 with phorbol 12-myristate 13-acetate (PMA). The cPGES/p23$^{-/-}$ fibroblasts had a similar induction of collagenase-3 compared to the wild-type fibroblasts suggesting that the ability of AP-1 to induce gene transcription is not affected by loss of cPGES/p23. Wild-type fibroblasts treated with dexamethasone and

PMA had a significant reduction in collagenase-3 expression (Figure 10b). However, the AP-1-induced expression of collagenase-3 in the cPGES/p23$^{-/-}$ fibroblasts was not inhibited upon treatment with dexamethasone suggesting that loss of cPGES/p23 reduces the ability of GR to negatively regulate transcription factors such as AP-1.

Defective nuclear translocation of GR in cPGES/p23$^{-/-}$ fibroblasts

To determine the mechanism for the reduction in GR transactivation and tethering in the cPGES/p23$^{-/-}$ fibroblasts, we investigated the ability of GR to translocate to the nucleus after dexamethasone stimulation. Using immunofluorescent staining, the wild-type fibroblasts showed an increase in GR in the nucleus after 30 and 60 minutes of dexamethasone stimulation (Figure 11a). cPGES/p23$^{-/-}$ fibroblasts showed no increase in GR in the nucleus after 30 and 60 minutes of dexamethasone stimulation. The nuclear localization of GR was quantitated by measuring mean pixel density of the nucleus. A slight increase in GR in the nucleus was measured at 60 minutes of dexamethasone stimulation in the cPGES/p23$^{-/-}$ fibroblasts; however, only the wild-type measurements taken at 30 and 60 minutes of dexamethasone stimulation had a statistically significant increase in pixel density in the nucleus compared to the non-stimulated cells.

To further verify the translocation defect, western blot analysis was performed on nuclear and cytosolic extracts from the fibroblasts after stimulation with dexamethasone. Similar to the immunofluorescence, the wild-type fibroblasts had an increase of GR in the nucleus and a decrease of GR in the cytosol at both 30 and 60 minutes of dexamethasone treatment. The cPGES/p23$^{-/-}$ fibroblasts had no change in GR in either the nuclear or the cytosolic fraction (Figure 11b).

Figure 2.1

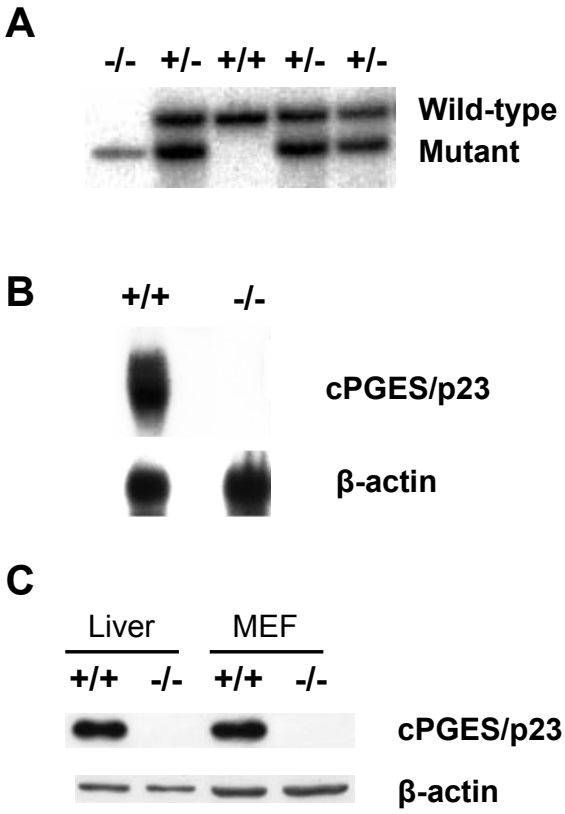
A
-/- +/- +/+ +/- +/-
Wild-type
Mutant
B
+/+ -/-
cPGES/p23
β-actin
C
Liver
MEF
+/+ -/- +/+ -/-
cPGES/p23
β-actin

Figure 2.1. Generation of cPGES/p23$^{-/-}$ mice. A) Southern blot analyses of DNA from embryonic day (E) 18.5 embryos generated by the intercross of mice heterozygous for the cPGES/p23 mutant allele. B) Northern blot analyses of cPGES/p23 mRNA expression in whole E18.5 embryos. Analysis with a β-actin-specific probe verifies equal RNA sample loading. C) Western blot analysis of cPGES/p23 protein expression in E18.5 liver and mouse embryonic fibroblasts (MEFs). β-actin expression shown as a loading control.

Figure 2.2

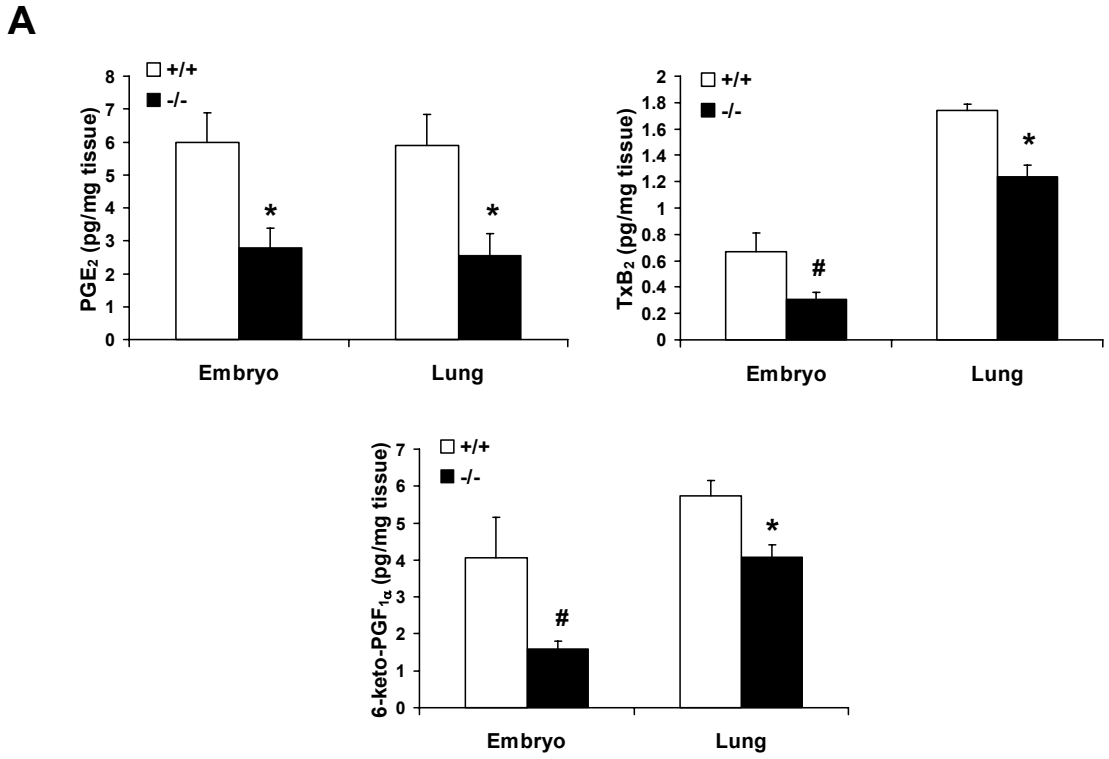
A
+/+
-/-
PGE2 (pg/mg tissue)
TxB2 (pg/mg tissue)
6-keto-PGF1α (pg/mg tissue)
Embryo
Lung
*
#

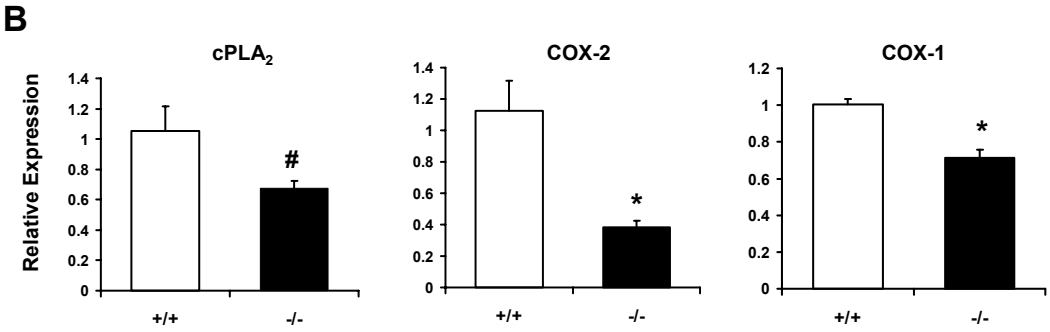
B
cPLA2
COX-2
COX-1
Relative Expression
+/+
-/-
*
#

Figure 2.2. cPGES/p23-deficient embryos have a significant decrease in prostanoid levels and a corresponding decrease in $cPLA_2$ and COX expression. A) PGE_2, thromboxane (TxB_2), and 6-keto-$PGF_{1\alpha}$ (a stable metabolite of prostacyclin (PGI_2)) levels in whole E18.5 embryos and lungs dissected from E18.5 embryos were measured by enzyme immunoassay (EIA). n = 4, * $p < .05$, # $p \leq .09$ by Student's t-test or $p \leq .05$ by Mann-Whitney. B) Determination of $cPLA_2$, COX-2, and COX-1 expression in total RNA isolated from E18.5 lungs by RT-PCR. Expression levels were normalized to β-actin, an endogenous control, and the results were expressed as fold change relative to wild-type expression levels. cPGES/$p23^{-/-}$ lungs, n = 7; wild-type lungs, n = 9; * $p < .05$, # $p = .06$.

Figure 2.3

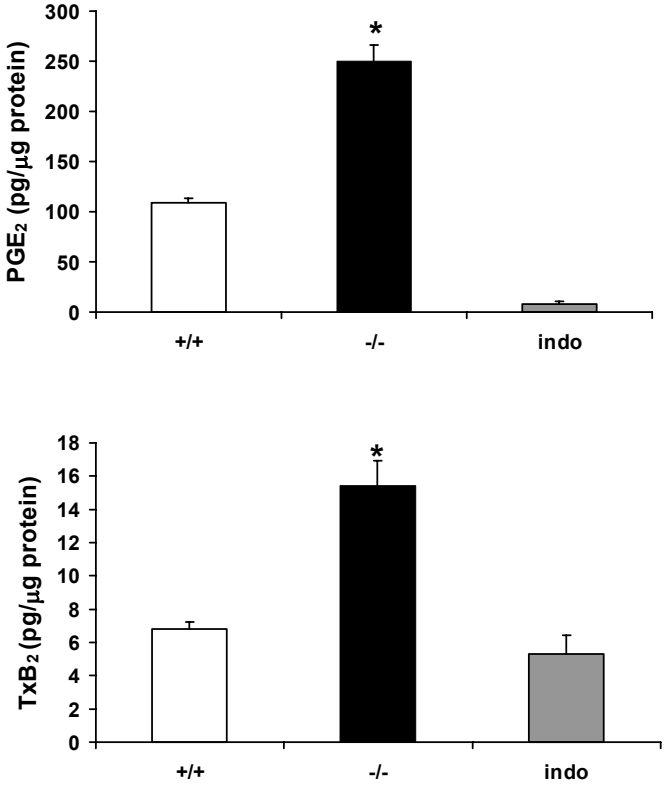
300
250
200
150
100
50
0
PGE2 (pg/µg protein)
*
+/+
-/-
indo
18
16
14
12
10
8
6
4
2
0
TxB2 (pg/µg protein)
*
+/+
-/-
indo

Figure 2.3. cPGES/p23-deficient primary fibroblasts have a significant increase in PGE_2 and TxB_2 levels. MEFs were isolated from cPGES/$p23^{-/-}$ and wild-type embryos. Cells were seeded in 24-well plates and grown to 80% confluence. After 1 hour incubation in serum-free media, the supernatant was removed, and PGE_2 and TxB_2 levels in the supernatant were determined by EIA. The cells in each well were harvested for total protein determination by the BCA method. Results are expressed as picograms of prostanoid per microgram of total cell protein per well. Parallel cultures treated with indomethacin, which inhibits the enzymatic activity of both COX-1 and COX-2, served as a negative control in this assay. $n = 6$, * $p < .01$.

Figure 2.4

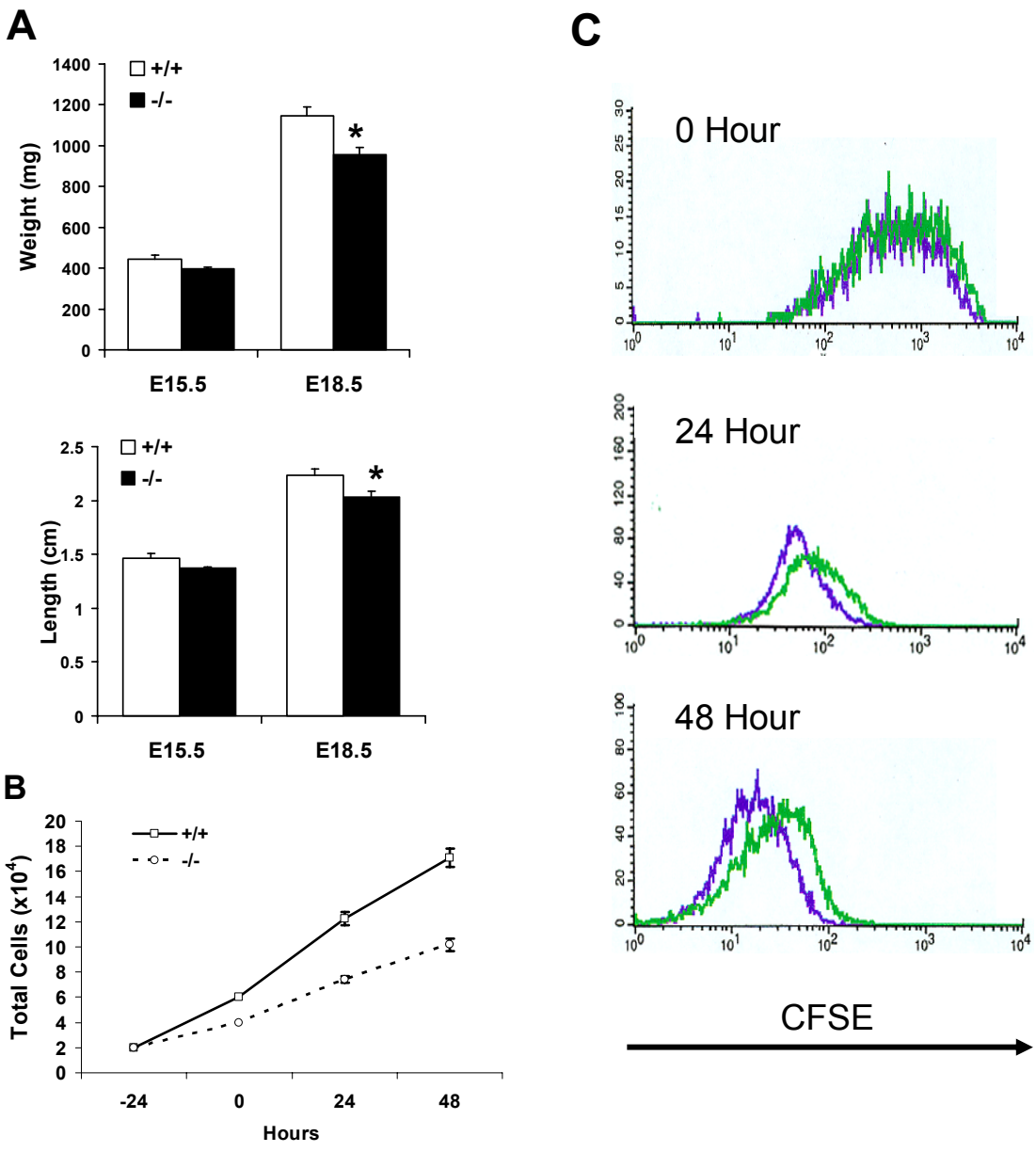
A
+/+
-/-
Weight (mg)
1400
1200
1000
800
600
400
200
0
*
E15.5
E18.5
Length (cm)
2.5
2
1.5
1
0.5
0
*
E15.5
E18.5
B
+/+
-/-
Total Cells (x10^4)
20
18
16
14
12
10
8
6
4
2
0
-24
0
24
48
Hours
C
0 Hour
24 Hour
48 Hour
CFSE

Figure 2.4. Loss of cPGES/p23 results in growth defects in embryos and proliferation defects in the primary embryonic fibroblasts. A) E15.5 and E18.5 embryos were removed by cesarean section and weight and crown-rump length determined. E15.5: cPGES/p23$^{-/-}$, n = 6; wild-type, n = 4; E18.5: cPGES/p23$^{-/-}$, n = 6; wild-type, n = 7; * $p < .05$. B) Growth curve for cPGES/p23$^{-/-}$ and wild-type primary embryonic fibroblasts. An equal number of cells of each genotype was plated in a 6-well plate (3 wells per time point for each genotype). At 24 hour intervals, cells were harvested and counted. The supernatant was collected from each well, and the number of dead cells present in the supernatant did not differ between samples. In contrast, a marked reduction in the number of cells present in the wells seeded with cPGES/p23$^{-/-}$ cells was observed. This data is representative of two independent experiments, each performed with two different -/- and +/+ MEF cultures. C) Proliferation assay comparing cPGES/p23$^{-/-}$ and wild-type primary fibroblasts. Cells were stained with CFSE and analyzed by flow cytometry 24 and 48 hours after staining. The CFSE intensity at the time of labeling is shown at 0 hr. A shift left at 24 and 48 hours represents a decrease in CFSE intensity which corresponds to the rate of proliferation in the population. Shown is the representative result from 3 independent experiments. Purple = wild-type; Green = cPGES/p23$^{-/-}$.

Figure 2.5

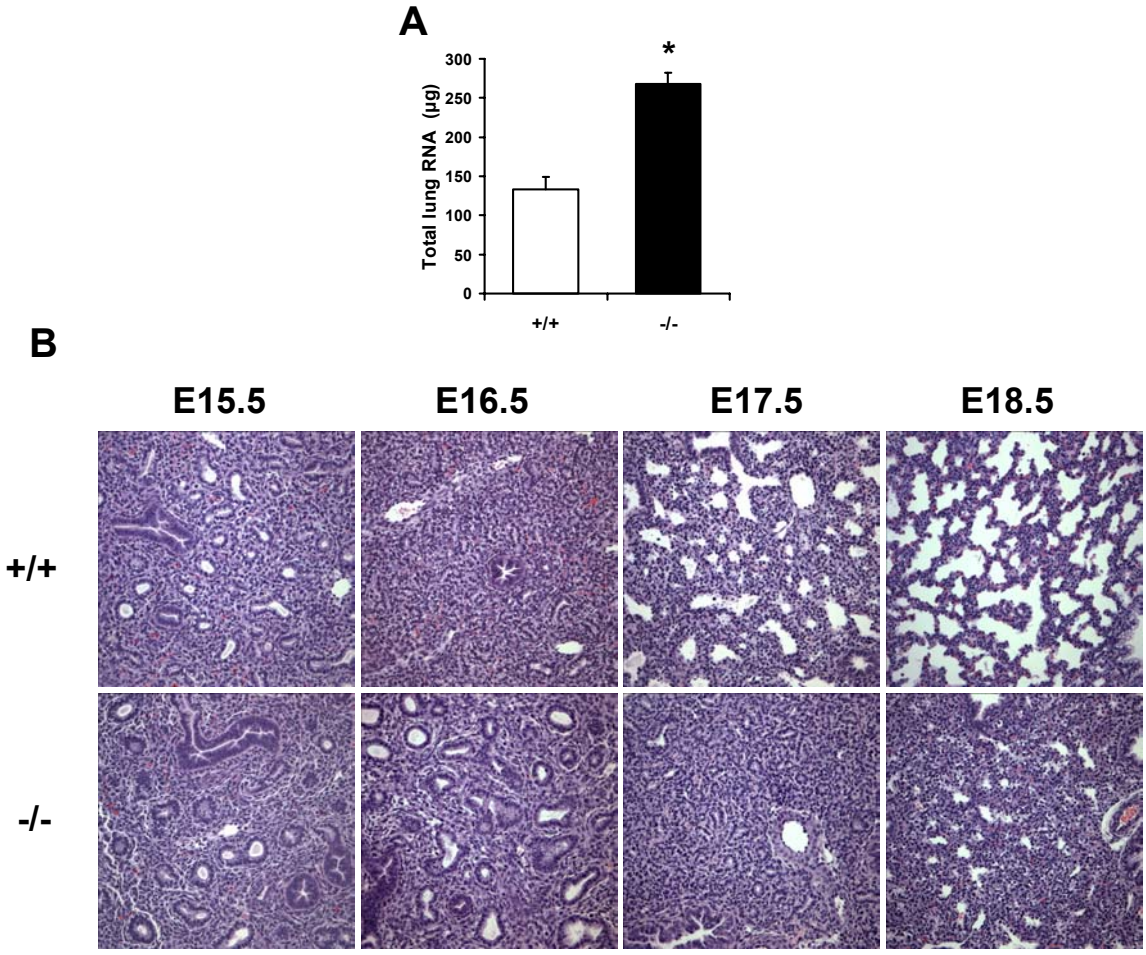
A
Total lung RNA (µg)
300
250
200
150
100
50
0
*
+/+
-/-
B
E15.5
E16.5
E17.5
E18.5
+/+
-/-

Figure 2.5. Histological analysis of lung tissue from E15.5-E18.5 wild-type and cPGES/p23$^{-/-}$ embryos by light microscopy. A) Total RNA was extracted from E18.5 embryo lungs. Quantitation of RNA revealed a significant increase in the cPGES/p23$^{-/-}$ lungs suggesting hypercellularity. B) Lungs were removed from embryos at E15.5, E16.5, E17.5, and E18.5 and fixed overnight in 10% formalin. Lung sections were stained with hematoxylin/eosin. The cPGES/p23$^{-/-}$ lung development appears arrested at the canalicular stage (E16.0-17.5). Notable is the failure of the development of terminal sacs. Original magnification, x10.

Figure 2.6

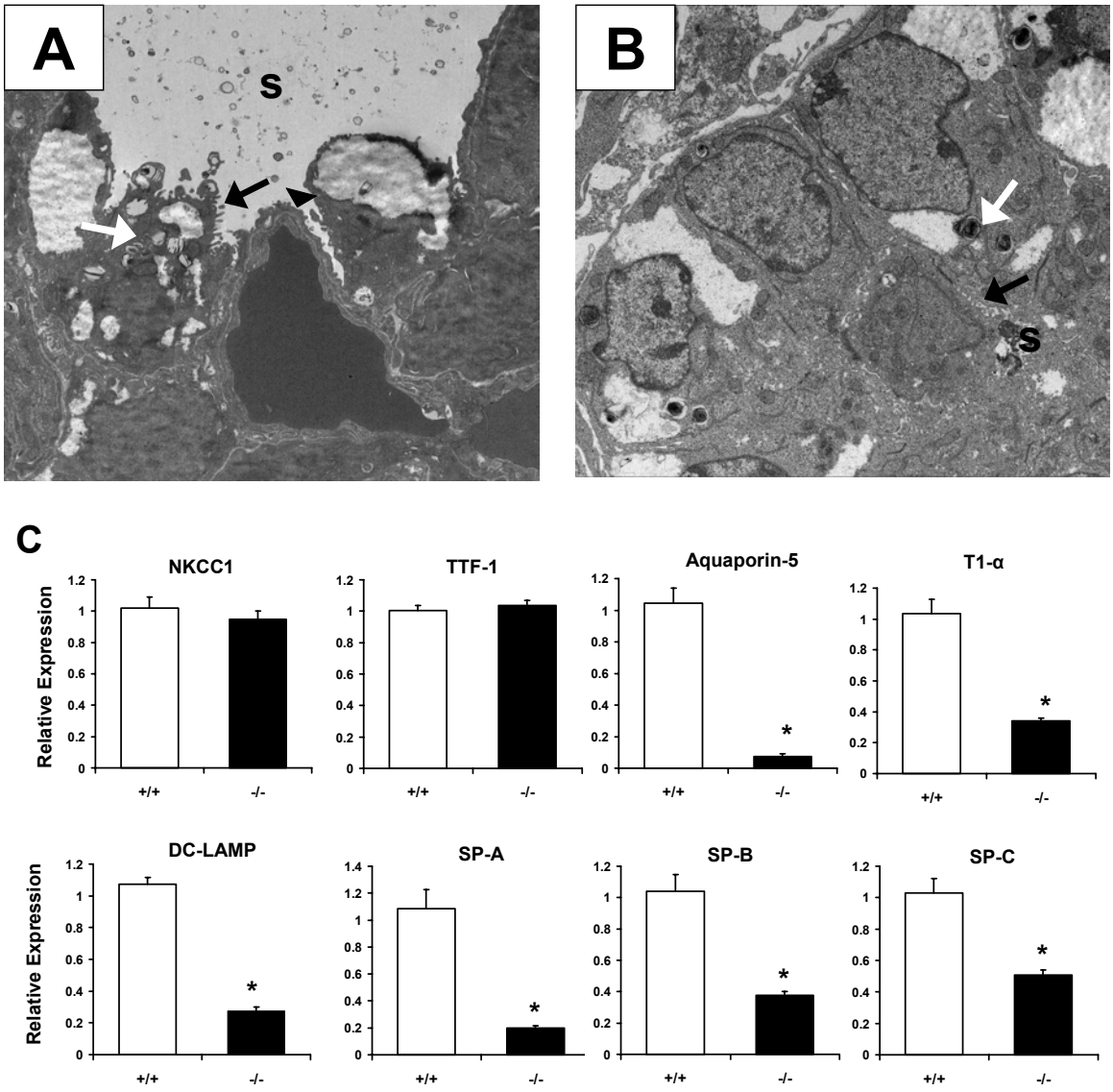
A
S
B
S
C
NKCC1
TTF-1
Aquaporin-5
T1-α
DC-LAMP
SP-A
SP-B
SP-C
Relative Expression
+/+
-/-
*

Figure 2.6. Abnormal ultrastructure of the distal airway in cPGES/p23$^{-/-}$ embryos. Transmission electron microscopy was used to analyze ultrastructural morphology in E18.5 lung tissue from wild-type (A) and cPGES/p23$^{-/-}$ (B) embryos. The electron micrographs demonstrate squamous type I AECs (black arrowhead) and cuboidal type II AECs containing lamellar bodies (white arrows) and apical microvilli (black arrows) in the wild-type lung. In contrast, while type II AECs were detected in the cPGES/p23$^{-/-}$ lungs, type I AECs could not be identified. s, surfactant. C) RT-PCR analysis was used to determine expression of a bronchial epithelial cell marker (NKCC1), a Clara cell-specific marker (TTF-1), type I AEC markers (aquaporin-5 and T1α), and type II AEC markers (DC-LAMP, SP-A, SP-B, SP-C). Expression levels were normalized to β-actin, an endogenous control, and the results were expressed as fold change relative to wild-type expression levels. cPGES/p23$^{-/-}$ lungs, n = 7; wild-type lungs, n = 9; * $p < .05$.

Figure 2.7

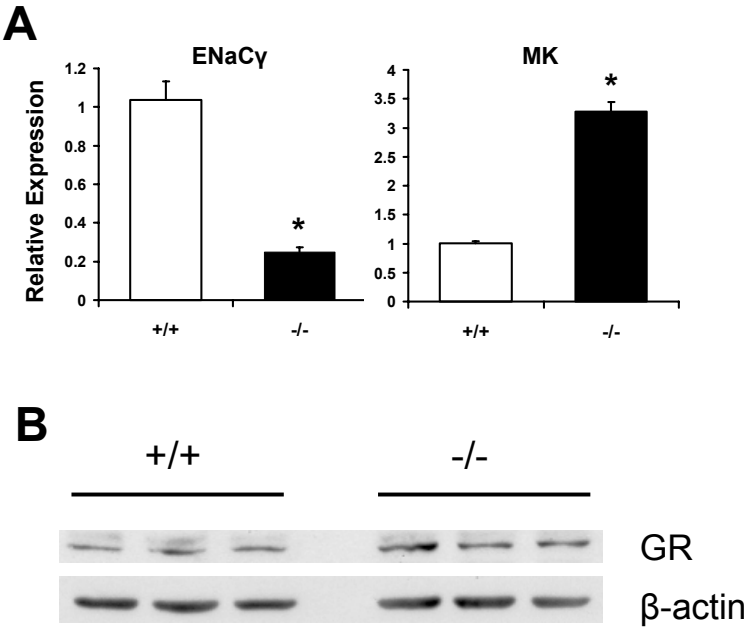
A
ENaCγ
MK
Relative Expression
1.2
1
0.8
0.6
0.4
0.2
0
4
3.5
3
2.5
2
1.5
1
0.5
0
*
*
+/+
-/-
+/+
-/-
B
+/+
-/-
GR
β-actin

Figure 2.7. cPGES/p23$^{-/-}$ mice have alterations in expression of glucocorticoid-regulated genes in the lung. A) RT-PCR analysis was used to determine expression levels of glucocorticoid-regulated genes, including ENaCγ and MK, in total RNA isolated from E18.5 lungs. Expression levels were normalized to β-actin, an endogenous control, and the results were expressed as fold change relative to wild-type expression levels. cPGES/p23$^{-/-}$ lungs, n = 7; wild-type lungs, n = 9; * $p < .05$. B) Western blot analysis of GR expression in E18.5 lungs from wild-type and cPGES/p23$^{-/-}$ embryos demonstrates similar GR protein levels. ß-actin expression verifies equal sample loading.

Figure 2.8

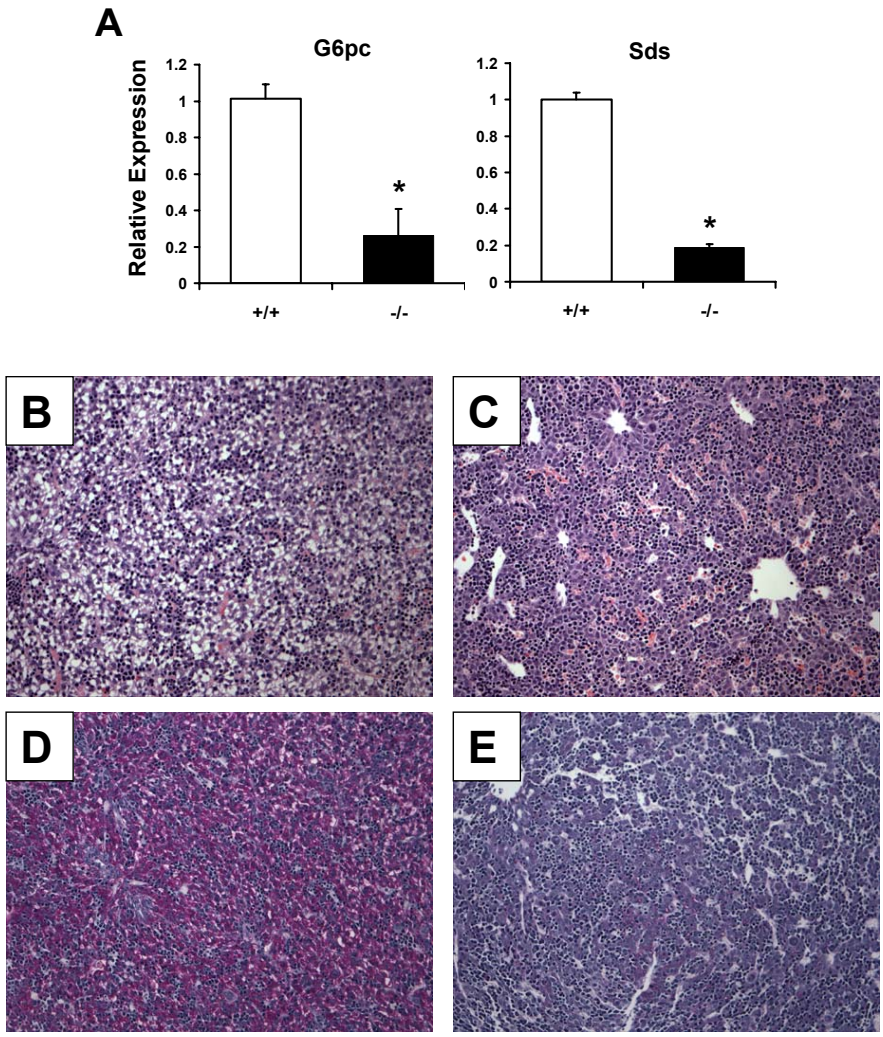

Figure 2.8. cPGES/p23$^{-/-}$ mice display abnormal liver morphology and have alterations in expression of glucocorticoid-regulated genes in the liver. A) RT-PCR analysis was used to determine expression levels of gluconeogenic enzymes, glucose-6-phosphatase (G6pc) and serine dehydratase (Sds), in total RNA isolated from E18.5 livers. Expression levels were normalized to β-actin, an endogenous control, and the results were expressed as fold change relative to wild-type expression levels. $n = 5$, * $p < .01$. B-E) Livers were removed from embryos at E17.5 and fixed overnight in 10% formalin. Liver sections from wild-type (B) and cPGES/p23$^{-/-}$ (C) embryos were stained with hematoxylin/eosin for routine histological examination. Glycogen content in the liver was assessed by periodic acid-Schiff (PAS) staining. Note the intense staining in the wild-type liver (D) compared to the cPGES/p23$^{-/-}$ liver (E). Representative of four embryo livers analyzed for each genotype. Original magnification, x10.

Figure 2.9

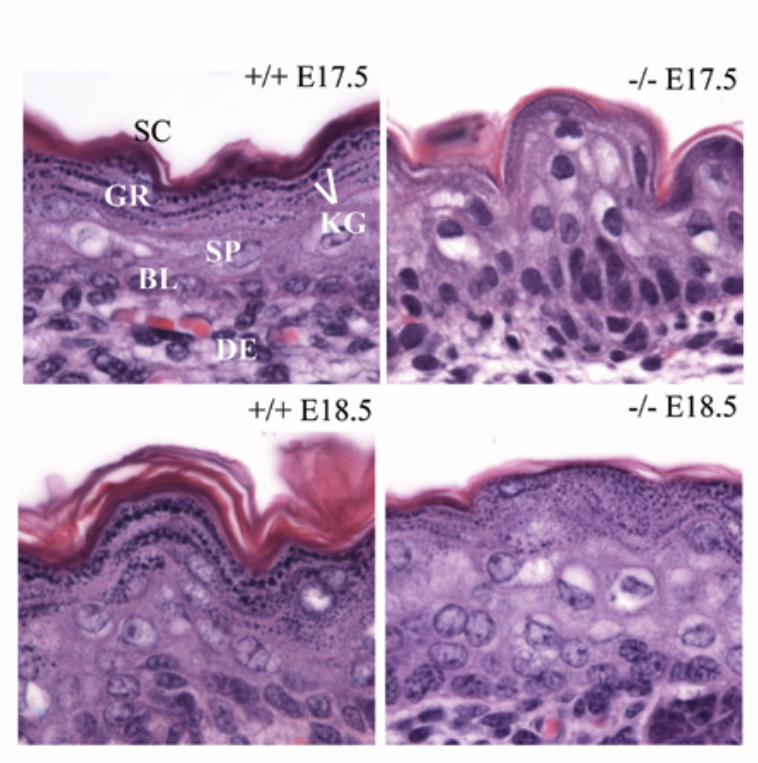

Figure 2.9. Delayed maturation of the skin in cPGES/p23$^{-/-}$ embryos.

Aberrations in differentiation and formation of the cornified envelope in cPGES/p23$^{-/-}$ stratified epithelia. Skin from wild-type and cPGES/p23$^{-/-}$ E17.5 and E18.5 fetuses was fixed in formalin, embedded in paraffin, and sections cut (5μm) and stained with hematoxylin and eosin. Sections correspond to the dorsal skin above the scapular region of the embryo. SC, stratum corneum; GR, granular layer; KG, kerotohyalin granules; SP, suprabasal layer; BL, basal layer; DE, dermis

Figure 2.10

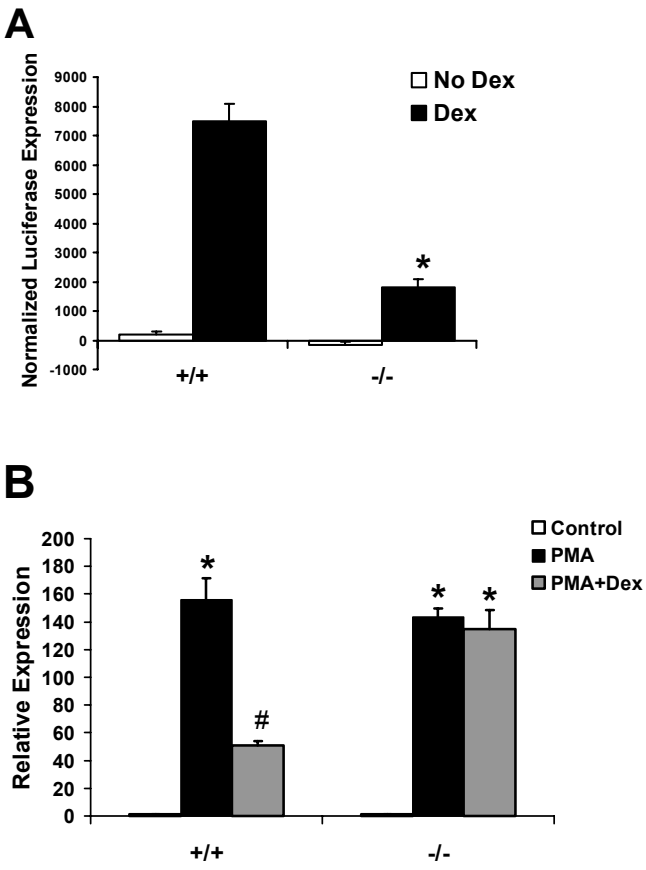
A
Normalized Luciferase Expression
9000
8000
7000
6000
5000
4000
3000
2000
1000
0
-1000
No Dex
Dex
*
+/+
-/-
B
Relative Expression
200
180
160
140
120
100
80
60
40
20
0
Control
PMA
PMA+Dex
*
#
*
*
+/+
-/-

Figure 2.10. Loss of cPGES/p23 results in defective GR transcriptional activation and protein-protein tethering mechanisms. A) Transformed fibroblasts were transfected with the reporters pGRE-luc or pTAL-luc (negative control) and pCMV-β to normalize for transfection efficiency. The transfected fibroblasts were incubated in the presence or absence of dexamethasone (10 nM) for 24hr. Luciferase and β-galactosidase expression were measured in the cell lysates. The luciferase values were normalized to the β-galactosidase values, and the values obtained from the fibroblasts transfected with the negative control (pTAL-luc) were subtracted from the values obtained from the fibroblasts transfected with pGRE-luc (3 replicates for each treatment and genotype). As expected, dexamethasone treatment resulted in a significant increase in luciferase expression in the wild-type fibroblasts. This induction was significantly attenuated in the fibroblasts lacking cPGES/p23. * $p < .01$. This data is representative of three independent experiments performed with two different cell cultures per genotype.

B) Treatment of embryonic fibroblasts with PMA (10^{-7} M for 6 hr.), which induces transcription of genes via AP-1, increased expression of collagenase-3 in both wild-type and cPGES/p23$^{-/-}$ cultures. However, subsequent treatment with dexamethasone (10^{-6} M for 6hr.) and PMA disrupts induction of this gene in wild-type but not in the cPGES/p23$^{-/-}$ fibroblasts. RT-PCR analysis was used to determine expression levels of collagenase-3 in total RNA isolated from the treated fibroblasts. Expression levels were normalized to β-actin, an endogenous control, and the results were expressed as fold change relative to untreated controls. Data is representative of two independent experiments with different MEF cultures. $n = 3$, * $p < .05$ compared to controls, # $p < .05$ compared to all groups by the Tukey-Kramer test for multiple comparisons.

Figure 2.11

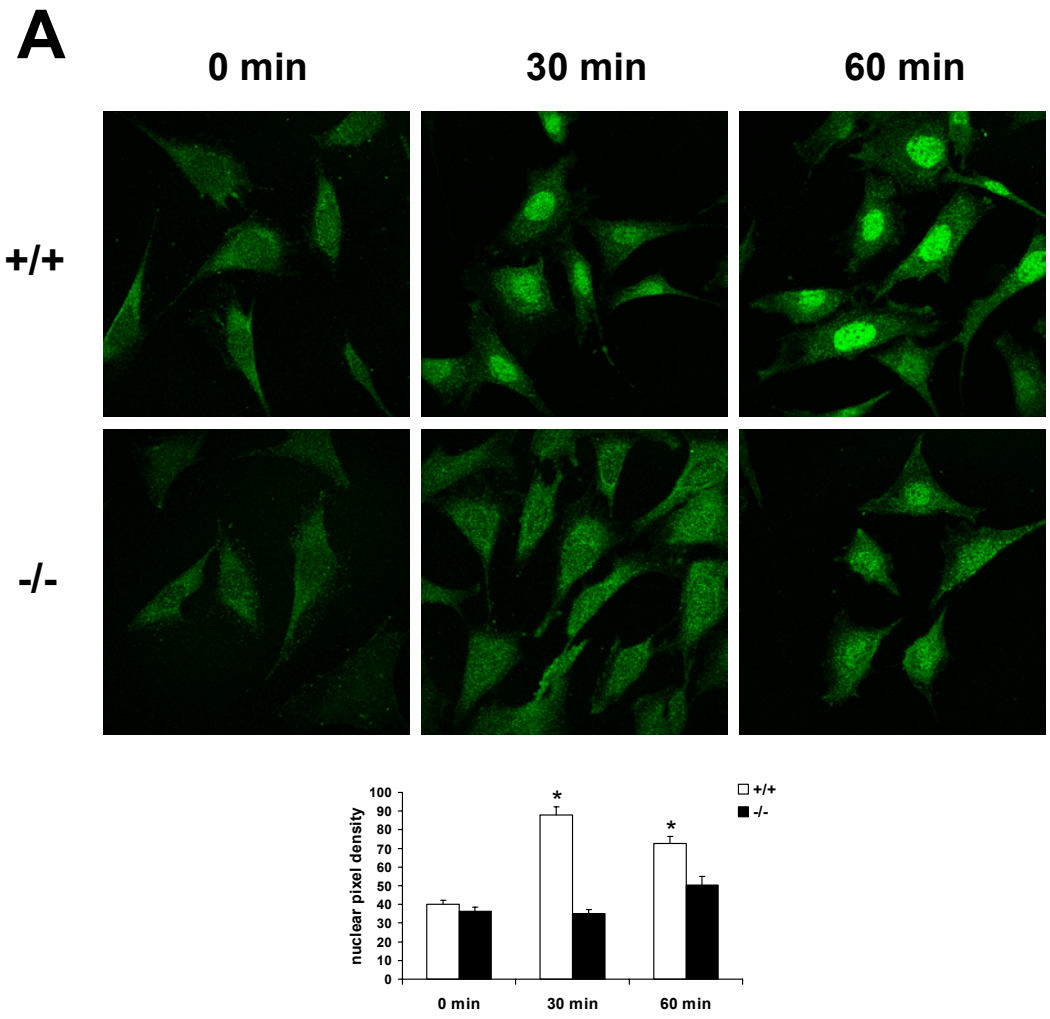
A
0 min
30 min
60 min
+/+
-/-
nuclear pixel density
100
90
80
70
60
50
40
30
20
10
0
*
*
+/+
-/-
0 min
30 min
60 min
B
Nuclear Fraction
+/+
-/-
Cytoplasmic Fraction
+/+
-/-
0 30 60 0 30 60 time (min)
GR
histone H1
1.0 1.5 1.5 1.0 0.9 0.8 fold change
0 30 60 0 30 60 time (min)
GR
α-tubulin
1.0 0.9 0.6 1.0 1.0 0.9 fold change

Figure 2.11. Defective nuclear translocation of GR in cPGES/p23$^{-/-}$ fibroblasts. A) Immunofluorescent staining of transformed fibroblasts for GR after treatment with dexamethasone demonstrates defective translocation in the cPGES/p23$^{-/-}$ fibroblasts. Fibroblasts were treated with dexamethasone (10nM) for 0, 30, and 60 minutes in serum-free medium. Software (ImageJ, NIH) was used to determine the mean pixel density of the nucleus of representative cells in each culture. $n = 12$; * $p < .05$ compared to all other groups by the Tukey-Kramer test for multiple comparisons. B) Western blot analysis demonstrates increases in GR in the nucleus and decreases in GR in the cytoplasm after dexamethasone stimulation (10nM) for 0, 30, and 60 minutes in the wild-type fibroblasts. No alterations in GR localization are observed in the cPGES/p23$^{-/-}$ fibroblasts after stimulation. Sample loading was verified by expression of α- tubulin for the cytoplasmic fraction and histone H1 for the nuclear fraction. Fold change was determined by densitometric analysis and normalized to the loading controls.

DISCUSSION

We show that cPGES/p23 is essential for progression of lung development from the early to the late canalicular stage and that pups lacking cPGES/p23 die in the perinatal period as a result of neonatal respiratory insufficiency. Loss of cPGES/p23 results in delayed maturation of the skin. cPGES/p23$^{-/-}$ pups also fail to induce high levels of gluconeogenic enzymes in the prenatal period. These phenotypes are consistent with the proposed function of cPGES/p23 as an Hsp90 co-chaperone essential for stabilization of GR. However, the cPGES/p23$^{-/-}$ embryos are smaller in size, and primary cultures of embryonic fibroblast show decreased proliferation. As these phenotypes are not observed in the GR-deficient mice, they likely define cPGES/p23 functions that are independent of GR. Evaluation of prostaglandin production in the cPGES/p23$^{-/-}$ embryos and in the embryo-derived primary fibroblasts does not support a direct role for cPGES/p23 in PGE_2 synthesis.

We noted differences in the terminal differentiation of the skin of the cPGES/p23$^{-/-}$ pups. In all mice, a severe deficiency in the cornification of the epithelium was noted both at 17.5 and 18.5 days gestation. However, at 17.5 days, the skin of the cPGES/p23$^{-/-}$ mice was also deficient in granulocytes, while this stratum was easily identified in wild-type mice. Interestingly, previous studies have shown that injection of glucocorticoids accelerate the functional, morphological, and lipid biochemical maturation of the permeability barrier of the skin (1). Later studies of the glucocorticoid-deficient animals supported the role of this hormone in the differentiation of this organ (20). Similar to the cPGES/p23$^{-/-}$ mice, differences between the wild-type and mutant animals were more pronounced earlier in development. At E17.5, neither a well-defined granular layer nor a stratum corneum was evident by light microscopy in the glucocorticoid-deficient fetuses; however, these deficits

diminished later in gestation. Taken together, this suggests that the alterations in differentiation of the skin of the cPGES/p23$^{-/-}$ mice are likely the consequence of loss of GR function.

Morphologically the lungs of the cPGES/p23 full-term embryos resemble those of the early canalicular stage of development (E16.5). Most notable is the absence of the terminal saccules characteristic of the full-term embryo. Examination of the ultrastructure of the lung and analysis of the expression of genes specific to distinct populations of airway epithelia indicates normal development of the airways, likely attenuated differentiation and/or maturation of type II AECs, and little to no differentiation of type I AECs from type II precursors. This phenotype is very similar to that described for GR-deficient mice. A GR hypomorphic (GR^{hypo}) mouse line, with extremely low levels of GR activity, was generated from ES cells in which the neomycin marker gene was inserted into exon 2 by homologous recombination (8, 63). While 10% of theses hypomorphs survive on a mixed genetic background, the co-isogenic 129 die of respiratory insufficiency in the immediate perinatal period. Similar to the cPGES/p23$^{-/-}$ pups, the lungs of these pups had failed to complete the final stages of maturation, and their architecture was comparable to that of an E16.5 embryo. However, unlike the cPGES/p23$^{-/-}$ embryonic lung, some type I AECs were identified in the GR^{hypo} lungs. Two possible explanations for these differences noted in the differentiation of the lungs and survival of the GR and cPGES/p23$^{-/-}$ mice are possible. First, this difference may reflect a GR-independent cPGES/p23 function in lung development. cPGES/p23 may play a role in stabilizing other Hsp90 clients, such as the retinoic acid receptor and the estrogen receptor, and many of these have documented roles in lung development (21, 28, 46, 74). An alternate possibility is that analysis of the GR^{hypo} mice may reflect residual activity

of the GR in these animals compared to the cPGES/p23$^{-/-}$ animals. Mice carrying a deletion of the second or third exon have a more severe phenotype with no animals surviving the perinatal period (GR^{null}); however, a detailed description of the lung phenotype, as in the GR^{hypo} mice, has not been described for these mice (5, 63). Final determination of whether GR-independent cPGES/p23 pathways contribute to lung development will require the direct comparison of congenic GR^{null} animals and cPGES/p23$^{-/-}$ animals under identical breeding and experimental conditions. However, the remarkable similarities in the phenotype of the GR^{hypo} and cPGES/p23$^{-/-}$ animals is consistent with the hypothesis that cPGES/p23 is essential for GR actions during lung development and that the failure of the cPGES/p23$^{-/-}$ lungs to mature reflects primarily the loss of this function of cPGES/p23.

The GR-regulated pathways critical for lung development have not been identified. Interestingly, a recent study showed that GR-deficient mice fail to downregulate the expression of midkine (MK), a heparin-binding growth/differentiation factor, which plays a role in mesenchymal-epithelial interactions during organogenesis (26, 27, 35). The expression pattern of MK during lung development is complex, but expression is dramatically reduced during sacculation of the lung at day 17 of gestation. It has been suggested that the decrease in expression of MK signals the lung to initiate maturation including the thinning of the mesenchyme critical to this stage of development (36). The high levels of MK in the lungs of E18.5 GR-deficient embryos are also observed in the cPGES/p23-deficient embryos. This continued expression of MK in the cPGES/p23$^{-/-}$ embryos supports the hypothesis that the failure to observe normal transition from the canalicular stage to the saccular stage of lung development is secondary to the loss of GR activity in the cPGES/p23$^{-/-}$ embryos.

The GR modulates gene expression through both DNA-binding-dependant and -independent mechanisms. The relative importance of these two pathways in development has been determined by generation of mice expressing a mutant GR (GR^{dim}) (52). This mutation prevents dimerization of the receptor, binding of the receptor to GRE sites in promoters, and transactivation of genes. Study of these mice showed that lung maturation requires DNA-binding-independent regulatory functions of GR since GR^{dim} mice survive into adulthood and have no severe respiratory defects. The cPGES/$p23^{-/-}$ mice die at birth, with a phenotype similar to that of the GR^{hypo} mice, indicating that cPGES/p23 is important in regulating the GR in its DNA-binding-independent processes. In contrast, similar to the GR-deficient mice, gluconeogenic enzymes are not induced in the post-natal period in GR^{dim} mice demonstrating that expression of these genes is dependant on DNA binding and transactivation (40). The loss of expression of glucose-6-phosphatase and serine dehydratase in the livers from full-term cPGES/$p23^{-/-}$ pups indicates that cPGES/p23 is essential for the prenatal activation of enzymes involved in gluconeogenesis. Again, the most likely interpretation of this phenotype is that cPGES/p23 is required for the stabilization of the GR receptor conformation required for ligand binding, subsequent nuclear translocation, and transactivation. Consistent with this, we show that the glucocorticoid dexamethasone failed to induce GRE-dependant expression of reporter genes in fibroblast lines established from the cPGES/p23-deficient mice. Our studies also indicate that cPGES/p23 is essential for the regulation of AP-1 by GR, a function that is not lost in the GR^{dim} mice and thus is a DNA-binding-independent function. Furthermore, we demonstrate that the loss of both DNA-binding-dependent and -independent mechanisms is due to the requirement of cPGES/p23 for the translocation of GR to the nucleus.

The cPGES/p23$^{-/-}$ pups are approximately 10% smaller in size than wild-type pups. No similar defect has been reported for GR-deficient pups, neither the GR^{hypo} or the GR^{null} lines, suggesting this growth retardation is not the result of decreased GR activity (5, 8). Primary fibroblasts derived from the cPGES/p23$^{-/-}$ embryos have a decreased rate of proliferation. Again, a similar defect has not been reported for the GR-deficient primary fibroblasts. In fact, addition of glucocorticoids to fibroblast cultures has been shown to inhibit proliferation (50, 71). cPGES/p23 together with Hsp90 has been implicated in a number of pathways which, if dysfunctional, could alter growth, cell cycle transition, and senescence of cells (3, 34, 39, 49). For example, the *Saccharomyces cerevisiae* homologue of p23, Sba1, and Wos2, the *Saccharomyces pombe* homologue, together with the corresponding Hsp90 analogues have been shown to regulate Cdc2, a protein kinase involved in mitotic control (37). A possible role for cPGES/p23 and Hsp90 in the function of telomerase has also been reported (22). However, it is unlikely that dysfunction of this complex would manifest itself in the first generation of the cPGES/p23$^{-/-}$ pups. Mouse chromosomes possess much longer telomeres than human cells, and several generations of breeding are required before loss of telomerase activity results in altered growth of mice (6). Additional studies will be required to fully characterize the role of cPGES/p23 in growth and proliferation.

cPGES/p23 was independently identified as a cytosolic protein with GSH-dependant PGE_2 synthase activity. The identification was based not only on the activity of protein purified from cellular extracts but also on the increase in PGE_2 production by cells co-transfected with a cDNA encoding this protein and COX-1 (60). This led to the hypothesis that the cPGES/COX1 pathway was responsible for the production of PGE_2 detected in mice

and cell lines lacking mPGES1 (62). Analysis of the cPGES/p23$^{-/-}$ mice fails to support the hypothesis that cPGES/p23 is a bona fide PGE_2 synthase. While loss of cPGES/p23 altered PGE_2 production, a corresponding alteration in the production of other COX-dependant prostanoids suggests a more complex and indirect role for cPGES/p23 in this pathway.

Our demonstration that cPGES/p23 is essential for the non-DNA-binding actions of GR and extensive studies documenting a role for GR in regulation of the arachidonic acid pathway provides an explanation for our results as well as the assignment of a synthase function to this protein. A number of negative regulatory targets for GR in the arachidonic acid pathway have been identified including lipocortin-1 and p11, proteins capable of modifying the release of arachidonic from membrane phospholipids (11, 77). The primary enzyme responsible for the release of arachadonic acid from the membrane for metabolism by the prostanoid pathway is $cPLA_2$ (4, 17). Glucocorticoids have been shown to inhibit the expression and activity of this protein during inflammatory responses (13, 23, 42). Glucocorticoids have also been shown to reduce COX-2 activity in cells by decreasing COX-2 transcription via tethering of transcription factors, such as NF-κB, essential for induction of this gene during inflammation (40-42, 51). Furthermore, post-transcriptional and translational regulation of COX-2 activity have been reported (29, 43, 44). Consistent with our studies of primary embryonic fibroblasts, decreased GR activity secondary to loss of cPGES/p23 would result in loss of this inhibitory pathway resulting in an increase in PGE_2 and other COX-2-dependant metabolites. Transfection of cell lines with p23 expression vectors has been reported, similar to loss of cPGES/p23, to result in inhibition of GR activity in cells lines (16, 73). This raises the possibility that the increased PGE_2 production noted in

cells transfected with cPGES/p23 was the indirect consequence of decreased GR function in this line.

Interestingly, the impact of loss of cPGES/p23 on prostanoid production by fetal tissues was very different from that observed with cultured cells. Here loss of this protein resulted in decreased levels of PGE_2 and other COX-dependant prostanoids. A number of possible explanations can be proposed. First, the ability of GR to stimulate the production of prostanoids in specific cell types has been reported, particularily in primary amniotic fibroblasts (15, 58, 78). These studies show that dexamethasone increases expression of both $cPLA_2$ and COX-2 in these cells. Consistent with this finding, prenatal dexamethasone increased prostaglandin synthesis in rat fetal lung (64). Potential GRE elements have been defined in the COX-2 and $cPLA_2$ promoters which may play a role in the induction of gene transcription (61, 75). It is interesting to speculate that, in the mouse embryo, glucocorticoids, which increase in levels as gestation progress, contribute to the increase in prostaglandin production observed late in gestation. Alternatively, the diminished prostanoid production might be the indirect consequence of alterations in development of the cPGES/p23$^{-/-}$ embryos. Finally, the decreases in prostanoids in the cPGES/p23$^{-/-}$ mice may reflect an, as of yet unidentified GR-independent function for cPGES/p23 in regulation of the arachidonic acid pathway. For example, cPGES/p23 has been shown to facilitate signaling of the aryl hydrocarbon receptor which in turn modulates the COX-2 pathway (10, 69). While additional experiments will be necessary to address these questions, taken together our data does not support the designation of cPGES/p23 as the third PGE_2 synthase, cPGES, and we suggest that this protein simply be referred to as p23.

While this manuscript was in preparation, Grad *et al.* reported the generation of mice from the identical ES cell clone carrying an insertional mutation in the *cPGES/p23* gene (19). A similar defect in lung and skin development was noted, and co-transfection of a GR reporter construct and a GR-expressing construct in fibroblasts derived from the embryos demonstrated decreased GR-dependant transcription. In contrast to the results shown here, the growth retardation of the pups and decreased proliferation in the primary fibroblasts were not noted in these studies. We also report the defective induction of gluconeogenic enzymes and decreased glycogen accumulation in the fetal livers. In addition, we show that the ability of GR to regulate the activity of other transcription factors, namely AP-1, is dependant on expression of p23. These deficiencies, as well as decreased expression of genes involved in lung development, suggests a role for p23 in both the DNA-binding-dependent and -independent mechanisms of GR. Lastly, our analysis of prostanoids in the p23-deficient animals and primary fibroblasts failed to support a role for this protein as a PGE_2 synthase.

ACKNOWLEDGMENTS

The authors thank Anne Latour, Leigh Jania, MyTrang Nguyen, and Subhashini Chandrashekaran for their technical assistance and helpful discussions, Jay Snouwaert for designing the probe for Southern blot analysis, and Bob Bagnell and Victoria Madden at UNC Microscopy Services.

This work was supported by National Institutes of Health grants HL-68141 (B.H. Koller) and American Heart Association grant 0415427U (A. Kern Lovgren).

REFERENCES

1. Aszterbaum, M., K. R. Feingold, G. K. Menon, and M. L. Williams. 1993. Glucocorticoids accelerate fetal maturation of the epidermal permeability barrier in the rat. J Clin Invest 91:2703-8.

2. Beaudry, J. B., C. E. Pierreux, G. P. Hayhurst, N. Plumb-Rudewiez, M. C. Weiss, G. G. Rousseau, and F. P. Lemaigre. 2006. Threshold levels of hepatocyte nuclear factor 6 (HNF-6) acting in synergy with HNF-4 and PGC-1alpha are required for time-specific gene expression during liver development. Mol Cell Biol 26:6037-46.

3. Betsholtz, C., L. Karlsson, and P. Lindahl. 2001. Developmental roles of platelet-derived growth factors. Bioessays 23:494-507.

4. Bonventre, J. V., Z. Huang, M. R. Taheri, E. O'Leary, E. Li, M. A. Moskowitz, and A. Sapirstein. 1997. Reduced fertility and postischaemic brain injury in mice deficient in cytosolic phospholipase A2. Nature 390:622-5.

5. Brewer, J. A., O. Kanagawa, B. P. Sleckman, and L. J. Muglia. 2002. Thymocyte apoptosis induced by T cell activation is mediated by glucocorticoids in vivo. J Immunol 169:1837-43.

6. Chang, S. 2005. Modeling aging and cancer in the telomerase knockout mouse. Mutat Res 576:39-53.

7. Cole, T. J., J. A. Blendy, A. P. Monaghan, K. Krieglstein, W. Schmid, A. Aguzzi, G. Fantuzzi, E. Hummler, K. Unsicker, and G. Schutz. 1995. Targeted disruption of the glucocorticoid receptor gene blocks adrenergic chromaffin cell development and severely retards lung maturation. Genes Dev 9:1608-21.

8. Cole, T. J., N. M. Solomon, R. Van Driel, J. A. Monk, D. Bird, S. J. Richardson, R. J. Dilley, and S. B. Hooper. 2004. Altered epithelial cell proportions in the fetal lung of glucocorticoid receptor null mice. Am J Respir Cell Mol Biol 30:613-9.

9. Costa, R. H., V. V. Kalinichenko, and L. Lim. 2001. Transcription factors in mouse lung development and function. Am J Physiol Lung Cell Mol Physiol 280:L823-38.

10. Cox, M. B., and C. A. Miller, 3rd. 2002. The p23 co-chaperone facilitates dioxin receptor signaling in a yeast model system. Toxicol Lett 129:13-21.

11. Croxtall, J. D., Q. Choudhury, H. Tokumoto, and R. J. Flower. 1995. Lipocortin-1 and the control of arachidonic acid release in cell signalling. Glucocorticoids (changed from glucorticoids) inhibit G protein-dependent activation of cPLA2 activity. Biochem Pharmacol 50:465-74.

12. Dittmar, K. D., D. R. Demady, L. F. Stancato, P. Krishna, and W. B. Pratt. 1997. Folding of the glucocorticoid receptor by the heat shock protein (hsp) 90-based chaperone machinery. The role of p23 is to stabilize receptor.hsp90 heterocomplexes formed by hsp90.p60.hsp70. J Biol Chem 272:21213-20.

13. Dolan-O'keefe, M., and H. S. Nick. 1999. Inhibition of cytoplasmic phospholipase A2 expression by glucocorticoids in rat intestinal epithelial cells. Gastroenterology 116:855-64.

14. Durant, S., D. Duval, and F. Homo-Delarche. 1988. Mouse embryo fibroblasts in culture: characteristics of arachidonic acid metabolism during early passages. Prostaglandins Leukot Essent Fatty Acids 32:129-37.

15. Economopoulos, P., M. Sun, B. Purgina, and W. Gibb. 1996. Glucocorticoids stimulate prostaglandin H synthase type-2 (PGHS-2) in the fibroblast cells in human amnion cultures. Mol Cell Endocrinol 117:141-7.

16. Freeman, B. C., and K. R. Yamamoto. 2002. Disassembly of transcriptional regulatory complexes by molecular chaperones. Science 296:2232-5.

17. Fujishima, H., R. O. Sanchez Mejia, C. O. Bingham, 3rd, B. K. Lam, A. Sapirstein, J. V. Bonventre, K. F. Austen, and J. P. Arm. 1999. Cytosolic phospholipase A2 is essential for both the immediate and the delayed phases of eicosanoid generation in mouse bone marrow-derived mast cells. Proc Natl Acad Sci U S A 96:4803-7.

18. Girard, J., P. Ferre, J. P. Pegorier, and P. H. Duee. 1992. Adaptations of glucose and fatty acid metabolism during perinatal period and suckling-weaning transition. Physiol Rev 72:507-62.

19. Grad, I., T. A. McKee, S. M. Ludwig, G. W. Hoyle, P. Ruiz, W. Wurst, T. Floss, C. A. Miller, 3rd, and D. Picard. 2006. The Hsp90 Cochaperone p23 Is Essential for Perinatal Survival. Mol Cell Biol 26:8976-83.

20. Hanley, K., K. R. Feingold, L. G. Komuves, P. M. Elias, L. J. Muglia, J. A. Majzoub, and M. L. Williams. 1998. Glucocorticoid deficiency delays stratum corneum maturation in the fetal mouse. J Invest Dermatol 111:440-4.

21. Holley, S. J., and K. R. Yamamoto. 1995. A role for Hsp90 in retinoid receptor signal transduction. Mol Biol Cell 6:1833-42.

22. Holt, S. E., D. L. Aisner, J. Baur, V. M. Tesmer, M. Dy, M. Ouellette, J. B. Trager, G. B. Morin, D. O. Toft, J. W. Shay, W. E. Wright, and M. A. White. 1999. Functional requirement of p23 and Hsp90 in telomerase complexes. Genes Dev 13:817-26.

23. Hong, S. L., and L. Levine. 1976. Inhibition of arachidonic acid release from cells as the biochemical action of anti-inflammatory corticosteroids. Proc Natl Acad Sci U S A 73:1730-4.

24. Jakobsson, P. J., S. Thoren, R. Morgenstern, and B. Samuelsson. 1999. Identification of human prostaglandin E synthase: a microsomal, glutathione-dependent, inducible enzyme, constituting a potential novel drug target. Proc Natl Acad Sci U S A 96:7220-5.

25. Johnson, J. L., T. G. Beito, C. J. Krco, and D. O. Toft. 1994. Characterization of a novel 23-kilodalton protein of unactive progesterone receptor complexes. Mol Cell Biol 14:1956-63.

26. Kadomatsu, K., R. P. Huang, T. Suganuma, F. Murata, and T. Muramatsu. 1990. A retinoic acid responsive gene MK found in the teratocarcinoma system is expressed in spatially and temporally controlled manner during mouse embryogenesis. J Cell Biol 110:607-16.

27. Kaplan, F., J. Comber, R. Sladek, T. J. Hudson, L. J. Muglia, T. Macrae, S. Gagnon, M. Asada, J. A. Brewer, and N. B. Sweezey. 2003. The growth factor midkine is modulated by both glucocorticoid and retinoid in fetal lung development. Am J Respir Cell Mol Biol 28:33-41.

28. Knoblauch, R., and M. J. Garabedian. 1999. Role for Hsp90-associated cochaperone p23 in estrogen receptor signal transduction. Mol Cell Biol 19:3748-59.

29. Lasa, M., M. Brook, J. Saklatvala, and A. R. Clark. 2001. Dexamethasone destabilizes cyclooxygenase 2 mRNA by inhibiting mitogen-activated protein kinase p38. Mol Cell Biol 21:771-80.

30. Liggins, G. C. 1969. Premature delivery of foetal lambs infused with glucocorticoids. J Endocrinol 45:515-23.

31. Loftin, C. D., D. B. Trivedi, H. F. Tiano, J. A. Clark, C. A. Lee, J. A. Epstein, S. G. Morham, M. D. Breyer, M. Nguyen, B. M. Hawkins, J. L. Goulet, O. Smithies, B. H. Koller, and R. Langenbach. 2001. Failure of ductus arteriosus closure and remodeling in neonatal mice deficient in cyclooxygenase-1 and cyclooxygenase-2. Proc Natl Acad Sci U S A 98:1059-64.

32. McDevitt, T. M., L. Gonzales, R. C. Savani, and P. L. Ballard. 2006. Role of Endogenous TGF-{beta} in Glucocorticoid-Induced Lung Type II Cell Differentiation. Am J Physiol Lung Cell Mol Physiol.

33. Mendelson, C. R. 2000. Role of transcription factors in fetal lung development and surfactant protein gene expression. Annu Rev Physiol 62:875-915.

34. Miettinen, P. J., J. E. Berger, J. Meneses, Y. Phung, R. A. Pedersen, Z. Werb, and R. Derynck. 1995. Epithelial immaturity and multiorgan failure in mice lacking epidermal growth factor receptor. Nature 376:337-41.

35. Mitsiadis, T. A., T. Muramatsu, H. Muramatsu, and I. Thesleff. 1995. Midkine (MK), a heparin-binding growth/differentiation factor, is regulated by retinoic acid and epithelial-mesenchymal interactions in the developing mouse tooth, and affects cell proliferation and morphogenesis. J Cell Biol 129:267-81.

36. Morrisey, E. E., and R. C. Savani. 2003. Midkine: a potential bridge between glucocorticoid and retinoid effects on lung vascular development. Am J Respir Cell Mol Biol 28:5-8.

37. Munoz, M. J., E. R. Bejarano, R. R. Daga, and J. Jimenez. 1999. The identification of Wos2, a p23 homologue that interacts with Wee1 and Cdc2 in the mitotic control of fission yeasts. Genetics 153:1561-72.

38. Murakami, M., K. Nakashima, D. Kamei, S. Masuda, Y. Ishikawa, T. Ishii, Y. Ohmiya, K. Watanabe, and I. Kudo. 2003. Cellular prostaglandin E2 production by membrane-bound prostaglandin E synthase-2 via both cyclooxygenases-1 and -2. J Biol Chem 278:37937-47.

39. Nakamura, S., H. Watanabe, M. Miura, and T. Sasaki. 1997. Effect of the insulin-like growth factor I receptor on ionizing radiation-induced cell death in mouse embryo fibroblasts. Exp Cell Res 235:287-94.

40. Newton, R. 2000. Molecular mechanisms of glucocorticoid action: what is important? Thorax 55:603-13.

41. Newton, R., L. M. Kuitert, M. Bergmann, I. M. Adcock, and P. J. Barnes. 1997. Evidence for involvement of NF-kappaB in the transcriptional control of COX-2 gene expression by IL-1beta. Biochem Biophys Res Commun 237:28-32.

42. Newton, R., L. M. Kuitert, D. M. Slater, I. M. Adcock, and P. J. Barnes. 1997. Cytokine induction of cytosolic phospholipase A2 and cyclooxygenase-2 mRNA is suppressed by glucocorticoids in human epithelial cells. Life Sci 60:67-78.

43. Newton, R., J. Seybold, L. M. Kuitert, M. Bergmann, and P. J. Barnes. 1998. Repression of cyclooxygenase-2 and prostaglandin E2 release by dexamethasone occurs by transcriptional and post-transcriptional mechanisms involving loss of polyadenylated mRNA. J Biol Chem 273:32312-21.

44. Newton, R., J. Seybold, S. F. Liu, and P. J. Barnes. 1997. Alternate COX-2 transcripts are differentially regulated: implications for post-transcriptional control. Biochem Biophys Res Commun 234:85-9.

45. Nguyen, M., T. Camenisch, J. N. Snouwaert, E. Hicks, T. M. Coffman, P. A. Anderson, N. N. Malouf, and B. H. Koller. 1997. The prostaglandin receptor EP4 triggers remodelling of the cardiovascular system at birth. Nature 390:78-81.

46. Patrone, C., T. N. Cassel, K. Pettersson, Y. S. Piao, G. Cheng, P. Ciana, A. Maggi, M. Warner, J. A. Gustafsson, and M. Nord. 2003. Regulation of postnatal lung development and homeostasis by estrogen receptor beta. Mol Cell Biol 23:8542-52.

47. Pfahl, M. 1993. Nuclear receptor/AP-1 interaction. Endocr Rev 14:651-8.

48. Pratt, W. B. 1998. The hsp90-based chaperone system: involvement in signal transduction from a variety of hormone and growth factor receptors. Proc Soc Exp Biol Med 217:420-34.

49. Pratt, W. B., and D. O. Toft. 2003. Regulation of signaling protein function and trafficking by the hsp90/hsp70-based chaperone machinery. Exp Biol Med (Maywood) 228:111-33.

50. Ramalingam, A., A. Hirai, and E. A. Thompson. 1997. Glucocorticoid inhibition of fibroblast proliferation and regulation of the cyclin kinase inhibitor p21Cip1. Mol Endocrinol 11:577-86.

51. Ray, A., and K. E. Prefontaine. 1994. Physical association and functional antagonism between the p65 subunit of transcription factor NF-kappa B and the glucocorticoid receptor. Proc Natl Acad Sci U S A 91:752-6.

52. Reichardt, H. M., K. H. Kaestner, J. Tuckermann, O. Kretz, O. Wessely, R. Bock, P. Gass, W. Schmid, P. Herrlich, P. Angel, and G. Schutz. 1998. DNA binding of the glucocorticoid receptor is not essential for survival. Cell 93:531-41.

53. Rochelle, L. G., D. C. Li, H. Ye, E. Lee, C. R. Talbot, and R. C. Boucher. 2000. Distribution of ion transport mRNAs throughout murine nose and lung. Am J Physiol Lung Cell Mol Physiol 279:L14-24.

54. Salaun, B., B. de Saint-Vis, N. Pacheco, Y. Pacheco, A. Riesler, S. Isaac, C. Leroux, V. Clair-Moninot, J. J. Pin, J. Griffith, I. Treilleux, S. Goddard, J. Davoust, M. Kleijmeer, and S. Lebecque. 2004. CD208/dendritic cell-lysosomal associated membrane protein is a marker of normal and transformed type II pneumocytes. Am J Pathol 164:861-71.

55. Smith, D. F., L. E. Faber, and D. O. Toft. 1990. Purification of unactivated progesterone receptor and identification of novel receptor-associated proteins. J Biol Chem 265:3996-4003.

56. Snyder, J. M., H. F. Rodgers, J. A. O'Brien, N. Mahli, S. A. Magliato, and P. L. Durham. 1992. Glucocorticoid effects on rabbit fetal lung maturation in vivo: an ultrastructural morphometric study. Anat Rec 232:133-40.

57. Stryke, D., M. Kawamoto, C. C. Huang, S. J. Johns, L. A. King, C. A. Harper, E. C. Meng, R. E. Lee, A. Yee, L. L'Italien, P. T. Chuang, S. G. Young, W. C. Skarnes, P. C. Babbitt, and T. E. Ferrin. 2003. BayGenomics: a resource of insertional mutations in mouse embryonic stem cells. Nucleic Acids Res 31:278-81.

58. Sun, K., R. Ma, X. Cui, B. Campos, R. Webster, D. Brockman, and L. Myatt. 2003. Glucocorticoids induce cytosolic phospholipase A2 and prostaglandin H synthase type 2 but not microsomal prostaglandin E synthase (PGES) and cytosolic PGES expression in cultured primary human amnion cells. J Clin Endocrinol Metab 88:5564-71.

59. Tanikawa, N., Y. Ohmiya, H. Ohkubo, K. Hashimoto, K. Kangawa, M. Kojima, S. Ito, and K. Watanabe. 2002. Identification and characterization of a novel type of membrane-associated prostaglandin E synthase. Biochem Biophys Res Commun 291:884-9.

60. Tanioka, T., Y. Nakatani, N. Semmyo, M. Murakami, and I. Kudo. 2000. Molecular identification of cytosolic prostaglandin E2 synthase that is functionally coupled with cyclooxygenase-1 in immediate prostaglandin E2 biosynthesis. J Biol Chem 275:32775-82.

61. Tazawa, R., X. M. Xu, K. K. Wu, and L. H. Wang. 1994. Characterization of the genomic structure, chromosomal location and promoter of human prostaglandin H synthase-2 gene. Biochem Biophys Res Commun 203:190-9.

62. Trebino, C. E., J. L. Stock, C. P. Gibbons, B. M. Naiman, T. S. Wachtmann, J. P. Umland, K. Pandher, J. M. Lapointe, S. Saha, M. L. Roach, D. Carter, N. A. Thomas, B. A. Durtschi, J. D. McNeish, J. E. Hambor, P. J. Jakobsson, T. J. Carty, J. R. Perez, and L. P. Audoly. 2003. Impaired inflammatory and pain responses in mice lacking an inducible prostaglandin E synthase. Proc Natl Acad Sci U S A 100:9044-9.

63. Tronche, F., C. Kellendonk, H. M. Reichardt, and G. Schutz. 1998. Genetic dissection of glucocorticoid receptor function in mice. Curr Opin Genet Dev 8:532-8.

64. Tsai, M. Y., M. W. Josephson, B. Handschin, and D. M. Brown. 1983. The effect of prenatal dexamethasone on fetal rat lung prostaglandin synthesis. Prostaglandins Leukot Med 11:171-7.

65. Uematsu, S., M. Matsumoto, K. Takeda, and S. Akira. 2002. Lipopolysaccharide-dependent prostaglandin E(2) production is regulated by the glutathione-dependent prostaglandin E(2) synthase gene induced by the Toll-like receptor 4/MyD88/NF-IL6 pathway. J Immunol 168:5811-6.

66. Vander Kooi, B. T., H. Onuma, J. K. Oeser, C. A. Svitek, S. R. Allen, C. W. Vander Kooi, W. J. Chazin, and R. M. O'Brien. 2005. The glucose-6-phosphatase catalytic subunit gene promoter contains both positive and negative glucocorticoid response elements. Mol Endocrinol 19:3001-22.

67. Vanstapel, F., F. Dopere, and W. Stalmans. 1980. The role of glycogen synthase phosphatase in the glucocorticoid-induced deposition of glycogen in foetal rat liver. Biochem J 192:607-12.

68. Venkatesh, V. C., and H. D. Katzberg. 1997. Glucocorticoid regulation of epithelial sodium channel genes in human fetal lung. Am J Physiol 273:L227-33.

69. Vogel, C., A. M. Boerboom, C. Baechle, C. El-Bahay, R. Kahl, G. H. Degen, and J. Abel. 2000. Regulation of prostaglandin endoperoxide H synthase-2 induction by dioxin in rat hepatocytes: possible c-Src-mediated pathway. Carcinogenesis 21:2267-74.

70. Wallace, M. J., S. B. Hooper, and R. Harding. 1995. Effects of elevated fetal cortisol concentrations on the volume, secretion, and reabsorption of lung liquid. Am J Physiol 269:R881-7.

71. Wang, Z., and M. J. Garabedian. 2003. Modulation of glucocorticoid receptor transcriptional activation, phosphorylation, and growth inhibition by p27Kip1. J Biol Chem 278:50897-901.

72. Williams, M. C. 2003. Alveolar type I cells: molecular phenotype and development. Annu Rev Physiol 65:669-95.

73. Wochnik, G. M., J. C. Young, U. Schmidt, F. Holsboer, F. U. Hartl, and T. Rein. 2004. Inhibition of GR-mediated transcription by p23 requires interaction with Hsp90. FEBS Lett 560:35-8.

74. Wongtrakool, C., S. Malpel, J. Gorenstein, J. Sedita, M. I. Ramirez, T. M. Underhill, and W. V. Cardoso. 2003. Down-regulation of retinoic acid receptor alpha signaling is required for sacculation and type I cell formation in the developing lung. J Biol Chem 278:46911-8.

75. Wu, T., T. Ikezono, C. W. Angus, and J. H. Shelhamer. 1994. Characterization of the promoter for the human 85 kDa cytosolic phospholipase A2 gene. Nucleic Acids Res 22:5093-8.

76. Yang, H., M. M. Lu, L. Zhang, J. A. Whitsett, and E. E. Morrisey. 2002. GATA6 regulates differentiation of distal lung epithelium. Development 129:2233-46.

77. Yao, X. L., M. J. Cowan, M. T. Gladwin, M. M. Lawrence, C. W. Angus, and J. H. Shelhamer. 1999. Dexamethasone alters arachidonate release from human epithelial

cells by induction of p11 protein synthesis and inhibition of phospholipase A2 activity. J Biol Chem 274:17202-8.

78. Zakar, T., J. J. Hirst, J. E. Mijovic, and D. M. Olson. 1995. Glucocorticoids stimulate the expression of prostaglandin endoperoxide H synthase-2 in amnion cells. Endocrinology 136:1610-9.

79. Zhou, L., L. Lim, R. H. Costa, and J. A. Whitsett. 1996. Thyroid transcription factor-1, hepatocyte nuclear factor-3beta, surfactant protein B, C, and Clara cell secretory protein in developing mouse lung. J Histochem Cytochem 44:1183-93.

CHAPTER 3

COX-2-derived prostacyclin protects against bleomycin-induced pulmonary fibrosis

COX-2-derived Prostacyclin Protects Against Bleomycin-induced Pulmonary Fibrosis

Alysia Kern Lovgren,[1,3] Leigh A. Jania,[3] John M. Hartney,[1,3] Kelly K. Parsons,[1,3] Laurent P. Audoly,[4] Garret A. FitzGerald,[5] Stephen L. Tilley,[2] Beverly H. Koller[1-3]

[1]Curriculum in Genetics and Molecular Biology, [2]Department of Medicine, Division of Pulmonary and Critical Care Medicine, and [3]Department of Genetics, University of North Carolina at Chapel Hill, Chapel Hill, North Carolina 27599-7248; [4]Department of Pharmacology, Merck Frosst Canada, Quebec, Kirkland, Canada; [5]Department of Pharmacology, University of Pennsylvania, Philadelphia, Pennsylvania 19104-6084.

This chapter has been published in the August 2006 issue of the American Journal of Physiology – Lung Cellular and Molecular Physiology. I would like to thank the contributing authors: Leigh Jania for help collecting tissue samples, John Hartney for breeding the mPGES1 mice and establishing the use of the Flexivent in our laboratory, Kelly Parsons for the COX-1 hydroxyproline measurements, Laurent Audoly for supplying the mPGES1 mice, Garret FitzGerald for supplying the IP mice, Stephen Tilley for supplying the EP2 mice, and Bev Koller for her guidance and support.

ABSTRACT

Prostacyclin is one of a number of lipid mediators elaborated from the metabolism of arachidonic acid by the cyclooxygenase (COX) enzymes. This prostanoid is a potent inhibitor of platelet aggregation, and its production by endothelial cells and protective role in the vasculature are well established. In contrast, much less is known regarding the function of this prostanoid in other disease processes. We show here that COX-2-dependent production of prostacyclin plays an important role in the development of fibrotic lung disease, limiting both the development of fibrosis and the consequential alterations in lung mechanics. In stark contrast, loss of prostaglandin E_2 (PGE_2) synthesis and signaling through the G_s-coupled EP2 and EP4 receptors had no effect on the development of disease. These findings suggest that prostacyclin analogues will protect against bleomycin-induced pulmonary fibrosis in COX-$2^{-/-}$ mice. If such protection is observed, investigation of these agents as a novel therapeutic approach to pulmonary fibrosis in humans may be warranted.

INTRODUCTION

Idiopathic pulmonary fibrosis (IPF) is a relentless, progressive, and heterogeneous disease characterized by alternating areas of normal lung, fibrosis, and interstitial inflammation affecting the peripheral subpleural parenchyma (19). Hallmarks of fibrosis include subepithelial myofibroblast/fibroblastic foci and increased deposition of collagen and extracellular matrix. This excess scar tissue causes stiffening of the alveolar walls and a decrease in compliance, which leads to the irreversible loss of total lung capacity and the reduced ability to transport oxygen into the capillaries (1, 19, 38, 47). Prostanoids, COX-dependant arachidonic acid metabolites, have been implicated in the development of pulmonary fibrosis.

Two COX enzymes, COX-1 and COX-2, both capable of converting arachidonic acid into prostaglandin endoperoxide (PGH_2), have been characterized (48). PGH_2 produced by either COX isoenzyme is further metabolized by specific synthases into the various prostanoids, including prostaglandin F_2 (PGF_2), thromboxane, prostaglandin D_2 (PGD_2), prostacyclin, and PGE_2. While many cell types express both COX isoforms and multiple synthases, co-localization of various enzymes allows the metabolite of an enzyme to be directly transferred to a specific synthase for further metabolism. Many examples of cooperation between specific COX isoforms and synthases have been described. COX-1 and thromboxane synthase couple in the production of thromboxane by platelets (41). In contrast, increasing evidence suggests that COX-2 provides PGH_2 for production of prostacyclin by endothelial cells (30, 57). The pathways responsible for production of a particular prostanoid have important clinical implications. For example, the collaboration between COX-1 and thromboxane synthase in the production of thromboxane by platelets

forms the basis for the use of low dose aspirin for prevention of stroke (41). In contrast, dependence of prostanoid production by endothelial cells on COX-2 may result in loss of a critical pool of prostacyclin in patients using COX-2 specific inhibitors, leading to increased risk for cardiac events in high risk patients (7). Another important concept regarding the COX pathway relates to changes in COX expression following cellular stimulation. While constitutive expression of both COX isoforms has been described in certain tissues, COX-2, in contrast to COX-1, is highly inducible (48). As a result, the prostanoid profile of a resting cell can change following activation. For example, COX-1 and thromboxane synthase collaborate in production of thromboxane in resting macrophages. After activation, increased expression of microsomal PGE_2 synthase 1 (mPGES1) and COX-2 parallels a drop in thromboxane production and increased PGE_2 production by these cells (6). Such a shift in prostanoid profiles is believed to be an important protective response under various pathophysiological conditions including pulmonary fibrosis, where lack of PGE_2 is speculated to contribute to disease pathogenesis.

The biosynthesis of PGE_2 is mediated primarily by mPGES1, one of three enzymes capable of catalyzing the conversion of PGH_2 to PGE_2. Both *in vitro* studies and analysis of mice lacking mPGES1 support an important role for this enzyme in PGE_2 synthesis, especially during inflammatory responses (54, 56). Microsomal PGE_2 synthase 2 (mPGES2) and cytosolic PGE_2 synthase (cPGES) increase PGE_2 production when over-expressed in various cell lines (34, 52). However, the contribution of these two enzymes to PGE_2 production *in vivo* has not yet been defined. Similar to most eicosanoids, the half life of PGE_2 *in vivo* is very short due to rapid metabolism by 15-hydroxyprostaglandin

dehydrogenase (PGDH). Important to this study, PGDH is expressed at high levels in the healthy lung and mice lacking this enzyme have elevated lung PGE_2 levels (21).

Prostanoids mediate their actions by binding to G-protein-associated receptors. Thromboxane and prostacyclin each act through a single receptor, termed TP and IP, respectively. TP is G_q-coupled, and activation of this receptor leads to increased intracellular calcium levels while activation of the G_s-coupled IP receptor leads to increased intracellular cAMP. Unlike prostacyclin and thromboxane, PGE_2 binds four different E prostanoid receptors, designated EP1, EP2, EP3, and EP4 (11). These receptors have unique expression patterns and differ in their activation of intracellular signaling pathways. Activation of the EP1 receptor increases intracellular calcium (59). EP2 and EP4 are coupled to G_s and increase intracellular cAMP, although differential activation of downstream signaling components, specifically, MAPK and PI3K, has been noted (43). EP3 has multiple isoforms that can couple to G_i, G_s, or G_q proteins; however, G_i predominates in most systems and decreases cAMP levels (36, 51).

A number of lines of evidence suggest that PGE_2 may play a role in limiting fibrotic responses in the lung and that this pathway may be compromised in patients with pulmonary fibrosis. First, patients with IPF have decreased PGE_2 levels in bronchoalveolar fluid, and fibroblasts taken from these patients have decreased COX-2 expression and reduced PGE_2 production (5, 58, 60). *Ex vivo* studies have shown that PGE_2 can decrease proliferation and suppress collagen synthesis of lung fibroblasts (3, 9, 13, 14, 18, 31). Other studies have shown that PGE_2 is capable of inhibiting fibroblast migration and fibroblast to myofibroblast transition (26, 28). Myofibroblasts express α-smooth muscle actin and have increased collagen gene expression. Thus, the increased number of myofibroblasts is likely to

contribute to the morphological changes as well as the contractile changes of lung parenchyma characteristic of IPF (63, 64). The ability of PGE_2 to alter activity and gene expression of fibroblasts has been attributed to engagement of G_s-coupled receptors, as these actions can be mimicked by agents that elevate cAMP (8, 28). Prostacyclin, which is also capable of increasing cAMP levels in many cell types, including fibroblasts, may also have a role in the development of pulmonary fibrosis. A study on lung fibroblasts from patients with IPF demonstrated decreased levels of prostacyclin production in IPF fibroblasts versus normal fibroblasts (12).

The studies reported here were designed to elucidate the role of prostanoids in fibrotic lung disease *in vivo*. Using the well-established bleomycin mouse model, seven congenic mouse lines deficient in either the metabolism of a prostanoid or in the ability to respond to a prostanoid were examined. In addition to using traditional histological and biochemical methods for evaluation of disease progression, the impact of disease on lung mechanics was also evaluated. Our studies reveal an important role for the COX-2-prostacyclin synthetic pathway in limiting the fibrotic response to bleomycin.

MATERIAL AND METHODS

Experimental Animals

All studies were conducted in accordance with the National Institutes of Health Guide for the Care and Use of Laboratory Animals as well as the Institutional Animal Care and Use Committee guidelines of the University of North Carolina at Chapel Hill. All experiments were carried out using 8-12 week old mice unless otherwise specified. Mice lacking COX-2 (*Ptgs2*), COX-1 (*Ptgs1*), mPGES1 (*Ptges*), PGDH (*Hpgd*), EP2 (*Ptger2*), EP4 (*Ptger4*), and IP (*Ptgir*) were generated as previously described (7, 10, 29, 33, 39, 53, 54). Congenic COX-$1^{-/-}$, $EP2^{-/-}$, and $IP^{-/-}$ mice were generated by backcrossing onto a C57BL/6 background for at least 12 generations. The $PGDH^{-/-}$ mice were backcrossed onto a C57BL/6 background for 7 generations. The mPGES$1^{-/-}$ mice were generated on a DBA/1J genetic background and backcrossed five generations onto a C57BL/6 background. $EP4^{-/-}$ mice only survive on a recombinant inbred background (39). Few COX-$2^{-/-}$ mice survive on the 129Sv/Ev or C57BL/6 genetic background. Most die with a patent ductus arteriosis within 48 hours of birth. COX-$2^{-/-}$ mice were generated by the intercross of 129/SvEv co-isogenic COX-$2^{+/-}$ mice with congenic C57BL/6 COX-$2^{+/-}$ animals (N8). Thus, all offspring, including the COX-$2^{-/-}$ and control COX-$2^{+/+}$ animals generated from these intercrosses will carry maternal 129Sv/Ev alleles and paternal C57BL/6 alleles and will differ only at the COX-2 locus. Animals in different experimental groups were age- and sex-matched for each experiment. Body weights did not differ between the experimental and control mice for all genotypes. Lung mechanics were assessed first in each experimental group, and then the entire lung was removed for either histological analysis or hydroxyproline measurements.

Bleomycin Treatment

Mice were anesthetized with approximately 20µl/g body weight of 2,2,2-tribromoethanol and administered 50 µl of saline or bleomycin (.05U unless specified otherwise) diluted in saline by intratracheal instillation.

Measurements of lung mechanics

Mice were anesthetized 21 days after bleomycin administration with 70-90 mg/kg pentobarbital sodium (American Pharmaceutical Partners, Los Angeles, CA), tracheostomized, and mechanically ventilated at a rate of 350 breaths/min, tidal volume of 6 cc/kg, and positive end-expiratory pressure of 3-4 cm H_2O with a computer-controlled small-animal ventilator (Scireq, Montreal, Canada). Once ventilated, mice were paralyzed with 0.8 mg/kg pancuronium bromide (Baxter Healthcare Corp., Deerfield, IL). Using custom designed software (Flexivent, Scireq), airway pressure, volume, and airflow were recorded using a precisely controlled piston during maneuvers to evaluate lung mechanics.

Pressure-volume curves were generated by a sequential delivery of 7 increments of air into the lungs from resting pressure to total lung capacity followed by 7 expiratory steps during which air was incrementally released. Plateau pressure was recorded when airflow returned to zero at each step. The Salazar-Knowles equation (Equation 1) was applied to the plateau pressure measurements obtained between total lung capacity (TLC) and functional residual capacity (FRC) during the expiratory phase of the pressure-volume loop to determine static compliance (C_{st}) of the lung (45).

$V = V_{max} - Ae^{-KP}$ (Equation 1)

Where V_{max} = volume extrapolated to infinite P, V = lung volume above FRC, A and K are constants

Forced oscillation technique measures the impedance of the lung to an oscillatory flow of mutually prime frequencies. These impedance values are applied to a mathematical model of the lung developed by Hantos et al. (20) called the constant phase model. This model provides a means of distinguishing central airways from peripheral airways and lung parenchyma. The computer-controlled piston applies a 4-s perturbation to the lungs consisting of 13 sinusoidal components having mutually prime frequencies from 1 to 20.5 Hz with approximately hyperbolically decreasing amplitudes. Multiple linear regression is used to fit impedance spectra derived from measured pressure and volume changes to the constant phase model of the lung using Equation 2.

$$Z(f) = R_{aw} + iI_{aw} + (G_{ti} - iH_{ti}/(2\pi f)^{\alpha}) \qquad \text{(Equation 2)}$$

where i = square root of –1, Z(f) = resistance of the lung as a function of frequency, R_{aw} = a measure of central airways caliber, I_{aw} = airway inertance, G_{ti} = dissipative(resistive) mechanical properties of the lung tissue, H_{ti} = conservative (elastic) mechanical properties of the lung tissue. $\alpha = (2/\pi)\arctan(H_{ti}/G_{ti})$.

To ensure proper recruitment of all alveolar spaces, a pressure-volume curve was generated first for each animal. After this maneuver, a 4-s prime wave was performed followed

by a second pressure-volume curve to obtain reported values. Each perturbation was followed by 10 seconds of ventilation before the next measurement was taken.

Histology

After assessing lung mechanics, the lungs were inflated with 10% formalin via a tracheal cannula, removed from the thoracic cavity, and fixed overnight in formalin. Lung sections were stained with hematoxylin/eosin for routine histology and Masson's trichrome for evaluation of collagen deposition. Histology was quantitated by digital imaging of the hemotoxylin/eosin stained sections. While blinded to genotype and treatment, at least five images were captured of representative areas of each lung lobe and analyzed for septal thickening due to increased cellular infiltrate, extracellular matrix, and fibroblasts. Using software (ImageJ, NIH), the threshold was set to count the number of pixels contained within areas of the digital images that had increased inflammation and extracellular matrix deposition. The threshold number of pixels was then divided by the total number of pixels in the entire image and multiplied by 100 to generate a percentage of area affected by fibrosis and inflammation (2).

Hydroxyproline Assay

After assessing lung mechanics, mice were exsanguinated, and the lungs were perfused with sterile PBS and removed. Tissue samples were homogenized in 5ml PBS and sonicated. Aliquots (500µl) of each sample were lyophilized for 24 hours until dry and then hydrolyzed in 500µl 6N hydrochloric acid at 120°C overnight. Samples were then dried in a speed vacuum for two hours, resuspended in water, applied to a filter Eppendorf tube (Fisher Scientific), and spun at maximum speed for five minutes. Aliquots were assayed by adding chloramines-T for 20 minutes at room temperature and then developing with Ehrlich-perchloric acid at 65°C for 15

minutes. Absorbance was read at 561 nm in a spectrophotometer, and samples were compared to a standard curve generated from known concentrations of hydroxyproline standard (Sigma)(23).

PGE_2 Analysis

Mice were euthanized 7 days post-bleomycin instillation with sodium pentobarbital and exsanguinated. Lungs were removed and flash frozen in liquid nitrogen. Samples were homogenized in 1x PBS with 1mM EDTA pH 7.4 and 10 mM indomethacin and sonicated. Lipids were purified through a C18 column, and PGE_2 content was determined by using enzyme immunoassay kits (Assay Designs).

Statistical Analysis

Values are presented as mean +/- standard error of the mean and are analyzed by Student's two-tailed t-test or ANOVA followed by Tukey-Kramer HSD post-hoc test. A p-value less than 0.05 is considered statistically significant.

RESULTS

Contribution of COX-1- and COX-2-derived prostanoids to bleomycin-induced pulmonary fibrosis

A number of early studies using mice lacking COX-2 suggested that COX-2-derived prostanoids could limit some aspects of the histological changes and increases in collagen production observed in the bleomycin and vanadium pentoxide (V_2O_5) models of interstitial fibrosis (4, 25). However, in a recent study, this difference in disease progression in the COX-$2^{-/-}$ mice was not as apparent (22). A possible explanation for inconsistent findings is suggested on examination of genetic background of the COX-2 mice used in the various studies. To address this potential concern, we examined the role of COX-2 in the bleomycin model of fibrosis using congenic F1 animals. In addition to using traditional histological and biochemical methods for evaluating disease progression in the COX-$2^{-/-}$ mice, we assessed the impact of loss of COX-2 on changes in airway mechanics characteristic of pulmonary fibrosis.

Bleomycin or saline was administered to cohorts of sex-matched COX-$2^{-/-}$ mice and wild-type littermates. Lungs were harvested 21 days after treatment, and histological changes were assessed by analysis of hematoxylin/eosin and Masson's trichrome stained sections of lung. As expected, no histological changes were observed in the lungs from the saline-treated animals (Figure 1 A,B). As previously described for this model, remarkable structural alterations including increased collagen deposition and cellularity were observed in lungs from animals exposed to bleomycin. These histological changes appeared more pronounced in the COX-$2^{-/-}$ animals (Figure 1 C,D,E,F). A digital imaging program was used to quantitate the extent of fibrosis and inflammation in the lungs as described in the materials and methods (2). Figure 1G demonstrates increased disease progression in lungs of

the COX-2$^{-/-}$ mice compared to the congenic controls. The extent of collagen deposition was assessed biochemically by quantitating hydroxyproline levels in lung homogenates from similarly treated cohorts of COX-2$^{-/-}$ and COX-2$^{+/+}$ animals. Consistent with qualitative differences observed on examination of trichrome stained sections, COX2$^{-/-}$ mice had increased levels of hydroxyproline after bleomycin administration compared to wild-type mice (Table 1).

In humans, interstitial fibrosis leads to alterations in lung mechanics characterized by a decrease in lung compliance. We, therefore, determined whether similar changes in airway mechanics could be observed in the bleomycin model of pulmonary fibrosis and, furthermore, whether these changes were sensitive to the presence or absence of COX-2-derived prostanoids. For this analysis, we utilized a computer-controlled small animal ventilator, highly sensitive pressure transducers, and software (Flexivent) to record airway opening pressures, volume, and airflow. Changes in lung mechanics were determined using two different methods. Static compliance (C_{st}) was determined from analysis of pressure-volume curves, and tissue elastance (H) was measured by applying the constant phase model to prime wave impedance values obtained using the forced oscillation technique. Decreases in compliance and increases in elastance are anticipated in the bleomycin-exposed lung if this treatment indeed models pulmonary fibrosis. Consistent with this expectation, wild-type bleomycin-injured mice showed a significant decrease in static compliance (C_{st}) and a significant increase in tissue elastance (H) compared to saline-treated mice ($p < .005$). The constant phase model of the lung also provides information concerning two additional parameters, airway resistance (R_{aw}) and tissue resistance (G). Consistent with the sparing of the conducting airways in this model, no change in R_{aw} was observed in the mice after

bleomycin treatment. A small, but significant, increase in G was observed in all animals treated with bleomycin; however, this parameter did not allow us to distinguish between mice with differences in disease severity.

Sex-matched COX-$2^{-/-}$ mice and their littermate controls were administered either bleomycin or saline, and lung mechanics were assessed 21 days later. Both groups had a significant decrease in static compliance after bleomycin administration compared to the saline controls. However, the static compliance of the bleomycin-treated COX-$2^{-/-}$ mice was significantly lower than the static compliance of the bleomycin-treated COX-$2^{+/+}$ mice (Figure 2A). Accordingly, a significantly higher tissue elastance was measured in the COX-$2^{-/-}$ mice compared to COX-$2^{+/+}$ mice after bleomycin administration (Figure 2B). The significant increase in tissue elastance and significant decrease in static compliance along with the histological and biochemical differences suggest that COX-2-derived prostanoid(s) protect against the development of bleomycin-induced pulmonary fibrosis.

In addition to COX-2, the lung expresses high levels of COX-1. We next determined whether a similar role for COX-1-derived prostanoids could be observed in this model. As COX-$1^{-/-}$ mice survive on the C57BL/6 genetic background, C57BL/6 COX-$1^{-/-}$ animals and their congenic controls were used for these studies. Unlike the COX-$2^{-/-}$ mice, no discernable difference in disease pathogenesis was observed between the COX-$1^{-/-}$ animals and their controls in any of the disease parameters. Table 1 shows a similar increase in hydroxyproline content in the COX-$1^{-/-}$ and COX-$1^{+/+}$ mice after bleomycin administration. Consistent with this, both histological analysis and measurements of lung mechanics demonstrate no difference in disease progression between the two groups (Supplemental Figure S1). Thus,

development of fibrotic lung disease after exposure to bleomycin is modulated by COX-2-, but not COX-1-, dependant prostanoid production.

Alterations in PGE_2 levels fail to alter susceptibility to bleomycin-induced pulmonary fibrosis

COX-2-derived PGH_2 can be further metabolized into prostacyclin, thromboxane, and the prostaglandins - PGE_2, PGD_2, and PGF_2. Both anti-inflammatory and anti-fibrotic properties have been attributed to PGE_2, which suggests that this prostanoid, acting through either the EP2 or EP4 G_s-coupled receptor, can limit progression of fibrotic lung disease. To test this hypothesis, we examined the development of lung disease after bleomycin treatment in mice lacking mPGES1, the inducible PGE_2 synthase.

Three enzymes have been reported to metabolize PGH_2 into PGE_2 *in vitro*; however, only one of these, mPGES1, has been demonstrated to contribute to PGE_2 production *in vivo*. We first established the contribution of mPGES1 to the increases in PGE_2 levels in the lungs observed after exposure to bleomycin. Mice lacking mPGES1 and congenic control animals were treated with bleomycin or saline. PGE_2 levels were measured in whole lung homogenates seven days after treatment. As expected, significant increases in lung PGE_2 levels were observed in wild-type mice following bleomycin treatment. In contrast, increases in lung PGE_2 was severely attenuated in mPGES1$^{-/-}$ mice (Figure 3). Thus, the marked increase in PGE_2 levels after bleomycin administration is almost completely dependant on mPGES1 expression.

We next determined the impact of this relative PGE_2 deficiency on the pathogenesis of bleomycin-induced fibrotic lung disease. C57BL/6 mPGES1$^{-/-}$ mice and congenic controls were administered bleomycin or saline, and histological changes in the lung were evaluated

21 days after treatment. Surprisingly, no difference could be discerned in development of disease in the two groups. Quantitation of inflammation and extracellular matrix deposition by digital analysis demonstrated a similar extent and severity of interstitial inflammation and fibrosis (Figure 4A). We further evaluated disease progression in the mPGES1$^{-/-}$ mice by measuring changes in lung function following bleomycin administration. Both loss of compliance and increase in elastance as a result of bleomycin exposure were of similar magnitude in mPGES1$^{-/-}$ vs. mPGES1$^{+/+}$ mice (Figure 4 B,C).

We next considered the possibility that an increase in disease severity resulting from decreased PGE_2 production may be difficult to observe in these experiments because of the extensive disease induced even in the wild-type controls. To address this concern, we repeated our comparison of the mPGES1$^{-/-}$ and control animals inducing a milder disease by decreasing the dose of bleomycin (0.025U rather than 0.05U). As expected, the severity of the fibrotic response was reduced in the wild-type mice. However, no difference could be discerned between the mPGES1$^{-/-}$ and mPGES1$^{+/+}$ mice. Both the mPGES1$^{-/-}$ and mPGES1$^{+/+}$ mice had a significant but similar decrease in static compliance and increase in tissue elastance after both high and low dose bleomycin administration compared to the saline-treated controls (Figure 4 B,C). Thus, loss of mPGES1-dependent PGE_2 production does not cause enhanced susceptibility to bleomycin-induced fibrosis.

To further address the role of PGE_2 in bleomycin-induced pulmonary fibrosis, we examined mice lacking PGDH, the major catabolic enzyme for PGE_2. Previous studies in our laboratory have shown that these mice have increased lung PGE_2 levels (21). If PGE_2 can limit the initiation or progression of fibrosis, we anticipate that the loss of PGDH and consequential increased PGE_2 levels might protect these mice from developing pulmonary

fibrosis. However, both pathological and physiological measurements revealed no difference in disease progression between the $PGDH^{-/-}$ and $PGDH^{+/+}$ mice after bleomycin administration (Supplemental Figure S2).

Loss of PGE_2 G_s-coupled receptors does not enhance susceptibility to bleomycin-induced fibrosis

While the majority of PGE_2 production in the bleomycin-treated mouse lung is dependant on mPGES1, it is possible that it is the loss of local discrete pools of mPGES1-independent PGE_2 that plays a critical role in limiting the extent of fibrosis within the lung parenchyma. To address this possibility, mice lacking the receptors through which PGE_2 activates fibroblasts and other cell types important to disease pathogenesis were examined. Development of disease in the $EP2^{-/-}$ mice was examined first, anticipating that the G_s-coupled EP2 and EP4 receptors, rather than the G_i/G_q-coupled EP3 receptor or the G_q-coupled EP1 receptor, would be more likely to mediate the protective actions of PGE_2 in the lung. Quantitative analysis of the histological changes revealed no significant differences between the $EP2^{-/-}$ mice and wild-type mice in the extent and severity of interstitial inflammation and fibrosis after bleomycin administration (Figure 5A). Consistent with these findings, hydroxyproline analysis revealed similar increases in collagen deposition after bleomycin administration in the wild-type and $EP2^{-/-}$ mice (Table 1). Disease progression in the $EP2^{-/-}$ mice was further analyzed by assessing alterations in lung mechanics. Both $EP2^{-/-}$ and wild-type mice had a similar decrease in static compliance and increase in tissue elastance after bleomycin administration (Figure 5 B,C). A similar result was obtained following treatment of 4-6 month old $EP2^{-/-}$ and wild-type animals with 0.1U of bleomycin (Figure 5 D,E).

Since $EP4^{-/-}$ mice only survive on a mixed genetic background, a recombinant inbred (RI) background permissive to this mutation was generated (39). Congenic animals have been produced by the successive intercross of -/- and +/- animals for twenty generations, after which $EP4^{-/-}$ and control animals were generated. This recombinant inbred strain is sensitive to bleomycin-induced lung injury, with treated mice showing both histological changes and alterations in lung function characteristic of this model. In fact, exposure to bleomycin induces a more robust increase in collagen deposition in the RI mouse strain than is observed in either C57BL/6 or the F1 (C57BL/6 and 129/SvEv) mice. The RI strain also displays a lower basal lung compliance than other mouse strains. Age- and sex-matched $EP4^{-/-}$ mice and their congenic controls were administered either bleomycin or saline, and lung mechanics were assessed 21 days later. A similar decrease in static compliance and increase in tissue elastance was observed in both $EP4^{-/-}$ and control animals after exposure to bleomycin (Figure 6). Consistent with these physiological observations, hydroxyproline levels were similar between the $EP4^{-/-}$ mice and the $EP4^{+/+}$ controls after bleomycin administration (Table 1). Taken together, these studies with mice lacking the G_s-coupled PGE_2 receptors and mice lacking the dominant enzyme responsible for PGE_2 synthesis in the lung suggest that a COX-2-derived prostanoid other than PGE_2 is responsible for limiting lung fibrosis in this model.

$IP^{-/-}$ mice are more susceptible to bleomycin-induced fibrosis

The failure to observe increased disease in mice deficient in PGE_2 production, together with a recent collaborative study showing increased fibrotic lesions in the hearts of mice lacking the IP receptor (16), suggested that COX-2-dependent production of

prostacyclin, and not PGE_2, may be critical in limiting development of fibrotic lung disease. To test this hypothesis, congenic C57BL/6 $IP^{-/-}$ and wild-type mice were administered bleomycin or saline, and disease was assessed 21 days later by histological analysis, hydroxyproline measurements, and lung mechanics. As expected, no difference was observed between the histology of the saline-treated $IP^{-/-}$ and wild-type lungs (Figure 7 A,B). Interestingly, and similar to the COX-$2^{-/-}$ mice, the $IP^{-/-}$ mice had more severe disease demonstrated by a significant increase in all disease parameters. Histological analysis of the $IP^{-/-}$ mice demonstrated increased collagen deposition and cellularity after bleomycin administration compared to the wild-type mice (Figure 7 C,D,E,F). This correlated with a significant increase in the quantitative histology score and lung hydroxyproline levels in the $IP^{-/-}$ mice compared to the wild-type mice (Figure 7G and Table 1). These increased morphological and structural changes corresponded to a more pronounced decrease in lung function in the bleomycin-treated $IP^{-/-}$ mice compared to controls. No difference was observed in the $IP^{-/-}$ mice compared to the wild-type controls after saline administration. However, after bleomycin administration, the $IP^{-/-}$ mice had a significant decrease in static compliance and increase in tissue elastance compared to the wild-type mice (Figure 8 A,B). Collectively, these results suggest that the increased fibrotic lung disease observed in the absence of COX-2 is due to loss of prostacyclin, acting through the IP receptor, rather than loss of PGE_2. Moreover, the similar magnitude of changes, physiologically, biochemically, and histopathologically, in $COX2^{-/-}$ and $IP^{-/-}$ mice following exposure to bleomycin suggests that loss of prostacyclin alone may account for the enhanced disease observed in $COX2^{-/-}$ animals.

Table 3.I **Changes in Hydroxyproline Content (µg/lung)**

	+/+	-/-
COX-2	50.85 ± 10.86	125.12 ± 27.94*
COX-1	64.75 ± 19.82	75.95 ± 22.55
EP2	78.77 ± 25.29	56.46 ± 20.93
EP4	212.78 ±19.46	193.50 ± 17.40
IP	51.22 ± 8.81	105.48 ± 18.03*

Lungs were removed for hydroxyproline analysis 21 days after treatment. Mean saline value for each experimental group was subtracted from the bleomycin-treated values to obtain the change in hydroxyproline content in µg/lung. Values presented are mean ± SEM. * $p < .05$ compared to corresponding wild-type value; n = 8-11.

Figure 3.1

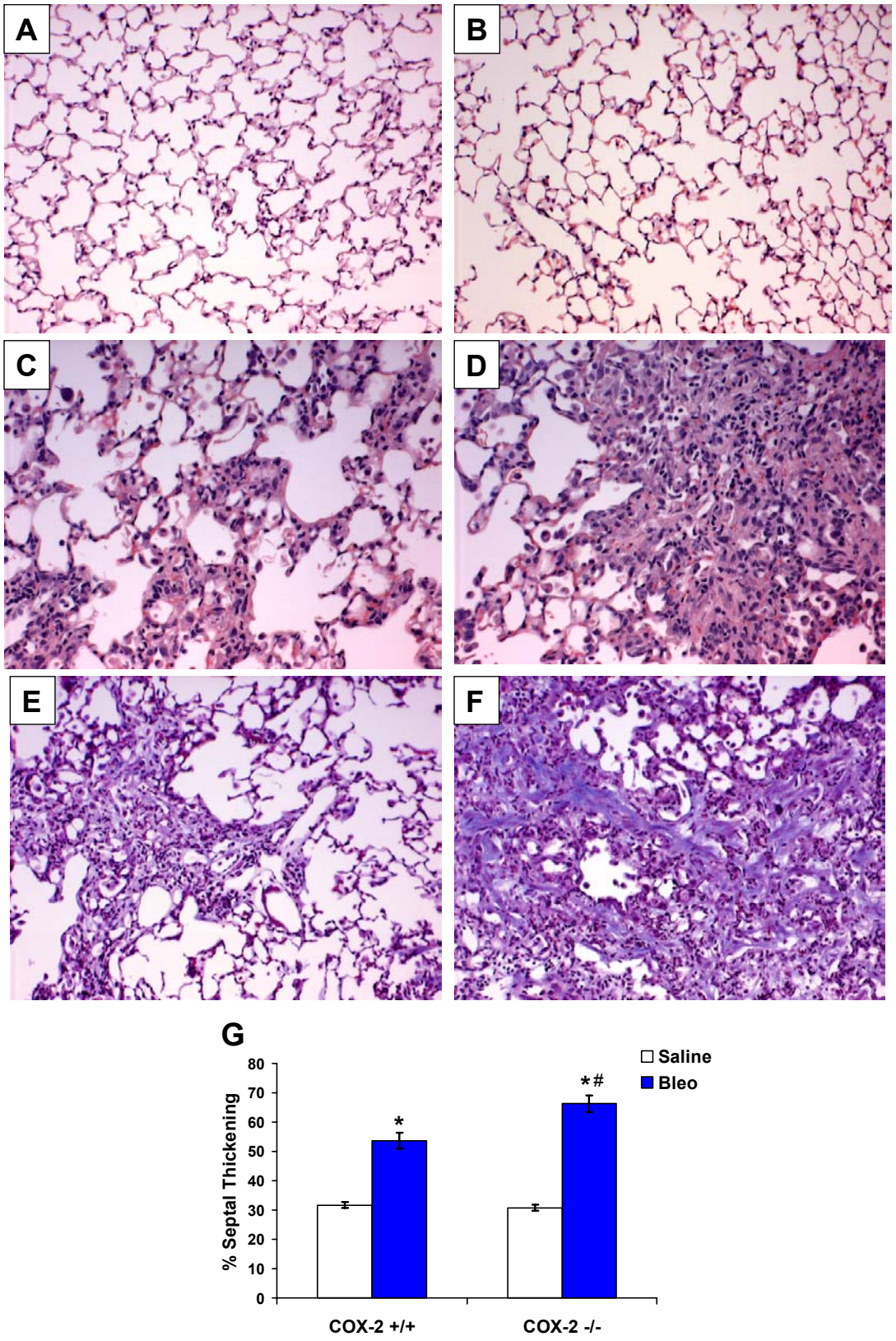
A
B
C
D
E
F
G
% Septal Thickening
80
70
60
50
40
30
20
10
0
*
*#
Saline
Bleo
COX-2 +/+
COX-2 -/-

Figure 3.1. Histological analysis reveals increased cellularity and deposition of collagen in the lungs of COX-2$^{-/-}$ mice compared to wild-type mice after bleomycin instillation. Lungs were harvested 21 days following treatment and fixed overnight in formalin. Lung sections were stained with hematoxylin/eosin or Masson's trichrome. Original magnification, 10x. **A)** Saline-treated wild-type mouse, hematoxylin/eosin stain. **B)** Saline-treated COX-2$^{-/-}$ mouse, hematoxylin/eosin stain. **C)** Bleomycin-treated wild-type mouse, hematoxylin/eosin stain. **D)** Bleomycin-treated COX-2$^{-/-}$ mouse, hematoxylin/eosin stain. **E)** Bleomycin-treated wild-type mouse, Masson's trichrome stain. **F)** Bleomycin-treated COX-2$^{-/-}$ mouse, Masson's trichrome stain. **G)** Morphological changes observed in lungs obtained from bleomycin-treated mice were quantitated by digital imaging of hematoxylin/eosin stained lung sections and presented as a percentage of septal thickening. Saline-treated COX-2$^{+/+}$, n = 9; saline-treated COX-2$^{-/-}$, n = 6; bleomycin-treated COX-2$^{+/+}$, n = 12; bleomycin-treated COX-2$^{-/-}$, n = 11. * $p < .01$ compared with corresponding saline value, # $p < .01$ compared with COX-2$^{+/+}$ bleomycin value.

Figure 3.2

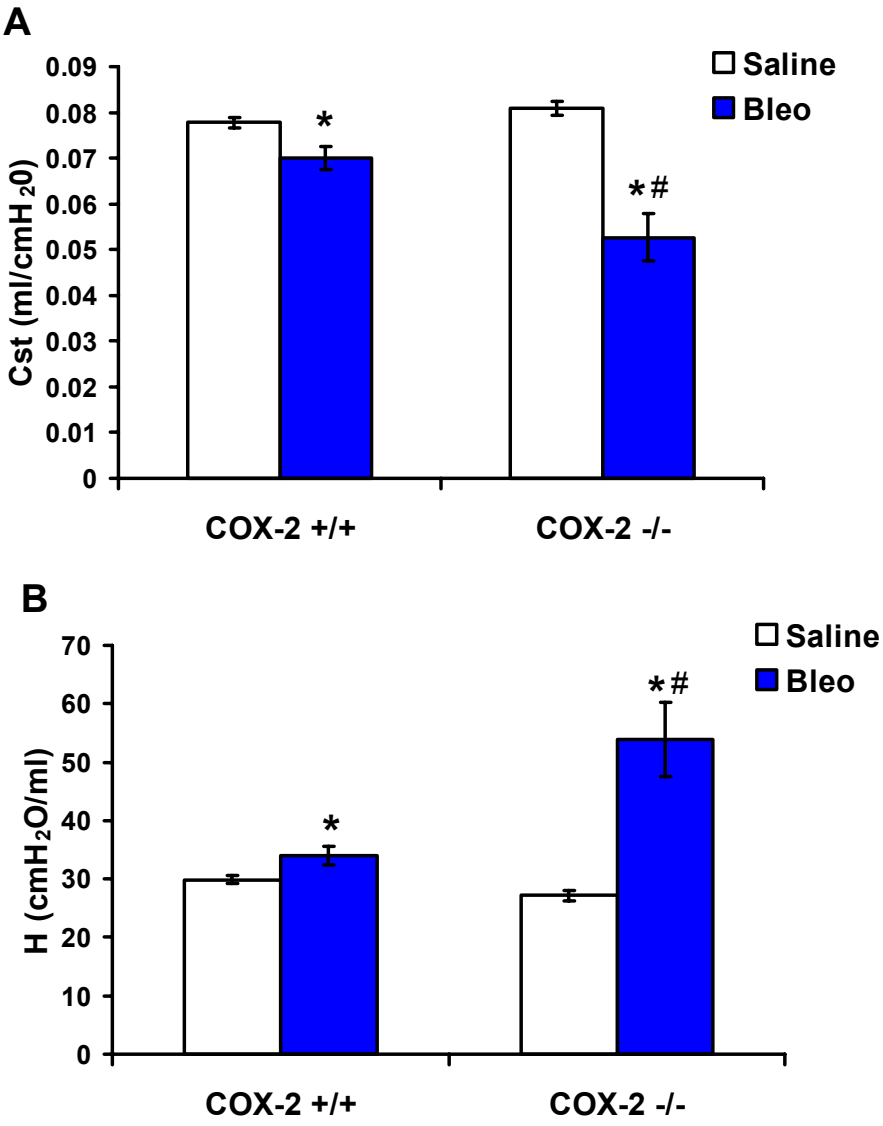
A
Saline
Bleo
0.09
0.08
0.07
0.06
0.05
0.04
0.03
0.02
0.01
0
Cst (ml/cmH20)
*
*#
COX-2 +/+
COX-2 -/-
B
Saline
Bleo
70
60
50
40
30
20
10
0
H (cmH2O/ml)
*
*#
COX-2 +/+
COX-2 -/-

Figure 3.2. Analysis of lung mechanics demonstrates increased disease susceptibility in the COX-2$^{-/-}$ mice. Lung mechanics were measured in anesthetized, paralyzed, and mechanically ventilated mice 21 days following bleomycin or saline instillation. **A)** Static compliance (Cst) determined by fitting the Salazar-Knowles equation to pressure-volume curves; n = 6-9 animals; * $p < .05$ compared with corresponding saline value, # $p < .05$ compared with COX-2$^{+/+}$ bleomycin value. **B)** Tissue elastance (H) determined by applying prime wave impedance values to the constant phase model; n = 9-11 animals; * $p < .05$ compared with corresponding saline value, # $p < .05$ compared with COX-2$^{+/+}$ bleomycin value.

Figure 3.3

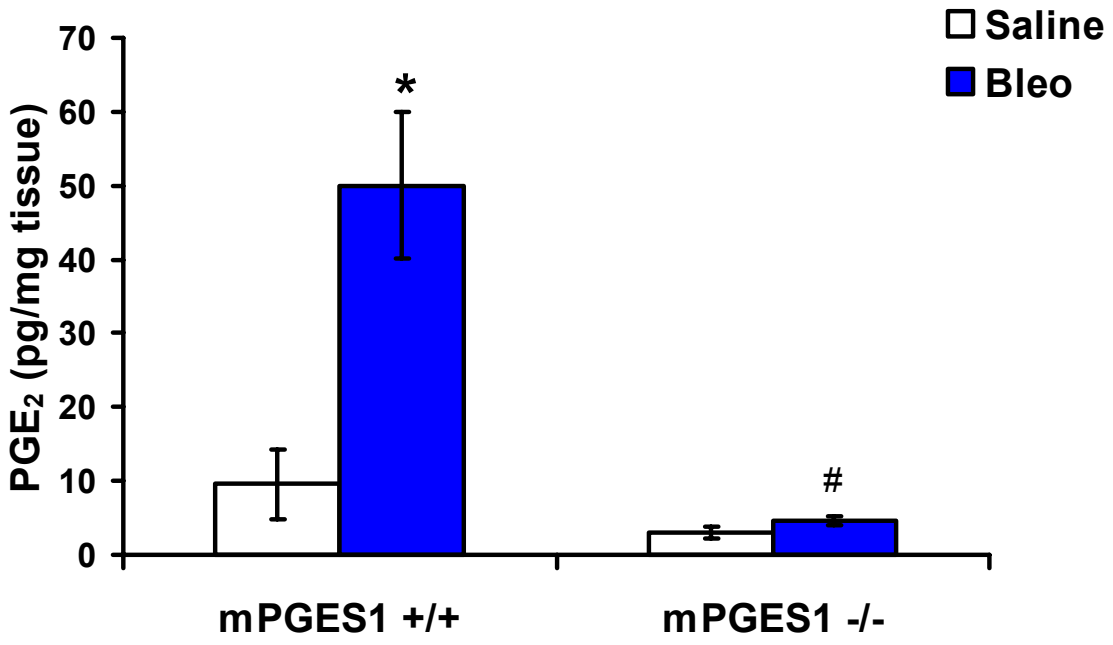
Saline
Bleo
70
60
50
40
30
20
10
0
PGE2 (pg/mg tissue)
*
#
mPGES1 +/+
mPGES1 -/-

Figure 3.3. Reduced PGE_2 levels in the lung homogenates of mPGES1$^{-/-}$ mice compared to wild-type mice after bleomycin administration. The lungs were harvested 7 days after bleomycin or saline administration. n = 3; * $p < .01$ compared with corresponding saline value, # $p < .01$ compared with mPGES1$^{+/+}$ bleomycin value.

Figure 3.4

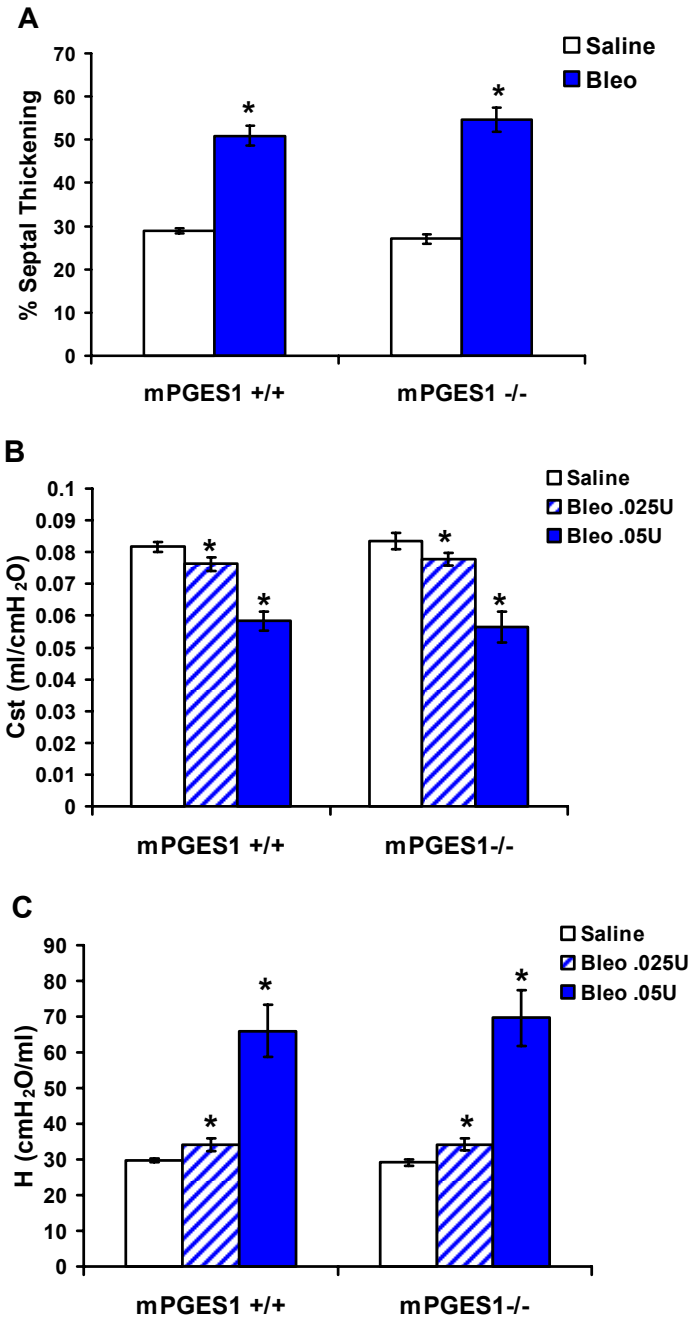
A
Saline
Bleo
% Septal Thickening
70
60
50
40
30
20
10
0
*
*
mPGES1 +/+
mPGES1 -/-
B
Saline
Bleo .025U
Bleo .05U
Cst (ml/cmH2O)
0.1
0.09
0.08
0.07
0.06
0.05
0.04
0.03
0.02
0.01
0
*
*
*
*
mPGES1 +/+
mPGES1-/-
C
Saline
Bleo .025U
Bleo .05U
H (cmH2O/ml)
90
80
70
60
50
40
30
20
10
0
*
*
*
*
mPGES1 +/+
mPGES1-/-

Figure 3.4. Histological analysis and measurements of lung mechanics fail to distinguish mPGES1$^{-/-}$ mice from wild-type mice after bleomycin administration. A) Morphological changes observed in lungs obtained from bleomycin-treated mice were quantitated by digital imaging of hematoxylin/eosin stained lung sections and presented as a percentage of septal thickening. Saline-treated groups, n = 6; bleomycin-treated groups, n = 15; * $p < .05$ compared with corresponding saline values. **B)** Static compliance (Cst) in the mPGES1$^{-/-}$ and wild-type mice after .05U and .025U of bleomycin. **C)** Tissue elastance (H) in the mPGES1$^{-/-}$ and wild-type mice after .05U and .025U of bleomycin. Saline-treated groups and bleomycin-treated groups for .025 dose, n = 8-10; saline-treated groups and bleomycin-treated groups for .05 dose, n = 14-18. * $p < .05$ compared to corresponding saline values.

Figure 3.5

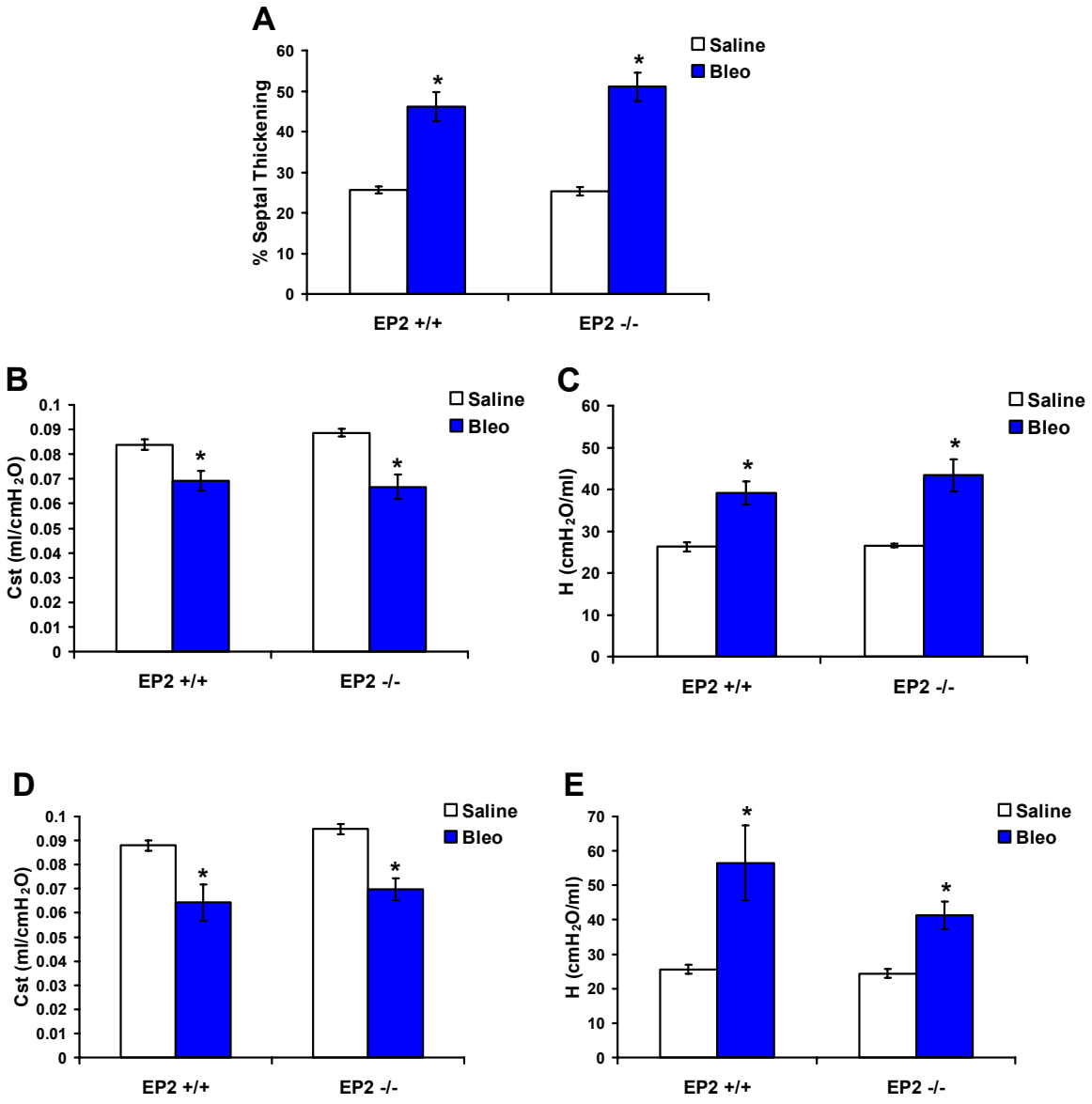
A
% Septal Thickening
60
50
40
30
20
10
0
Saline
Bleo
*
*
EP2 +/+
EP2 -/-
B
Cst (ml/cmH2O)
0.1
0.09
0.08
0.07
0.06
0.05
0.04
0.03
0.02
0.01
0
Saline
Bleo
*
*
EP2 +/+
EP2 -/-
C
H (cmH2O/ml)
60
50
40
30
20
10
0
Saline
Bleo
*
*
EP2 +/+
EP2 -/-
D
Cst (ml/cmH2O)
0.1
0.09
0.08
0.07
0.06
0.05
0.04
0.03
0.02
0.01
0
Saline
Bleo
*
*
EP2 +/+
EP2 -/-
E
H (cmH2O/ml)
70
60
50
40
30
20
10
0
Saline
Bleo
*
*
EP2 +/+
EP2 -/-

Figure 3.5. Histological analysis and lung mechanics demonstrate similar disease susceptibility in the EP2$^{-/-}$ and wild-type mice after bleomycin administration. A) Morphological changes observed in lungs obtained from bleomycin-treated mice were quantitated by digital imaging of hematoxylin/eosin stained lung sections and presented as a percentage of septal thickening. Saline-treated groups, n = 7; bleomycin-treated groups, n = 10. * $p < .05$ compared with corresponding saline values. **B)** Static compliance (Cst) in the EP2$^{-/-}$ and wild-type mice (8-12 weeks) treated with .05U of bleomycin. **C)** Tissue elastance (H) in the EP2$^{-/-}$ and wild-type mice (8-12 weeks) treated with .05U of bleomycin. **D)** Static compliance (Cst) in an older cohort of mice (4-6 months) treated with 0.1U of bleomycin. **E)** Tissue elastance (H) in an older cohort of mice (4-6 months) treated with 0.1U of bleomycin. Saline-treated and bleomycin-treated groups from younger cohort, n = 8-11; saline-treated and bleomycin-treated groups from older cohort, n = 7-10; * $p < .05$ compared with corresponding saline values.

Figure 3.6

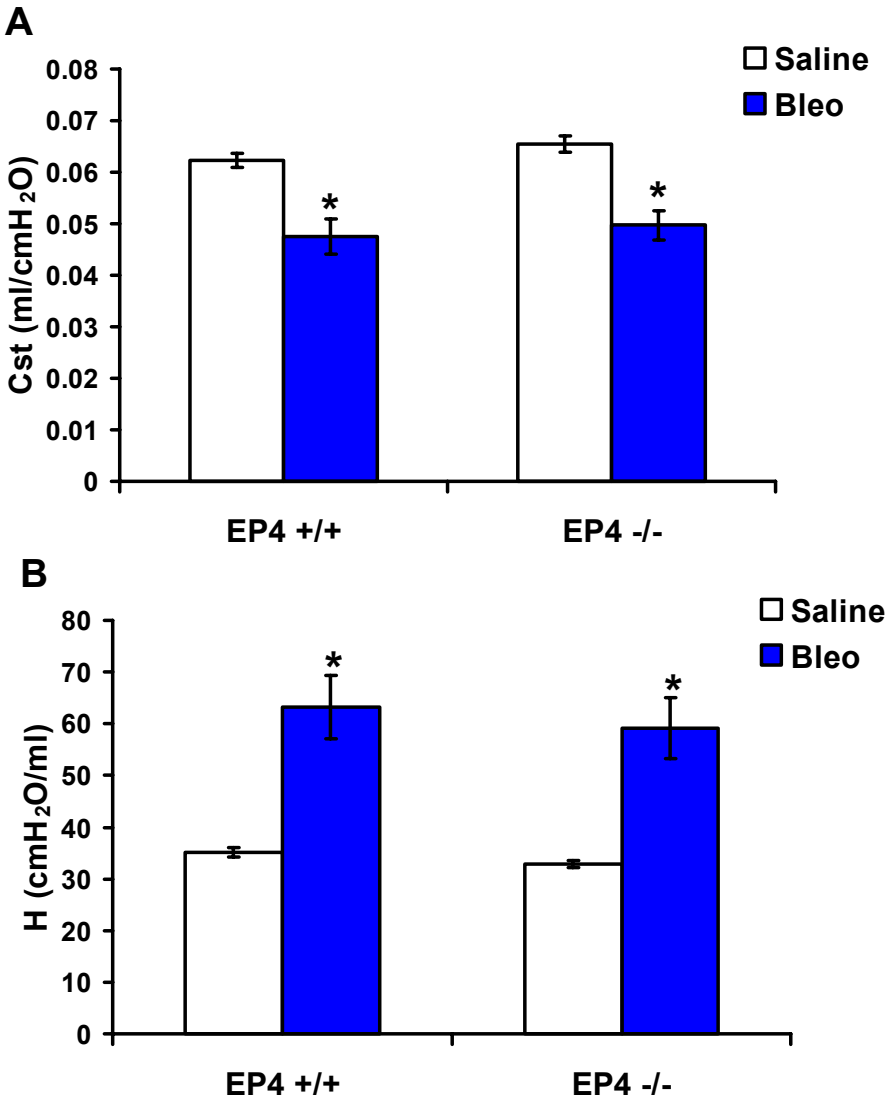
A
Saline
Bleo
0.08
0.07
0.06
0.05
0.04
0.03
0.02
0.01
0
Cst (ml/cmH2O)
*
*
EP4 +/+
EP4 -/-
B
Saline
Bleo
80
70
60
50
40
30
20
10
0
H (cmH2O/ml)
*
*
EP4 +/+
EP4 -/-

Figure 3.6. Analysis of lung mechanics reveal similar disease susceptibility in the EP4$^{-/-}$ and wild-type mice after bleomycin administration. Lung mechanics were measured in anesthetized, paralyzed, and mechanically ventilated mice 21 days following bleomycin or saline instillation. **A)** Static compliance (Cst) determined by fitting the Salazar-Knowles equation to pressure-volume curves. **B)** Tissue elastance (H) determined by applying prime wave impedance values to the constant phase model. n = 8-10 animals; * $p < .05$ compared with corresponding saline values.

Figure 3.7

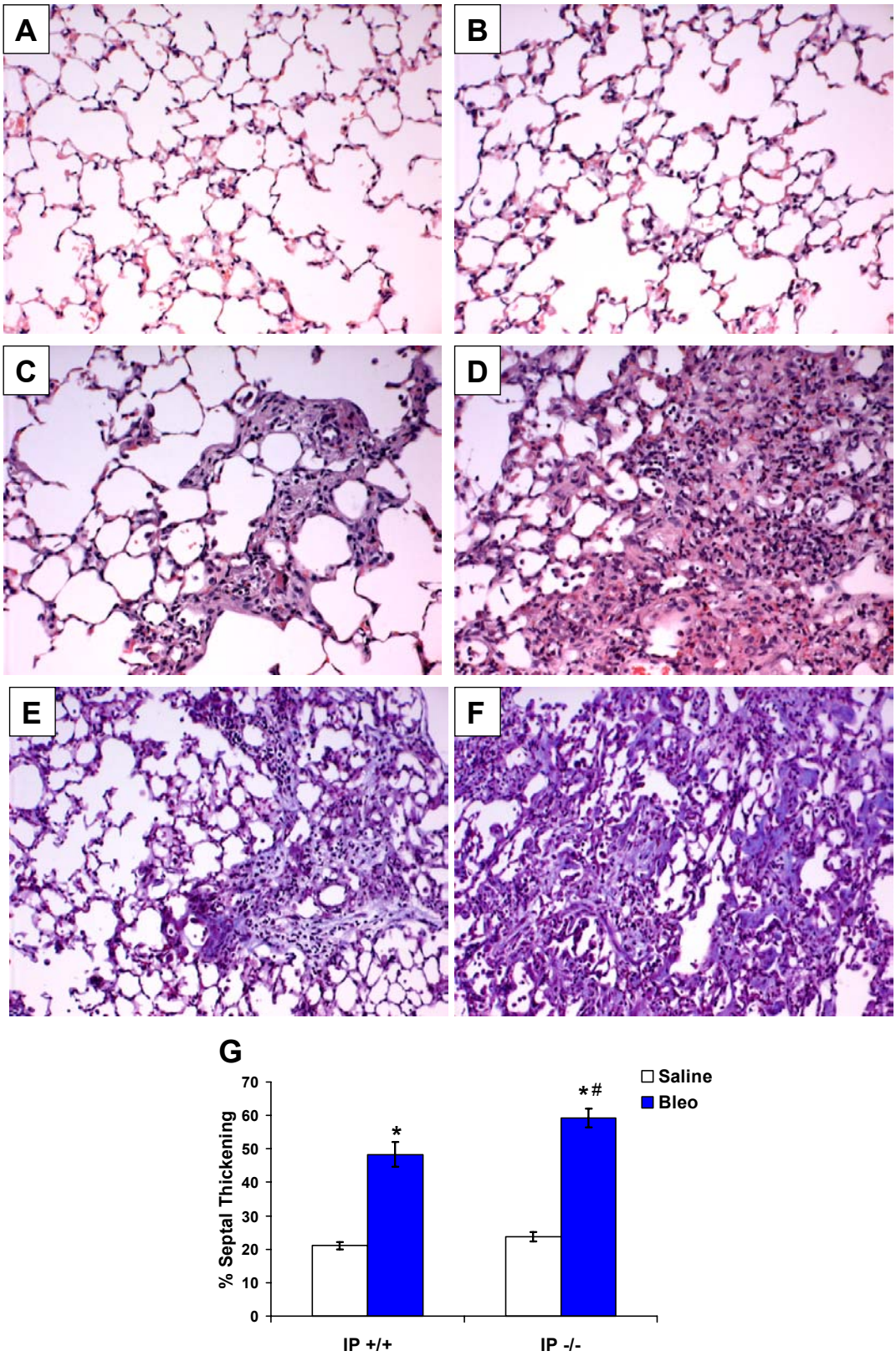
A
B
C
D
E
F
G
% Septal Thickening
70
60
50
40
30
20
10
0
*
*#
Saline
Bleo
IP +/+
IP -/-

Figure 3.7. Histological analysis reveals increased cellularity and deposition of collagen in the lungs of $IP^{-/-}$ mice compared to wild-type mice after bleomycin instillation. Lungs were harvested 21 days following treatment and fixed overnight in formalin. Lung sections were stained with hematoxylin/eosin or Masson's trichrome. Original magnification, x10. **A)** Saline-treated wild-type mouse, hematoxylin/eosin stain. **B)** Saline-treated $IP^{-/-}$ mouse, hematoxylin/eosin stain. **C)** Bleomycin-treated wild-type mouse, hematoxylin/eosin stain. **D)** Bleomycin-treated $IP^{-/-}$ mouse, hematoxylin/eosin stain. **E)** Bleomycin-treated wild-type mouse, Masson's trichrome stain. **F)** Bleomycin-treated $IP^{-/-}$ mouse, Masson's trichrome stain. **G)** Morphological changes observed in lungs obtained from bleomycin-treated mice were quantitated by digital imaging of hematoxylin/eosin stained lung sections and presented as a percentage of septal thickening. Saline-treated $IP^{+/+}$, n = 5; saline-treated $IP^{-/-}$, n = 5; bleomycin-treated $IP^{+/+}$, n = 13; bleomycin-treated $IP^{-/-}$, n = 10; * $p < .05$ compared with corresponding saline value, # $p < .05$ compared with $IP^{+/+}$ bleomycin value.

Figure 3.8

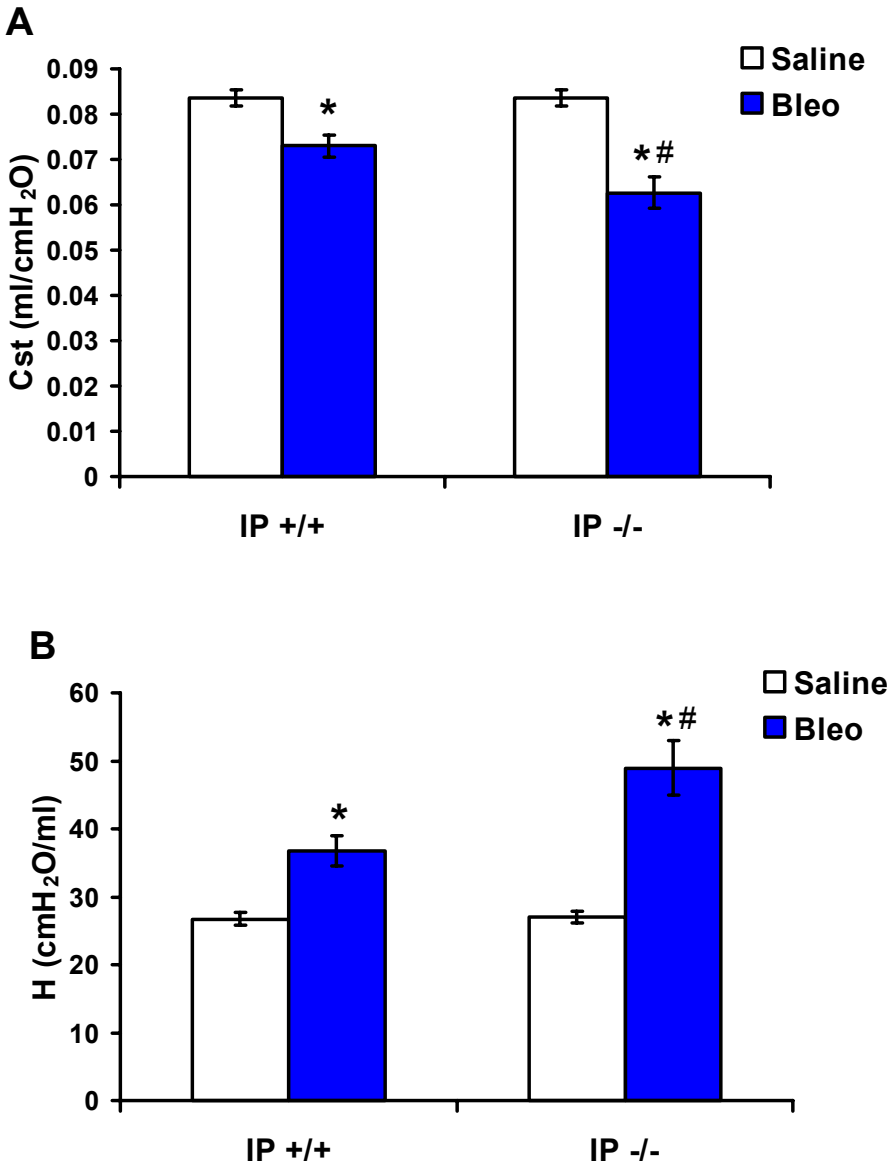
A
Saline
Bleo
0.09
0.08
0.07
0.06
0.05
0.04
0.03
0.02
0.01
0
Cst (ml/cmH2O)
*
*#
IP +/+
IP -/-
B
Saline
Bleo
60
50
40
30
20
10
0
H (cmH2O/ml)
*
*#
IP +/+
IP -/-

Figure 3.8. Analysis of lung mechanics demonstrates increased disease susceptibility in the $IP^{-/-}$ mice. Lung mechanics were measured in anesthetized, paralyzed, and mechanically ventilated mice 21 days following bleomycin or saline instillation. **A)** Static compliance (Cst) determined by fitting the Salazar-Knowles equation to pressure-volume curves. **B)** Tissue elastance (H) determined by applying prime wave impedance values to the constant phase model. Saline-treated, n = 8-10; bleomycin-treated, n = 15-18. * $p < .05$ compared with corresponding saline value, # $p < .05$ compared with $IP^{+/+}$ bleomycin value.

Supplemental Figure S1.

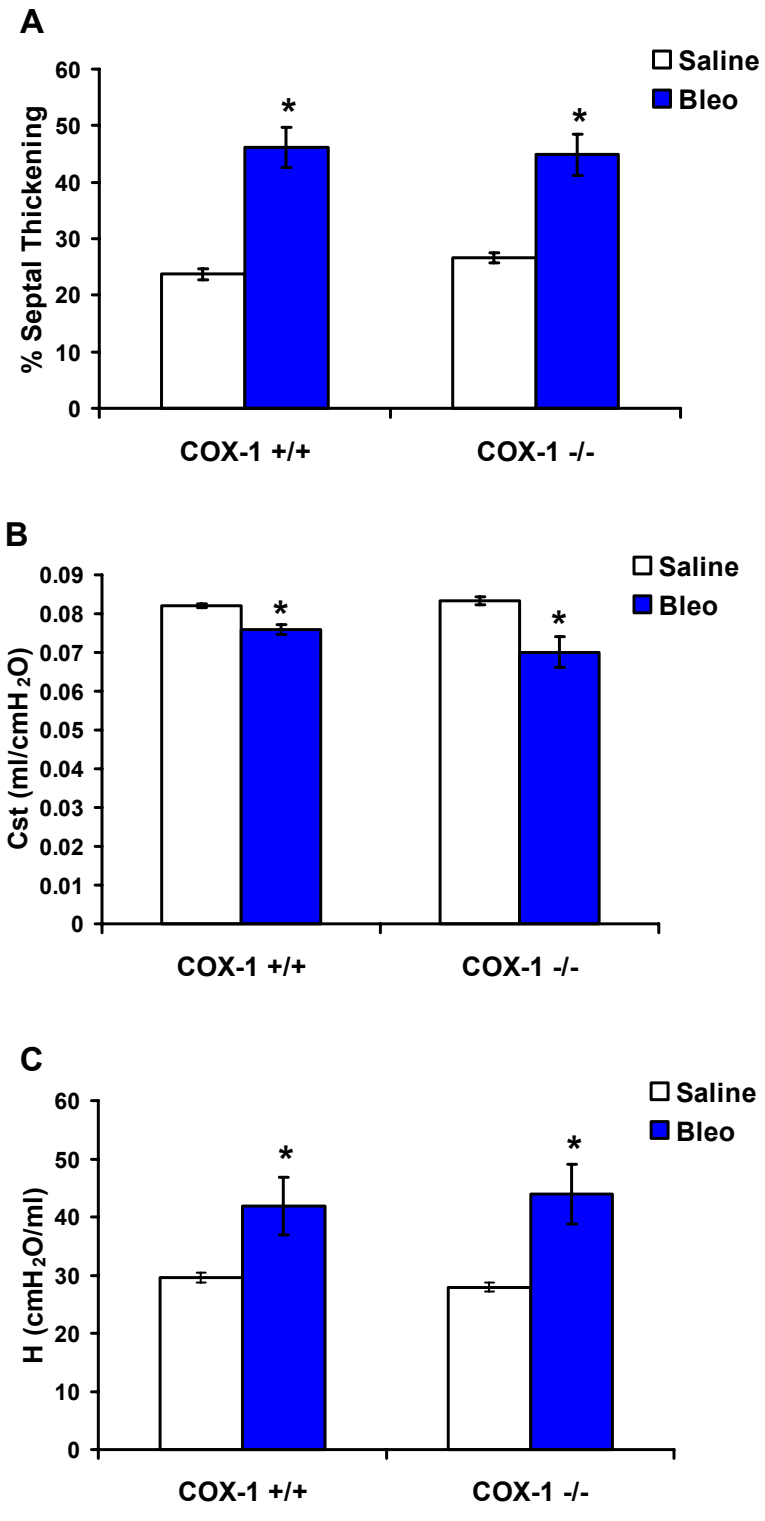

Supplemental Figure S1. Histological analysis and lung mechanics demonstrate similar disease susceptibility in the COX-1$^{-/-}$ and wild-type mice after bleomycin administration. Lung mechanics were measured in anesthetized, paralyzed, and mechanically ventilated mice 21 days following bleomycin or saline instillation, and then the lungs were inflated with 10% formalin via a tracheal cannula, removed from the thoracic cavity, and fixed overnight in formalin. **A)** Morphological changes observed in lungs obtained from bleomycin-treated mice were quantitated by digital imaging of hematoxylin/eosin stained lung sections and presented as a percentage of septal thickening. No difference was measured between the two bleomycin-treated groups. * $p < .05$ compared with corresponding saline values. n = 8-12. **B)** Static compliance (Cst) determined by fitting the Salazar-Knowles equation to pressure-volume curves. **C)** Tissue elastance (H) determined by applying prime wave impedance values to the constant phase model. No difference in either static compliance or tissue elastance was measured between the two bleomycin-treated groups. * $p < .05$ compared with corresponding saline values. Saline-treated animals, n = 14; bleomycin-treated animals, n = 20.

Supplemental Figure S2.

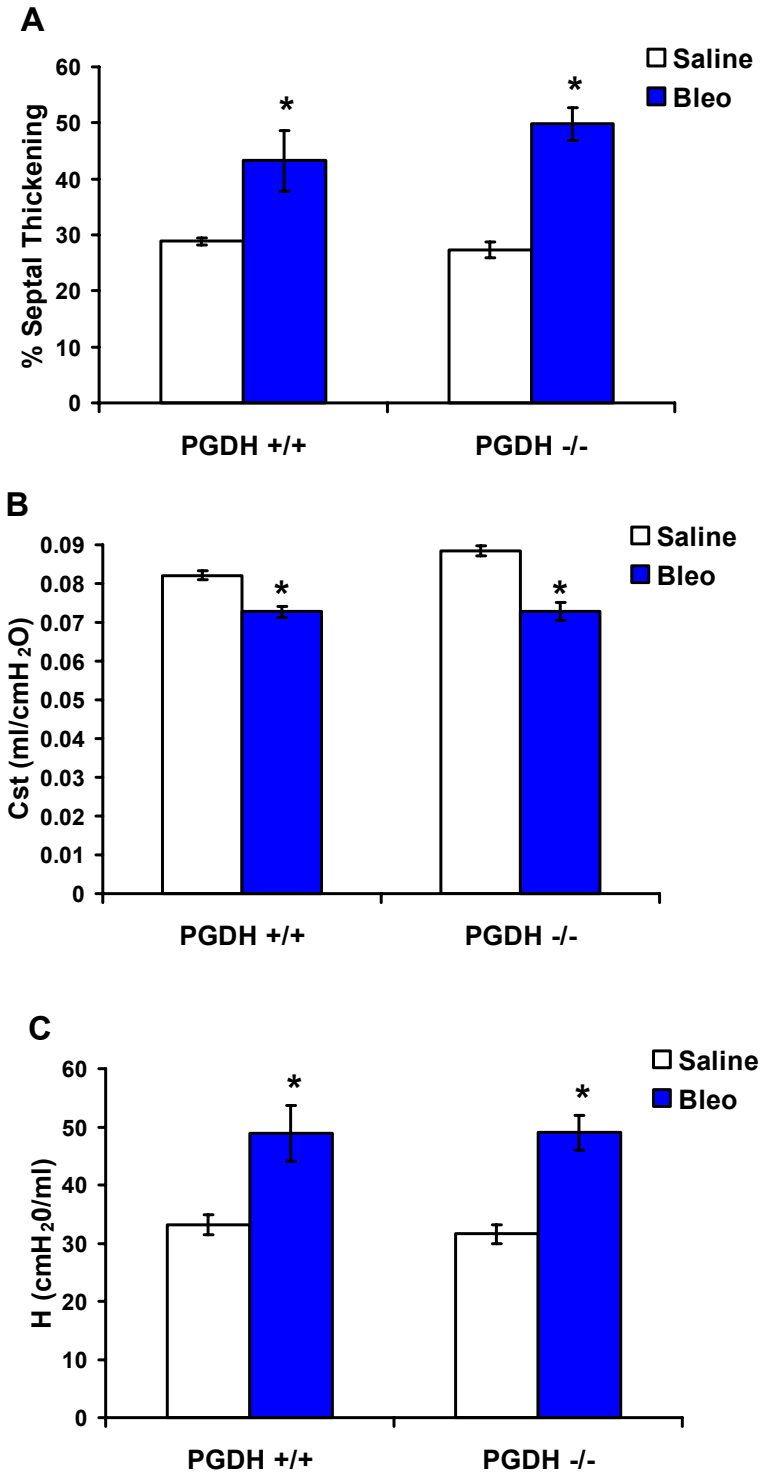

Supplemental Figure S2. Histological analysis and lung mechanics demonstrate similar disease susceptibility in the PGDH$^{-/-}$ and wild-type mice after bleomycin administration. Lung mechanics were measured in anesthetized, paralyzed, and mechanically ventilated mice 21 days following bleomycin or saline instillation, and then the lungs were inflated with 10% formalin via a tracheal cannula, removed from the thoracic cavity, and fixed overnight in formalin. **A)** Morphological changes observed in lungs obtained from bleomycin-treated mice were quantitated by digital imaging of hematoxylin/eosin stained lung sections and presented as a percentage of septal thickening. No difference was measured between the two bleomycin-treated groups. * $p < .05$ compared with corresponding saline values. n = 6-8. **A)** Static compliance (Cst) determined by fitting the Salazar-Knowles equation to pressure-volume curves. **B)** Tissue elastance (H) determined by applying prime wave impedance values to the constant phase model. No difference in either static compliance or tissue elastance was measured between the two bleomycin-treated groups. * $p < .05$ compared with corresponding saline values. Saline-treated animals, n = 9; bleomycin-treated animals, n = 15.

Supplemental Figure S3.

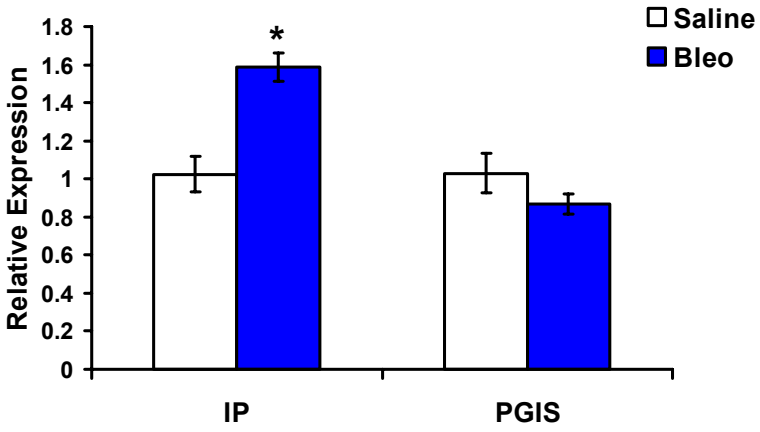

Supplemental Figure S3. Real-time quantitative PCR analysis of expression levels of IP and PGIS in total RNA isolated from day 21 bleomycin-treated and saline-treated lungs. Each sample was subjected to quantitative RT-PCR analysis on an ABI Prism 7900 Thermocycler. Expression of each was detected using commercially available primer and probe sets (Applied Biosystems). Expression levels were normalized to an endogenous control, 18s, and the results were expressed as fold change relative to saline-treated expression levels. Quantification of samples was performed using the comparative Ct ($\Delta\Delta$Ct) method, as described in the Assays-on-Demand Users Manual (Applied Biosystems). Relative gene expression was determined by the formula $x = 2^{-\Delta\Delta Ct}$. Saline-treated lungs, n = 7; bleomycin-treated lungs, n = 9; * $p < .05$.

DISCUSSION

Bleomycin-induced fibrosis is extensively used to model aspects of the pathogenesis of interstitial pulmonary fibrosis. Here we show that intratracheally administered bleomycin leads to changes in lung mechanics that parallel those observed in patients with pulmonary fibrosis, providing an additional means of assessing the severity of disease in the mouse. We examined the development of fibrotic lung disease in seven congenic mouse lines, each carrying a null allele in a gene required for the normal synthesis or response to prostanoids. These studies show that COX-2-dependant prostacyclin production limits the development of fibrosis and subsequent loss of lung function after exposure to bleomycin. In contrast, alterations in PGE_2 levels or in the ability of mice to respond to PGE_2 have no effect on the development of disease.

Pulmonary function testing is commonly used to monitor the progression of pulmonary fibrosis in humans. Reductions in forced vital capacity reflect changes in lung compliance as collagen is synthesized by myofibroblasts and deposited within the interstitium of the lung parenchyma. Similar measurements have not typically been utilized in evaluation of disease in this mouse model of interstitial pulmonary fibrosis. Rather, the severity of disease induced by bleomycin treatment is assessed using semi-quantitative histological examination and changes in lung hydroxyproline content. In our studies, in addition to these traditional criteria, we measured lung mechanics of both saline and bleomycin-exposed animals. In all experiments, treatment of both wild-type and congenic lines with bleomycin results in a significant decrease in static compliance, determined by analysis of pressure-volume loops from tracheostomized, mechanically ventilated animals. In addition to detecting differences between control and bleomycin-treated animals,

assessment of static compliance allows us to distinguish differences in disease severity in various experimental groups. The increase in fibrotic disease in the bleomycin-treated COX-$2^{-/-}$ and $IP^{-/-}$ animals detected using histological and biochemical measurements was paralleled by a significant decrease in static compliance of the lungs. In the other mice tested, when histological evaluation and hydroxyproline measurements failed to distinguish between the two experimental groups of mice, no difference could be observed in the static lung compliance of these animals.

We also evaluated the changes in lung mechanics after bleomycin exposure using the forced oscillatory technique. This method, pioneered by Schuessler, Bates, and Irvin (24, 46), measures the impedance of the lung to an oscillatory flow of mutually prime frequencies. The constant phase model of the lung developed by Hantos et al. (20) is then utilized to calculate a value termed tissue elastance (H), which reflects the conservative (elastic) mechanical properties of the lung tissue. Tissue elastance was increased in all mice exposed to bleomycin. Experimental groups with more severe disease, based on histological and biochemical parameters, also displayed a significant increase in tissue elastance. Thus, both tissue elastance and static compliance provide a sensitive means of assessing changes in lung mechanics that parallel the morphological changes induced by exposure to bleomycin.

Our observation of increased disease in the COX-$2^{-/-}$ bleomycin-treated mice is consistent with the report by Keerthisingam et al. (25) using this same model of fibrotic lung disease. In their study, histological examination of a small group of mice of mixed genetic background revealed more severe disease in the COX-$2^{-/-}$ animals. However, in a more recent report by these investigators, the degree of fibrosis in the lungs was similar between bleomycin-treated COX-$2^{-/-}$ mice and similarily treated wild-type controls (22). Mice used in

these studies were generated from selection and breeding of populations of F2 mice carrying both 129Sv/Ev and C57BL/6 genes, mice much less susceptible to patent ductus arteriosis. Over time, this breeding scheme likely results in a skewing of the genetic background of the mice in favor of a particular complement of 129Sv/Ev and C57BL/6 alleles. Differences in the response of the COX-$2^{-/-}$ animals used in the various experiments could be attributed at least in part to distorted representation of 129Sv/Ev and C57BL/6 alleles in control and COX-$2^{-/-}$ animals. Bonner et al. (4) examined COX-$1^{-/-}$ and COX-$2^{-/-}$ mice of mixed genetic background using a V_2O_5 model of pulmonary fibrosis. V_2O_5 exposure does not result in fibrotic disease in wild-type mice. While loss of COX-1 did not result in an increase in collagen deposition, a measurable increase in fibrosis was observed in the COX-$2^{-/-}$ animals. These results correlate well with our studies of the C57BL/6 congenic COX-$1^{-/-}$ mice and the F1 COX-$2^{-/-}$ mice in the bleomycin model. We also failed to observe a difference in the development of disease in mice lacking COX-1 expression, and, on the other hand, we found that the fibrotic response to bleomycin is exaggerated in the COX-$2^{-/-}$ mice. Taken together, histological and biochemical studies of the COX-deficient mice in both the bleomycin and V_2O_5 models of pulmonary fibrosis and analysis of lung mechanics after exposure to bleomycin suggest a role for COX-2-derived prostanoids in limiting fibrotic lung disease.

A number of lines of evidence indicate that the protective prostanoid produced by the COX-2 pathway is PGE_2 and that the protective actions of PGE_2 are mediated by the EP2 receptor. This model, however, is not supported by the studies reported here. First, we found no increase in disease parameters in the mice lacking mPGES1, despite our finding that this synthase is responsible for the increase in PGE_2 levels measured in the mouse lung after exposure to bleomycin. Two other proteins capable of metabolizing PGH_2 to PGE_2

have been identified, although a role for these proteins in the *in vivo* production of PGE_2 has not yet been reported. However, as the phenotype of the mPGES1$^{-/-}$ does not recapitulate the phenotypes of the various receptor deficient mice, it is presumed that some mPGES1-independent pathways must be active *in vivo* (39, 53). It is possible that these alternative synthetic pathways provide discrete pools of PGE_2 essential for protecting mice against bleomycin-induced disease. We therefore examined mice lacking PGE_2 receptors, focusing on the two G_s-coupled PGE_2 receptors, EP2 and EP4. No difference in the response of the mice to bleomycin was observed in either the EP2$^{-/-}$ or EP4$^{-/-}$ mice compared to controls. Our results differ from a recent study carried out using EP2$^{-/-}$ mice. In this study, modest increases in collagen levels were measured in the EP2$^{-/-}$ animals compared to controls (32). The basis for these conflicting results is not apparent. However, our inability to observe changes physiologically, biochemically, and pathologically in mPGES1$^{-/-}$, PGDH$^{-/-}$, EP2$^{-/-}$, and EP4$^{-/-}$ mice does not support an anti-fibrotic role for PGE_2 in this model.

Prostacyclin production, similar to PGE_2, is dependant on COX metabolism of arachidonic acid. Prostacyclin binds with high affinity to the IP receptor, a seven transmembrane receptor which, like the EP2 and EP4 receptors, couples primarily to G_s to activate adenyl cyclase. IP receptors are expressed at high levels on platelets, and prostacyclin limits platelet aggregation and thrombi formation. Loss of COX-2-mediated prostacylin production by endothelial cells and the resultant unopposed activity of COX-1-dependant thromboxane action on platelets may underlie possible increased risks for cardiovascular events in patients treated with COX-2 specific inhibitors (15). Fewer studies have examined the role of prostacyclin in fibrotic lung diseases such as idiopathic pulmonary fibrosis.

A role for prostacyclin in pulmonary fibrosis is consistent with the expression of prostacyclin synthase (PGIS) and the IP receptor by many cell types present in the lung. PGIS expression has been demonstrated on pneumocytes, fibroblasts, endothelial cells, and resident leukocytes, and IP expression has been demonstrated on pneumocytes, fibroblasts, smooth muscle cells, and macrophages (12, 27, 40, 42, 44, 55). In addition, IP receptors are expressed by many hematopoietic cells, including lymphocytes and neutrophils, recruited to the lung after exposure to bleomycin (37, 61). We have examined the expression of PGIS and IP by quantitative RT-PCR in saline-treated and bleomycin-treated lungs. As expected, expression of both the synthase and the receptor was easily detected in the healthy lung. PGIS expression was not increased after induction of fibrosis with bleomycin. However, a small (50%) increase in the expression of the IP receptor was observed using this method (Supplemental Figure S3).

We recently reported that mice lacking IP receptors have elevated blood pressure, and the hearts of these animals showed extensive fibrosis (16). Interestingly, while fibrosis is an expected consequence of elevations in blood pressure and cardiac stress, the extent of fibrosis in the IP-deficient mice was exaggerated compared to the modest increase in blood pressure. This suggests that, while the fibrosis was likely triggered by the stress conferred by elevated blood pressure, the fibrotic response normally may be limited by the presence of IP receptors on cardiac fibroblasts. Consistent with this interpretation, stable prostacyclin analogues can inhibit migration of lung fibroblasts and proliferation of cardiac fibroblasts (27, 62). Exposure to IP agonists also decreased expression of types I and III collagen by cardiac fibroblasts (62). In fact, bradykinin-mediated decreases in collagen formation by these cells

are the indirect consequence of production of a prostanoid, particularily prostacyclin, the major prostanoid formed by cardiac fibroblasts (17).

Studies of dermal fibroblasts further support a role for prostacyclin in regulation of fibroblast growth and production of extracellular matrix components. The prostacyclin analogue, iloprost, suppressed type I collagen induction by TGF-β in dermal wounds and attenuated induction of connective tissue growth factor (CTGF) (49). Iloprost was also shown to suppress CTGF in the dermis of scleroderma patients (50). Further studies with dermal fibroblasts suggest a mechanism whereby stimulation of the IP receptor leads to PKA activation which in turn limits TGF-β induction of collagen and CTGF by suppressing the Ras/MEK/ERK cascade (49). Taken together, these studies support a model in which induction of COX-2 in the bleomycin-treated mice leads to increased production of prostacyclin. Prostacyclin acts on IP receptors expressed by fibroblasts to limit their response to injury, including their migration to the lung, proliferation, and production of collagen.

We cannot yet rule out the possibility that the increase in disease observed in the $IP^{-/-}$ mice is not the consequence of loss of the inhibitory actions of prostacyclin on the fibrotic response itself, but rather the result of an enhanced inflammatory response following bleomycin treatment. IP receptors are expressed on many leukocyte populations, and an increase in cAMP in these cells would be expected to limit migration and production of proinflammtory cytokines. In fact, the studies with the COX-2 mice in the V_2O_5 model support this interpretation (4). Future studies in which loss of the IP receptor is limited to specific populations should allow us to further define the mechanism by which COX-2-dependant prostacyclin production limits the development of fibrosis in the mouse lung.

In these studies, we show that loss of the prostacyclin receptor has a profound impact on the development of bleomycin-induced pulmonary fibrosis. $IP^{-/-}$ mice showed increased disease by all parameters examined. The magnitude of the physiological, biochemical, and pathological changes were similar to that of COX-$2^{-/-}$ mice, suggesting that loss of prostacyclin, and not loss of PGE_2, is responsible for the enhanced fibrotic response observed in our studies. The importance of COX-2-dependant prostacyclin production in limiting thrombotic events by counteracting the prothrombotic actions of thromboxane has been extensively explored (7). The studies reported here suggest that COX-2-dependant prostacyclin production may also have an important protective role in fibrotic diseases. In this regard, Murakami et al. recently examined the impact of a prostacyclin agonist on the development of fibrosis in the bleomycin model (35). Interpretation of their findings, however, is complicated by the fact that this compound also displays thromboxane synthase inhibitory activity. Treatment of mice with this agent provided protection against bleomycin-induced fibrosis when mice were treated throughout the entire three week time period over which the disease develops. In light of the reduced COX-2 expression observed in the lungs of humans with IPF (60), it will be important to determine whether IP receptor agonists can limit the severity of disease in the COX-$2^{-/-}$ mice. If prostacylin analogues can attenuate disease progression, particularly if administered after initial lung injury, then further exploration of these agents as a novel therapy for treatment of IPF and other causes of pulmonary fibrosis in humans may be warranted.

ACKNOWLEDGEMENTS

The authors thank Dr. Bob Bagnell and the UNC Microscopy Services Laboratory, Dr. Mitsuo Yamauchi and lab members for assistance in hydroxyproline measurements, Kim Burns for histology preparation, Dr. William Funkhouser and Subhashini Chandrashekaran for helpful discussions, and Anne Latour and Gita Madan for genotyping. This work was supported by National Institutes of Health grants HL-68141 (B.H. Koller), Cystic Fibrosis Foundation Grant Koller00Z0 (B.H. Koller), National Heart, Lung, and Blood Institute Grant HL-071802 (S.L. Tilley), and American Heart Association grant 0415427U (A. Kern Lovgren).

REFERENCES

1. American Thoracic Society. Idiopathic pulmonary fibrosis: diagnosis and treatment. International consensus statement. American Thoracic Society (ATS), and the European Respiratory Society (ERS). *Am J Respir Crit Care Med* 161: 646-664, 2000.

2. Beller TC, Friend DS, Maekawa A, Lam BK, Austen KF, and Kanaoka Y. Cysteinyl leukotriene 1 receptor controls the severity of chronic pulmonary inflammation and fibrosis. *Proc Natl Acad Sci U S A* 101: 3047-3052, 2004.

3. Bitterman PB, Wewers MD, Rennard SI, Adelberg S, and Crystal RG. Modulation of alveolar macrophage-driven fibroblast proliferation by alternative macrophage mediators. *J Clin Invest* 77: 700-708, 1986.

4. Bonner JC, Rice AB, Ingram JL, Moomaw CR, Nyska A, Bradbury A, Sessoms AR, Chulada PC, Morgan DL, Zeldin DC, and Langenbach R. Susceptibility of cyclooxygenase-2-deficient mice to pulmonary fibrogenesis. *Am J Pathol* 161: 459-470, 2002.

5. Borok Z, Gillissen A, Buhl R, Hoyt RF, Hubbard RC, Ozaki T, Rennard SI, and Crystal RG. Augmentation of functional prostaglandin E levels on the respiratory epithelial surface by aerosol administration of prostaglandin E. *Am Rev Respir Dis* 144: 1080-1084, 1991.

6. Brock TG, McNish RW, and Peters-Golden M. Arachidonic acid is preferentially metabolized by cyclooxygenase-2 to prostacyclin and prostaglandin E2. *J Biol Chem* 274: 11660-11666, 1999.

7. Cheng Y, Austin SC, Rocca B, Koller BH, Coffman TM, Grosser T, Lawson JA, and FitzGerald GA. Role of prostacyclin in the cardiovascular response to thromboxane A2. *Science* 296: 539-541, 2002.

8. Choung J, Taylor L, Thomas K, Zhou X, Kagan H, Yang X, and Polgar P. Role of EP2 receptors and cAMP in prostaglandin E2 regulated expression of type I collagen alpha1, lysyl oxidase, and cyclooxygenase-1 genes in human embryo lung fibroblasts. *J Cell Biochem* 71: 254-263, 1998.

9. Clark JG, Kostal KM, and Marino BA. Modulation of collagen production following bleomycin-induced pulmonary fibrosis in hamsters. Presence of a factor in lung that increases fibroblast prostaglandin E2 and cAMP and suppresses fibroblast proliferation and collagen production. *J Biol Chem* 257: 8098-8105, 1982.

10. Coggins KG, Latour A, Nguyen MS, Audoly L, Coffman TM, and Koller BH. Metabolism of PGE2 by prostaglandin dehydrogenase is essential for remodeling the ductus arteriosus. *Nat Med* 8: 91-92, 2002.

11. Coleman RA, Smith WL, and Narumiya S. International Union of Pharmacology classification of prostanoid receptors: properties, distribution, and structure of the receptors and their subtypes. *Pharmacol Rev* 46: 205-229, 1994.

12. Cruz-Gervis R, Stecenko AA, Dworski R, Lane KB, Loyd JE, Pierson R, King G, and Brigham KL. Altered prostanoid production by fibroblasts cultured from the lungs of human subjects with idiopathic pulmonary fibrosis. *Respir Res* 3: 17, 2002.

13. Fine A and Goldstein RH. The effect of PGE2 on the activation of quiescent lung fibroblasts. *Prostaglandins* 33: 903-913, 1987.

14. Fine A, Poliks CF, Donahue LP, Smith BD, and Goldstein RH. The differential effect of prostaglandin E2 on transforming growth factor-beta and insulin-induced collagen formation in lung fibroblasts. *J Biol Chem* 264: 16988-16991, 1989.

15. Fitzgerald GA. Coxibs and cardiovascular disease. *N Engl J Med* 351: 1709-1711, 2004.

16. Francois H, Athirakul K, Howell D, Dash R, Mao L, Kim HS, Rockman HA, Fitzgerald GA, Koller BH, and Coffman TM. Prostacyclin protects against elevated blood pressure and cardiac fibrosis. *Cell Metab* 2: 201-207, 2005.

17. Gallagher AM, Yu H, and Printz MP. Bradykinin-induced reductions in collagen gene expression involve prostacyclin. *Hypertension* 32: 84-88, 1998.

18. Goldstein RH and Polgar P. The effect and interaction of bradykinin and prostaglandins on protein and collagen production by lung fibroblasts. *J Biol Chem* 257: 8630-8633, 1982.

19. Gross TJ and Hunninghake GW. Idiopathic pulmonary fibrosis. *N Engl J Med* 345: 517-525, 2001.

20. Hantos Z, Daroczy B, Suki B, Nagy S, and Fredberg JJ. Input impedance and peripheral inhomogeneity of dog lungs. *J Appl Physiol* 72: 168-178, 1992.

21. Hartney JM, Coggins KG, Tilley SL, Jania LA, Kern Lovgren A, Audoly LP, and Koller BH. Prostaglandin E2 protects lower airways against broncoconstriction. *Am J Physiol Lung Cell Mol Physiol*, 2005.

22. Hodges RJ, Jenkins RG, Wheeler-Jones CP, Copeman DM, Bottoms SE, Bellingan GJ, Nanthakumar CB, Laurent GJ, Hart SL, Foster ML, and McAnulty RJ. Severity of lung injury in cyclooxygenase-2-deficient mice is dependent on reduced prostaglandin E(2) production. *Am J Pathol* 165: 1663-1676, 2004.

23. Huszar G, Maiocco J, and Naftolin F. Monitoring of collagen and collagen fragments in chromatography of protein mixtures. *Anal Biochem* 105: 424-429, 1980.

24. Irvin CG and Bates JH. Measuring the lung function in the mouse: the challenge of size. *Respir Res* 4: 4, 2003.

25. Keerthisingam CB, Jenkins RG, Harrison NK, Hernandez-Rodriguez NA, Booth H, Laurent GJ, Hart SL, Foster ML, and McAnulty RJ. Cyclooxygenase-2 deficiency results in a loss of the anti-proliferative response to transforming growth factor-beta in human fibrotic lung fibroblasts and promotes bleomycin-induced pulmonary fibrosis in mice. *Am J Pathol* 158: 1411-1422, 2001.

26. Kohyama T, Ertl RF, Valenti V, Spurzem J, Kawamoto M, Nakamura Y, Veys T, Allegra L, Romberger D, and Rennard SI. Prostaglandin E(2) inhibits fibroblast chemotaxis. *Am J Physiol Lung Cell Mol Physiol* 281: L1257-1263, 2001.

27. Kohyama T, Liu X, Kim HJ, Kobayashi T, Ertl RF, Wen FQ, Takizawa H, and Rennard SI. Prostacyclin analogs inhibit fibroblast migration. *Am J Physiol Lung Cell Mol Physiol* 283: L428-432, 2002.

28. Kolodsick JE, Peters-Golden M, Larios J, Toews GB, Thannickal VJ, and Moore BB. Prostaglandin E2 inhibits fibroblast to myofibroblast transition via E. prostanoid receptor 2 signaling and cyclic adenosine monophosphate elevation. *Am J Respir Cell Mol Biol* 29: 537-544, 2003.

29. Langenbach R, Morham SG, Tiano HF, Loftin CD, Ghanayem BI, Chulada PC, Mahler JF, Lee CA, Goulding EH, Kluckman KD, Kim HS, and Smithies O. Prostaglandin synthase 1 gene disruption in mice reduces arachidonic acid-induced inflammation and indomethacin-induced gastric ulceration. *Cell* 83: 483-492, 1995.

30. McAdam BF, Catella-Lawson F, Mardini IA, Kapoor S, Lawson JA, and FitzGerald GA. Systemic biosynthesis of prostacyclin by cyclooxygenase (COX)-2: the human pharmacology of a selective inhibitor of COX-2. *Proc Natl Acad Sci U S A* 96: 272-277, 1999.

31. McAnulty RJ, Hernandez-Rodriguez NA, Mutsaers SE, Coker RK, and Laurent GJ. Indomethacin suppresses the anti-proliferative effects of transforming growth factor-beta isoforms on fibroblast cell cultures. *Biochem J* 321 (Pt 3): 639-643, 1997.

32. Moore BB, Ballinger MN, White ES, Green ME, Herrygers AB, Wilke CA, Toews GB, and Peters-Golden M. Bleomycin-induced E prostanoid receptor changes alter fibroblast responses to prostaglandin E2. *J Immunol* 174: 5644-5649, 2005.

33. Morham SG, Langenbach R, Loftin CD, Tiano HF, Vouloumanos N, Jennette JC, Mahler JF, Kluckman KD, Ledford A, Lee CA, and Smithies O. Prostaglandin synthase 2 gene disruption causes severe renal pathology in the mouse. *Cell* 83: 473-482, 1995.

34. Murakami M, Nakashima K, Kamei D, Masuda S, Ishikawa Y, Ishii T, Ohmiya Y, Watanabe K, and Kudo I. Cellular prostaglandin E2 production by membrane-bound prostaglandin E synthase-2 via both cyclooxygenases-1 and -2. *J Biol Chem* 278: 37937-37947, 2003.

35. Murakami S, Nagaya N, Itoh T, Kataoka M, Iwase T, Horio T, Miyahara Y, Sakai Y, Kangawa K, and Kimura H. Prostacyclin agonist with thromboxane synthase inhibitory activity (ONO-1301) attenuates bleomycin-induced pulmonary fibrosis in mice. *Am J Physiol Lung Cell Mol Physiol* 290: L59-65, 2006.

36. Namba T, Sugimoto Y, Negishi M, Irie A, Ushikubi F, Kakizuka A, Ito S, Ichikawa A, and Narumiya S. Alternative splicing of C-terminal tail of prostaglandin E receptor subtype EP3 determines G-protein specificity. *Nature* 365: 166-170, 1993.

37. Narumiya S, Sugimoto Y, and Ushikubi F. Prostanoid receptors: structures, properties, and functions. *Physiol Rev* 79: 1193-1226, 1999.

38. Nava S and Rubini F. Lung and chest wall mechanics in ventilated patients with end stage idiopathic pulmonary fibrosis. *Thorax* 54: 390-395, 1999.

39. Nguyen M, Camenisch T, Snouwaert JN, Hicks E, Coffman TM, Anderson PA, Malouf NN, and Koller BH. The prostaglandin receptor EP4 triggers remodelling of the cardiovascular system at birth. *Nature* 390: 78-81, 1997.

40. Oida H, Namba T, Sugimoto Y, Ushikubi F, Ohishi H, Ichikawa A, and Narumiya S. In situ hybridization studies of prostacyclin receptor mRNA expression in various mouse organs. *Br J Pharmacol* 116: 2828-2837, 1995.

41. Patrono C. Aspirin as an antiplatelet drug. *N Engl J Med* 330: 1287-1294, 1994.

42. Plum J, Huang C, Grabensee B, Schror K, and Meyer-Kirchrath J. Prostacyclin enhances the expression of LPS/INF-gamma-induced nitric oxide synthase in human monocytes. *Nephron* 91: 391-398, 2002.

43. Regan JW. EP2 and EP4 prostanoid receptor signaling. *Life Sci* 74: 143-153, 2003.

44. Rose F, Zwick K, Ghofrani HA, Sibelius U, Seeger W, Walmrath D, and Grimminger F. Prostacyclin enhances stretch-induced surfactant secretion in alveolar epithelial type II cells. *Am J Respir Crit Care Med* 160: 846-851, 1999.

45. Salazar E and Knowles JH. An Analysis of Pressure-Volume Characteristics of the Lungs. *J Appl Physiol* 19: 97-104, 1964.

46. Schuessler TF and Bates JH. A computer-controlled research ventilator for small animals: design and evaluation. *IEEE Trans Biomed Eng* 42: 860-866, 1995.

47. Selman M, King TE, and Pardo A. Idiopathic pulmonary fibrosis: prevailing and evolving hypotheses about its pathogenesis and implications for therapy. *Ann Intern Med* 134: 136-151, 2001.

48. Smith WL, Garavito RM, and DeWitt DL. Prostaglandin endoperoxide H synthases (cyclooxygenases)-1 and -2. *J Biol Chem* 271: 33157-33160, 1996.

49. Stratton R, Rajkumar V, Ponticos M, Nichols B, Shiwen X, Black CM, Abraham DJ, and Leask A. Prostacyclin derivatives prevent the fibrotic response to TGF-beta by inhibiting the Ras/MEK/ERK pathway. *Faseb J* 16: 1949-1951, 2002.

50. Stratton R, Shiwen X, Martini G, Holmes A, Leask A, Haberberger T, Martin GR, Black CM, and Abraham D. Iloprost suppresses connective tissue growth factor production in fibroblasts and in the skin of scleroderma patients. *J Clin Invest* 108: 241-250, 2001.

51. Sugimoto Y, Negishi M, Hayashi Y, Namba T, Honda A, Watabe A, Hirata M, Narumiya S, and Ichikawa A. Two isoforms of the EP3 receptor with different carboxyl-terminal domains. Identical ligand binding properties and different coupling properties with Gi proteins. *J Biol Chem* 268: 2712-2718, 1993.

52. Tanioka T, Nakatani Y, Semmyo N, Murakami M, and Kudo I. Molecular identification of cytosolic prostaglandin E2 synthase that is functionally coupled with cyclooxygenase-1 in immediate prostaglandin E2 biosynthesis. *J Biol Chem* 275: 32775-32782, 2000.

53. Tilley SL, Audoly LP, Hicks EH, Kim HS, Flannery PJ, Coffman TM, and Koller BH. Reproductive failure and reduced blood pressure in mice lacking the EP2 prostaglandin E2 receptor. *J Clin Invest* 103: 1539-1545, 1999.

54. Trebino CE, Stock JL, Gibbons CP, Naiman BM, Wachtmann TS, Umland JP, Pandher K, Lapointe JM, Saha S, Roach ML, Carter D, Thomas NA, Durtschi BA, McNeish JD, Hambor JE, Jakobsson PJ, Carty TJ, Perez JR, and Audoly LP. Impaired inflammatory and pain responses in mice lacking an inducible prostaglandin E synthase. *Proc Natl Acad Sci U S A* 100: 9044-9049, 2003.

55. Tuder RM, Cool CD, Geraci MW, Wang J, Abman SH, Wright L, Badesch D, and Voelkel NF. Prostacyclin synthase expression is decreased in lungs from patients with severe pulmonary hypertension. *Am J Respir Crit Care Med* 159: 1925-1932, 1999.

56. Uematsu S, Matsumoto M, Takeda K, and Akira S. Lipopolysaccharide-dependent prostaglandin E(2) production is regulated by the glutathione-dependent prostaglandin E(2) synthase gene induced by the Toll-like receptor 4/MyD88/NF-IL6 pathway. *J Immunol* 168: 5811-5816, 2002.

57. Ueno N, Murakami M, Tanioka T, Fujimori K, Tanabe T, Urade Y, and Kudo I. Coupling between cyclooxygenase, terminal prostanoid synthase, and phospholipase A2. *J Biol Chem* 276: 34918-34927, 2001.

58. Vancheri C, Sortino MA, Tomaselli V, Mastruzzo C, Condorelli F, Bellistri G, Pistorio MP, Canonico PL, and Crimi N. Different expression of TNF-alpha receptors and prostaglandin E(2)Production in normal and fibrotic lung fibroblasts: potential implications for the evolution of the inflammatory process. *Am J Respir Cell Mol Biol* 22: 628-634, 2000.

59. Watabe A, Sugimoto Y, Honda A, Irie A, Namba T, Negishi M, Ito S, Narumiya S, and Ichikawa A. Cloning and expression of cDNA for a mouse EP1 subtype of prostaglandin E receptor. *J Biol Chem* 268: 20175-20178, 1993.

60. Wilborn J, Crofford LJ, Burdick MD, Kunkel SL, Strieter RM, and Peters-Golden M. Cultured lung fibroblasts isolated from patients with idiopathic pulmonary fibrosis have a diminished capacity to synthesize prostaglandin E2 and to express cyclooxygenase-2. *J Clin Invest* 95: 1861-1868, 1995.

61. Wise H, Qian YM, and Jones RL. A study of prostacyclin mimetics distinguishes neuronal from neutrophil IP receptors. *Eur J Pharmacol* 278: 265-269, 1995.

62. Yu H, Gallagher AM, Garfin PM, and Printz MP. Prostacyclin release by rat cardiac fibroblasts: inhibition of collagen expression. *Hypertension* 30: 1047-1053, 1997.

63. Zhang HY, Gharaee-Kermani M, Zhang K, Karmiol S, and Phan SH. Lung fibroblast alpha-smooth muscle actin expression and contractile phenotype in bleomycin-induced pulmonary fibrosis. *Am J Pathol* 148: 527-537, 1996.

64. Zhang K, Rekhter MD, Gordon D, and Phan SH. Myofibroblasts and their role in lung collagen gene expression during pulmonary fibrosis. A combined immunohistochemical and in situ hybridization study. *Am J Pathol* 145: 114-125, 1994.

CHAPTER 4

Role of thromboxane and inflammation in the enhanced disease susceptibility of $IP^{-/-}$ mice

INTRODUCTION

Idiopathic pulmonary fibrosis is a relentless, fatal disease characterized by proliferation of mesenchymal cell populations and extracellular matrix deposition. This leads to alterations in lung architecture and impaired gas exchange. Current concepts highlight the pathobiology of pulmonary fibrosis as an epithelial-fibroblastic disorder. Microinjuries to the lung induce epithelial cell activation which causes the release of cytokines and other mediators to activate fibroblasts. This activation includes migration to the injured site, proliferation, and transformation into myofibroblasts. Myofibroblasts disrupt the basement membrane and may enhance epithelial cell apoptosis. The role of inflammation in the progression of disease is currently debatable. The lack in efficacy of corticosteroid therapy for patients with idiopathic pulmonary fibrosis has largely prompted the current concept that inflammation plays little to no role in disease pathogenesis. However, inflammatory cells can not be ignored due to their release of profibrotic and antifibrotic mediators that can alter the phenotype of epithelial and fibroblast cells.

In the previous chapter, we demonstrated an important role for prostacyclin in the protection against pulmonary fibrosis. Prostacyclin is best known for its role in preventing platelet aggregation and being a potent vasodilator. Due to these primary roles, prostacyclin analogues are the primary treatment for patients with pulmonary hypertension. However, in the context of the pathobiology of pulmonary fibrosis, prostacyclin can inhibit fibroblast proliferation and migration (9, 26). Also, prostacyclin analogues can inhibit collagen production in cardiac and dermal fibroblasts (20, 21, 26). In addition, the prostacyclin receptor, IP, is expressed by lymphocytes and neutrophils, which are recruited to the lung after bleomycin administration and secrete mediators that play intricate roles in disease

development (13, 25). Thus, prostacyclin has many potential mechanisms for inhibiting the progression of bleomycin-induced pulmonary fibrosis.

Thromboxane is another lipid mediator produced from COX-derived PGH_2. The actions of thromboxane antagonize those of prostacyclin. The best known role of thromboxane is as a vasoconstrictor and a facilitator of platelet aggregation. However, thromboxane also has both pro-inflammatory and pro-fibrotic mechanisms that oppose prostacyclin. The balance between these two mediators has recently been demonstrated to be an important homeostatic mechanism, and disruption of this intricate balance leads to disease pathogenesis. Recent studies have demonstrated that loss of prostacyclin increases salt-sensitive blood pressure, cardiac hypertrophy, and cardiac fibrosis as well as the proliferative response to vascular injury (5, 7). In all cases, simultaneous loss of thromboxane ameliorates this increase in disease.

In this chapter, we investigate the role that prostacyclin and its counterpart thromboxane play in the development of pulmonary fibrosis. The bleomycin-induced fibrosis model is characterized by an initial influx of leukocytes that instigate the fibrotic process. Our data suggests that prostacyclin may have an inhibitory effect on inflammatory cell recruitment within the early stages of inflammation, particularily neutrophil recruitment. We show that TNF-α, a key pro-inflammatory cytokine in the development of pulmonary fibrosis, may not play a role in this increase in neutrophil recruitment and disease susceptibility. Interestingly, we demonstrate that an alteration in the intricate balance between thromboxane and prostacyclin may play an important role in disease pathogenesis.

MATERIALS AND METHODS

Experimental Animals

All studies were conducted in accordance with the National Institutes of Health Guide for the Care and Use of Laboratory Animals as well as the Institutional Animal Care and Use Committee guidelines of the University of North Carolina at Chapel Hill. All experiments were carried out using 8-12 week old mice unless otherwise specified. Mice lacking IP and IP/TP were generated as previously described (5, 23).

Bleomycin Treatment

Mice were anesthetized with approximately 20µl/g body weight of 2,2,2-tribromoethanol and administered 50 µl of saline or bleomycin (.05U unless specified otherwise) diluted in saline by intratracheal instillation.

Bronchoalveolar Lavage

At various time points, bronchoalveolar lavage (BAL) was performed (1.0 ml of Hank's saline solution x 3). The total number of BALF cells was determined using a hemacytometer. A differential cell count was conducted on a cytospin prepared from 200 µl of BAL fluid and stained with Diff-Quik solution (Sigma) according to manufacturer's instructions.

Cytokine Measurements

Lung samples were homogenized in 2 ml PBS w/ protease inhibitors and sonicated. After centrifugation for 10 minutes at 3500rpm at 4°C, the supernatant was removed and frozen at -

80°C. Before use, samples were spun down at max speed to remove particulate matter. TNF-α levels were quantitated by using enzyme immunoassay kits (BD Opt EIA).

Measurements of lung mechanics

Mice were anesthetized 21 days after bleomycin administration with 70-90 mg/kg pentobarbital sodium (American Pharmaceutical Partners, Los Angeles, CA), tracheostomized, and mechanically ventilated at a rate of 350 breaths/min, tidal volume of 6 cc/kg, and positive end-expiratory pressure of 3-4 cm H_2O with a computer-controlled small-animal ventilator (Scireq, Montreal, Canada). Once ventilated, mice were paralyzed with 0.8 mg/kg pancuronium bromide (Baxter Healthcare Corp., Deerfield, IL). Using custom designed software (Flexivent, Scireq), airway pressure, volume, and airflow were recorded using a precisely controlled piston during maneuvers to evaluate lung mechanics.

Pressure-volume curves were generated by a sequential delivery of 7 increments of air into the lungs from resting pressure to total lung capacity followed by 7 expiratory steps during which air was incrementally released. Plateau pressure was recorded when airflow returned to zero at each step. The Salazar-Knowles equation (Equation 1) was applied to the plateau pressure measurements obtained between total lung capacity (TLC) and functional residual capacity (FRC) during the expiratory phase of the pressure-volume loop to determine static compliance (C_{st}) of the lung.

$V = V_{max} - Ae^{-KP}$ (Equation 1)

Where V_{max} = volume extrapolated to infinite P, V = lung volume above FRC, A and K are constants

RESULTS

Role of prostacyclin in leukocyte recruitment after bleomycin treatment

Prostanoids play an important role in modulating the inflammatory response in acute and chronic lung diseases. After exposure to vanadium pentoxide, COX-$2^{-/-}$ mice had a significant increase in inflammatory cell infiltration into the lung compared to wild-type mice 7 days after treatment suggesting an anti-inflammatory role for prostanoids in acute lung injury (2). Consistent with this, we measured a significant increase in neutrophils 7 days after bleomycin treatment in the COX-$2^{-/-}$ mice (18.1±6.0 for wild-type and 39.0±4.0 for COX-$2^{-/-}$, $p < .05$). To investigate the role of prostacyclin in the inflammatory response, we quantitated the total number of leukocytes in BALF 3 and 7 days after bleomycin administration in $IP^{-/-}$ and wild-type mice. Interestingly, quantitation of leukocytes in BALF 3 days after bleomycin treatment revealed a significant increase in the early inflammatory response in the $IP^{-/-}$ mice compared to the wild-type mice (Figure 1A). To determine whether the composition of the inflammatory response differed between groups, differential staining was performed to identify the leukocyte populations. The $IP^{-/-}$ mice exhibited a significant increase in neutrophils upon differential analysis of the BALF (Figure 1B). Thus, the magnitude and the composition of the initial inflammatory response are altered in the $IP^{-/-}$ mice.

Our preliminary studies demonstrated that, in wild-type mice, the initial influx of leukocytes is higher 7 days after bleomycin treatment compared to earlier time points (34.7±5.4 for day 7 compared to 24.3±2.6 on day 4 and 18.3±3.3 on day 1). To determine whether this increase in inflammatory cell recruitment continued through the peak of inflammation, we measured the total cell counts in BALF of $IP^{-/-}$ mice and wild-type mice 7

days after bleomycin treatment. As shown in Figure 2A, by day 7, both groups recruited a similar number of inflammatory cells to the lung. No significant alterations in the accumulation of neutrophils, macrophages, or lymphocytes was noted in the BALF 7 days after bleomycin treatment (Figure 2B).

After V_2O_5 exposure, along with increased inflammation, the COX-$2^{-/-}$ mice had a significant increase in TNF-α levels 7 days after bleomycin treatment (2). We analyzed whole lung homogenates from $IP^{-/-}$ and wild-type mice and demonstrated a significant increase in TNF-α levels 7 days after bleomycin administration. However, no significant difference was measured between the two genotypes (108.8 pg/ml increase above salines for wild-type mice and 108.7 pg/ml increase above salines for $IP^{-/-}$ mice).

Respiratory Mechanics in Aged $IP^{-/-}$ mice

Our collaborators recently reported an enhanced fibrotic response in hearts of $IP^{-/-}$ mice, and this response was dramatically increased in 17-month-old mice compared to 6-month-old mice (7). To determine if loss of prostacyclin can cause alterations in the fibroblast phenotypes in $IP^{-/-}$ mice without an initial inflammatory response, we analyzed the lung mechanics and examined the lung architecture of 12-month-old mice. In previous studies, we have used C57BL/6 mice; however, since 129/SvEv are more susceptible to fibrosis, we analyzed both strains of mice in these experiments. Analysis of static compliance measurements demonstrated no difference between the $IP^{-/-}$ mice and wild-type mice in either strain (Figure 3). In addition, histological analysis of the lungs revealed no alterations in lung architecture in the $IP^{-/-}$ mice.

Role of the thromboxane/prostacyclin balance in bleomycin-induced pulmonary fibrosis

Opposite of prostacyclin, thromboxane promotes fibroblast proliferation and lung inflammation (12). We demonstrated in the previous chapter that prostacyclin protects against bleomycin-induced pulmonary fibrosis. Since thromboxane has both pro-fibrotic and pro-inflammatory properties, we investigated the hypothesis that, contrary to prostacyclin, loss of this mediator may be protective against pulmonary fibrosis. We examined mice lacking the thromboxane receptor, TP. Congenic C57BL/6 $TP^{-/-}$ and wild-type mice were administered bleomycin or saline, and disease was assessed 21 days later by lung mechanics. As expected, no difference was observed between the static compliance of the saline-treated $TP^{-/-}$ and wild-type lungs. After bleomycin administration, both $TP^{-/-}$ and wild-type mice had a similar decrease in static compliance, so, unlike prostacyclin, loss of thromboxane alone is not enough to alter disease susceptibility (Figure 4A).

The balance of thromboxane and prostacyclin is important for maintaining cardiopulmonary homeostasis, and alterations in this balance can contribute to disease pathogenesis. Unrestrained thromboxane, upon loss of prostacyclin in the $IP^{-/-}$ mice, may be important for enhancing disease progression. To test this hypothesis, double knockouts, 129/SvEv $IP^{-/-}/TP^{-/-}$ mice, were administered bleomycin and disease progression was compared to 129/SvEv $IP^{-/-}$ mice and wild-type mice. As with the C57BL/6 $IP^{-/-}$ mice, the 129/SvEv $IP^{-/-}$ mice had a significant decrease in static compliance compared to the wild-type mice. Interestingly, the $IP^{-/-}/TP^{-/-}$ mice did not have a statistically significant decrease in static compliance compared to the wild-type mice (Figure 4B). Although the static compliance was not completely returned to wild-type values in the $IP^{-/-}/TP^{-/-}$ mice, these mice appear to have an ameliorated fibrotic response to bleomycin.

Figure 4.1

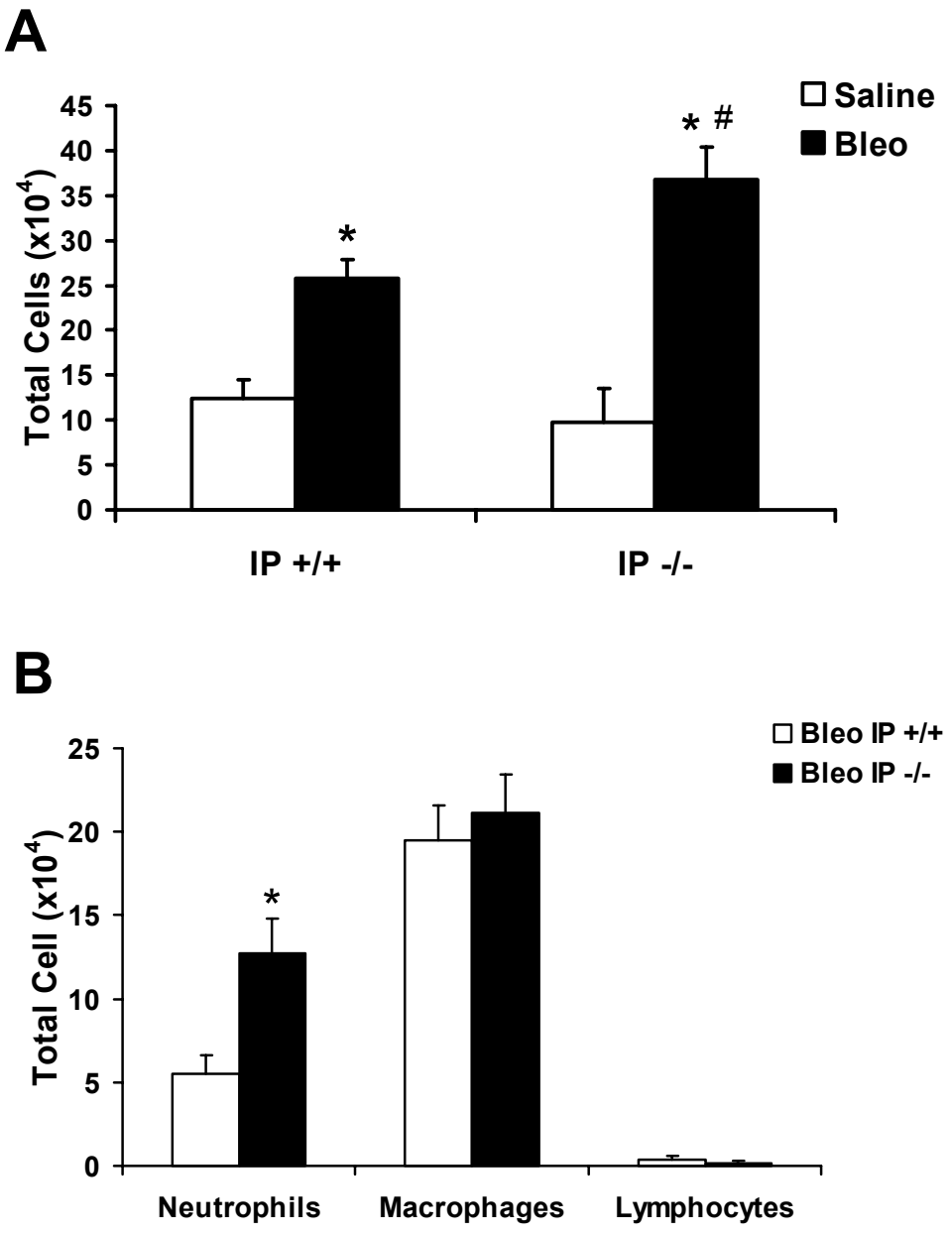
A
Saline
Bleo
Total Cells (x10^4)
45
40
35
30
25
20
15
10
5
0
*
* #
IP +/+
IP -/-
B
Bleo IP +/+
Bleo IP -/-
Total Cell (x10^4)
25
20
15
10
5
0
*
Neutrophils
Macrophages
Lymphocytes

Figure 4.1. Enhanced inflammatory response and neutrophilia in $IP^{-/-}$ mice 3 days after bleomycin administration. A) A significant increase in cellularity was measured in the bronchoalveolar lavage fluid (BALF) of $IP^{-/-}$ mice compared to wild-type mice 3 days after bleomycin treatment. * $p < .05$ compared to corresponding saline value. # $p < .05$ compared to wild-type bleomycin value. $n = 6$. B) Differential staining of leukocytes revealed an increased number of neutrophils in the BALF of the $IP^{-/-}$ mice compared to the wild-type mice. * $p < .05$ compared to wild-type bleomycin value. $n = 6$.

Figure 4.2

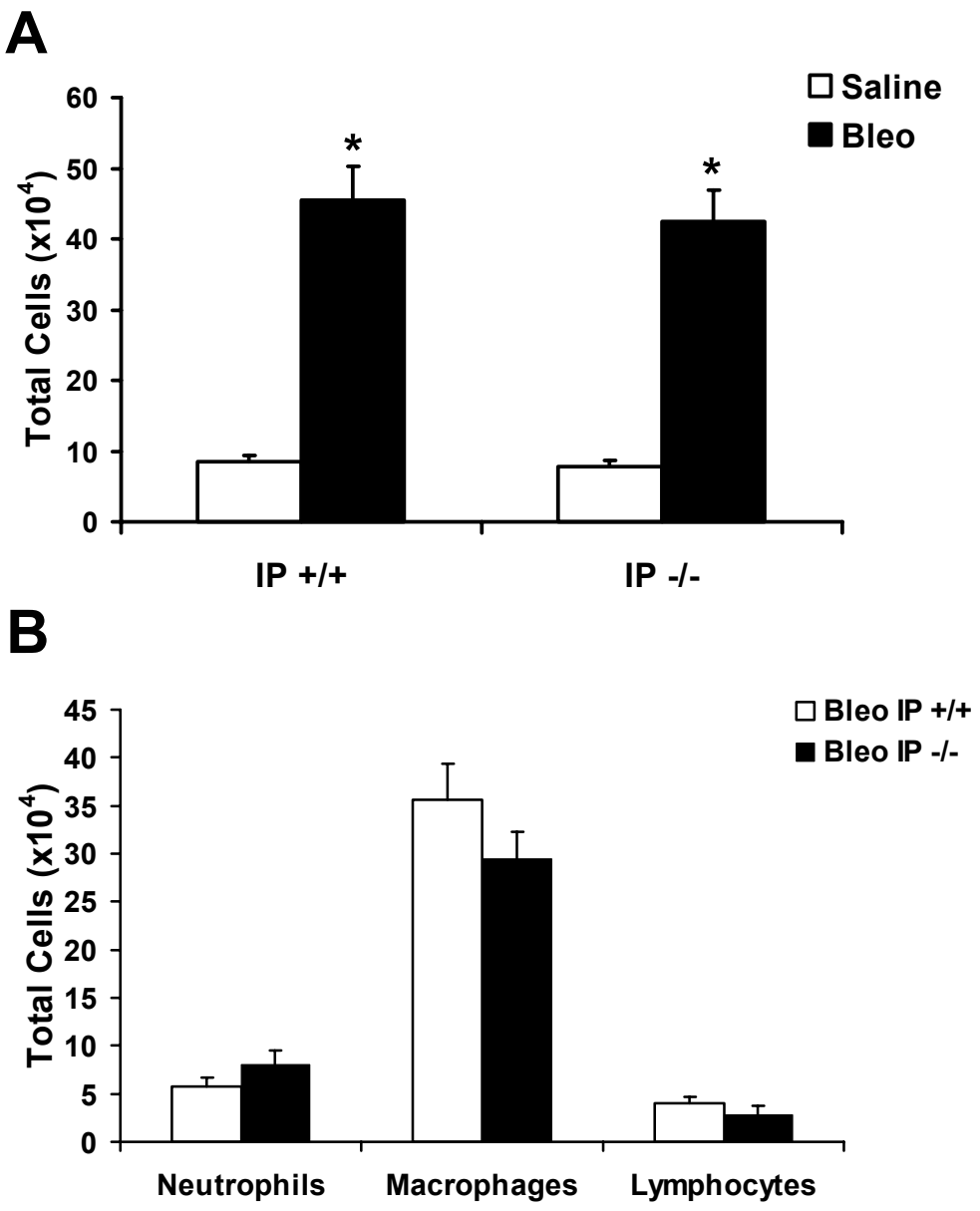
A
Saline
Bleo
Total Cells (x10^4)
60
50
40
30
20
10
0
*
*
IP +/+
IP -/-
B
Bleo IP +/+
Bleo IP -/-
Total Cells (x10^4)
45
40
35
30
25
20
15
10
5
0
Neutrophils
Macrophages
Lymphocytes

Figure 4.2 Similar magnitude of inflammatory cell recruitment 7 days after bleomycin administration in the $IP^{-/-}$ mice compared to the wild-type mice. A) Total inflammatory cell counts were similar in the BALF of $IP^{-/-}$ mice and wild-type mice 7 days after bleomycin treatment. * $p < .05$ compared to corresponding saline value. $n = 10$. B) Differential staining of leukocytes revealed similar recruitment of neutrophils, macrophages, and lymphocytes to the lungs of $IP^{-/-}$ mice compared to the wild-type mice 7 days after bleomycin treatment. $n = 10$.

Figure 4.3

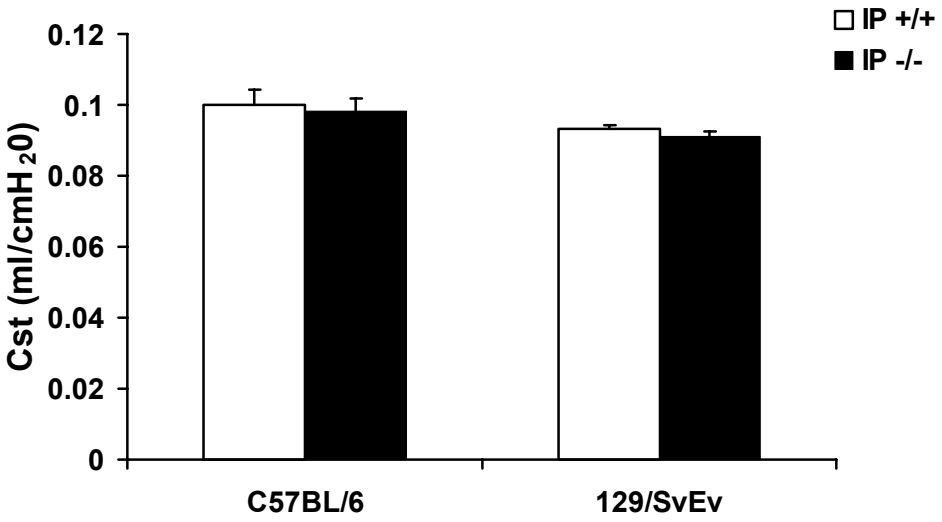

Figure 4.3 Similar lung mechanics in 12-month-old $IP^{-/-}$ and wild-type mice. Static compliance was measured in anesthetized, paralyzed, and mechanically ventilated mice and determined by fitting the Salazar-Knowles equation to pressure-volume curves. Two different background strains, C57BL/6 and 129/SvEv, were analyzed. C57BL/6 $IP^{+/+}$, n = 5; C57BL/6 $IP^{-/-}$, n = 9; 129/SvEv $IP^{+/+}$, n = 7; 129/SvEv $IP^{-/-}$, n = 6.

Figure 4.4

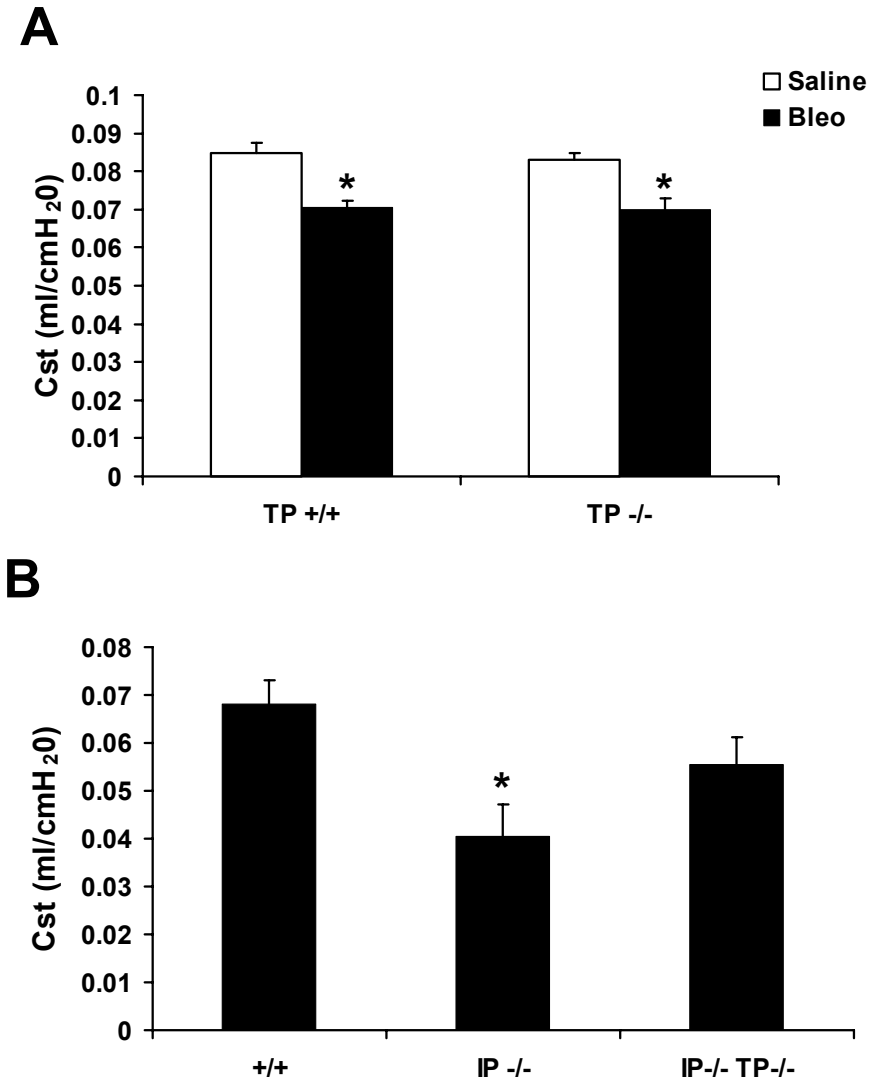
A
Saline
Bleo
0.1
0.09
0.08
0.07
0.06
0.05
0.04
0.03
0.02
0.01
0
Cst (ml/cmH20)
*
*
TP +/+
TP -/-
B
0.08
0.07
0.06
0.05
0.04
0.03
0.02
0.01
0
Cst (ml/cmH20)
*
+/+
IP -/-
IP-/- TP-/-

Figure 4.4 Analysis of lung mechanics in $TP^{-/-}$, $IP^{-/-}/TP^{-/-}$, and wild-type mice after bleomycin administration. Lung mechanics were measured in anesthetized, paralyzed, and mechanically ventilated mice 21 days following bleomycin or saline instillation. **A)** Static compliance (Cst) determined by fitting the Salazar-Knowles equation to pressure-volume curves revealed similar disease susceptibility in the $TP^{-/-}$ and wild-type mice after bleomycin administration. * $p < .05$ compared with corresponding saline values. n = 8-9 animals. **B)** 129/SvEv $IP^{-/-}$ mice demonstrate an increased susceptibility to disease, and this enhanced response is ameliorated in double knockout mice (129/SvEv $IP^{-/-}/TP^{-/-}$). * $p < .05$ compared with wild-type bleomycin value. n = 4-7 animals.

DISCUSSION

The magnitude of the initial inflammatory response in the bleomycin-induced fibrosis model is often correlated with enhanced fibrosis at later stages (19). However, numerous studies have also demonstrated an increase in fibrosis without alterations in the inflammatory response. For example, pulmonary fibrosis is more severe in mice deficient in GM-CSF despite the fact that the recruitment of inflammatory cells is similar compared to wild-type animals (10). In this chapter, we demonstrate that loss of prostacyclin signaling caused an increase of inflammatory cell recruitment to the lungs after the initial injury. In particular, a significant increase in neutrophils was observed. If future experiments confirm these preliminary studies, this suggests that prostacyclin may play an inhibitory role in the initial influx of leukocytes, especially neutrophils, after bleomycin treatment.

The data presented here only begins to unravel the complexity of the inflammatory process in the prostacyclin deficient mice. Of particular interest is the fact that the $IP^{-/-}$ mice had a significant increase in total cells and neutrophils in the BALF 3 days, but not 7 days, after treatment. The $IP^{-/-}$ mice may have an earlier peak in the inflammatory cell recruitment and then remain constant while the wild-type mice peak later. The possibility also exists that, at a certain point, large numbers of inflammatory cells become trapped in the interstitium, so cell counts from the BALF may not reflect the total number of cells actually recruited to the lung. Histological analysis or leukocyte purification from whole lung collagenase digests would reveal the localization and number of cells in the alveolar space and the pulmonary interstitium. In addition to cell recruitment, variations in cell count could reflect alterations in apoptosis and subsequent removal by macrophages. Failure to clear unwanted cells by apoptosis can lead to abnormal repair and continued release of toxic

mediators. Further experimentation will be necessary to determine the exact mechanism of cell recruitment and cell death in the $IP^{-/-}$ mice.

The alterations in the inflammatory response may or may not be relevant in enhancing disease susceptibility, especially since the precise cause-effect relationship of inflammation and disease progression is unclear. However, enhanced neutrophilia has been linked to a worse prognosis for disease progression. In one study, neutrophils were shown to induce apoptosis of lung epithelial cells, possibly leading to impaired reepithelialization, aberrant remodeling, and enhanced disease progression (18). Also, in an additional study, mice deficient in γ-glutamyl transpeptidase (GGT) were protected from pulmonary fibrosis, yet inflammation after exposure to bleomycin was generally similar to wild-type mice (16). However, on closer analysis, the $GGT^{-/-}$ were observed to have fewer neutrophils and more lymphocytes and macrophages than wild-type. Immunohistochemical analysis showed high expression of matrix metalloproteinase 9 (MMP-9) in neutrophils, as well as alveolar epithelia, and this expression was lacking in the $GGT^{-/-}$ mice. The authors conclude that an increased number of neutrophils and MMP-9 expression can enhance disease progression, so the $GGT^{-/-}$ animals were protected from disease as a result of decreased neutrophil infiltration and subsequent MMP activity.

MMP-9 is responsible for the degradation of extracellular matrix, primarily type IV collagen. Underneath the alveolar epithelium is the basement membrane, which is composed of type IV collagen, fibronectin, laminin, and proteoglycans. Disruption of this basement membrane and impaired re-epithelialization are key factors in the progression of pulmonary fibrosis. MMP-9 has been implicated as a factor responsible for the breakdown of the basement membrane and extracellular matrix components to perpetuate the fibrotic response

(8, 17). In support of its role in fibrosis, MMPs are highly expressed in the lung parenchyma and in the airways of IPF patients (8). In addition, studies have demonstrated that a substantial amount of MMPs are stored in the granules of neutrophils (1). Thus, the increased neutrophil recruitment in the $IP^{-/-}$ mice may lead to basement membrane disruption due to enhanced MMP-9 activity. Our preliminary experiments have demonstrated no significant increase in MMP-9 expression by RT-PCR in whole lung homogenates of $IP^{-/-}$ mice (data not shown). However, the localization or activation of MMP-9 may be more important than mRNA expression. Thus, immunohistochemical examination and zymography are required to confirm whether MMP-9 plays a role in enhanced disease progression.

Besides MMPs, neutrophils have a large number of toxic molecules in their granules, such as neutrophil elastase (3). Similar to MMP-9, neutrophil elastase can degrade elastin, collagen type III and IV, laminin, and fibronectin (24). Neutrophil elastase can also activate MMPs by cleaving their pro-enzyme form (15). In support of its role in disease progression, the amount of neutrophil elastase is enhanced in the BALF of IPF patients (14). Also, an inhibitor of neutrophil elastase limited the fibrotic response to bleomycin treatment in mice (22). Enhanced neutrophilia in the $IP^{-/-}$ mice may lead to alterations in any number of toxic enzymes, such as neutrophil elastase, which could be responsible for altering disease progression in the $IP^{-/-}$ mice.

The bleomycin-induced fibrosis model is currently the best characterized and most often utilized mouse model for studying idiopathic pulmonary fibrosis. Unfortunately, this model is characterized by an initial influx of leukocytes that is responsible for perpetuating the fibrotic response. In the human disease, the initial cause is unknown, and the role of

inflammation in disease progression is debatable and most likely not as dramatic as its role in the bleomycin model. Thus, when using this model to find novel therapeutics, this difference in the initial inflammatory response must be taken into account. A recent study demonstrated that the inflammatory phase is the first ten days after bleomycin administration and the fibrotic phase follows thereafter. This group demonstrated a peak in pro-inflammatory mediators from days 3-9, and pro-fibrotic mediators were elevated from day 9 through the end of the experiment suggesting a "switch" between these two phases (4). Novel therapeutics that are efficacious after administration during the fibrotic phase provide promise to patients with pulmonary fibrosis who usually present during late stages of disease. In this regard, a recent study examined the impact of a prostacyclin agonist on the development of fibrosis in the bleomycin model (11). Treatment of mice with this agent provided protection against bleomycin-induced fibrosis; however, protection was only noted when mice were treated throughout the entire three week time period over which the disease develops and not when given after the inflammatory phase. This is consistent with our finding that prostacyclin plays a role in the initial inflammatory response. However, in light of the reduced COX-2 expression observed in the lungs of humans with IPF, it will be important to determine whether delivery of prostacyclin analogues to COX-2$^{-/-}$ mice during the fibrotic stage could alter disease progression. This would shed light on whether prostacyclin indeed plays a role strictly in the inflammatory response or if it plays a role in the fibrotic process as well.

To determine if prostacyclin may play a role in altering fibrotic mediators without an initial inflammatory response, we analyzed the lung architecture and respiratory mechanics in 12-month-old mice lacking the prostacyclin receptor. IP$^{-/-}$ mice have enhanced cardiac

fibrosis as they age, so if prostacyclin is an important pro-fibrotic mediator, loss of this signaling over a lifetime may trigger alterations in the phenotype of lung fibroblasts. However, no difference was measured in the static compliance of these mice on either the C57BL/6 or 129/SvEv background. Upon histological analysis, no differences were noted in the architecture of the lung. Interestingly, the 129/SvEv strain had small areas of increased inflammation in their lungs at 12 months of age; however, this was not dependent on loss of IP.

The balance of thromboxane and prostacyclin has recently been implicated as essential for homeostasis, and alterations lead to enhanced disease susceptibility. For example, loss of cardioprotective prostacyclin and continued production of thromboxane is implicated in the increased risk of thrombotic events in patients taking COX-2-specific inhibitors (5). Also, in fibroblasts from IPF patients, altered prostanoid metabolism was measured, and the investigators highlighted the physiological imbalance between prostacyclin and thromboxane as important for altering fibroblast phenotypes toward fibrogenesis. They concluded that the lower ratio of prostacyclin to thromboxane may play an important role in the pathogenesis of IPF (6). Our data supports their conclusions. We demonstrated that the enhanced disease in the $IP^{-/-}$ mice after bleomycin treatment was ameliorated with simultaneous deletion of TP. If future experiments confirm these preliminary studies, our data suggests that an essential balance exists between thromboxane and prostacyclin in the bleomycin-induced fibrosis model. A shift in prostanoid profiles may lead to enhanced inflammation and subsequent fibrosis.

In this chapter, our data suggests that prostacyclin may play a role in the early inflammatory response to bleomycin-induced lung injury by inhibiting the initial influx of

leukocytes, especially neutrophils. This is consistent with the fact that IP is expressed on neutrophils, as well as other leukocyte populations (13, 25). Previous studies with the COX-$2^{-/-}$ mice demonstrated a significant increase in the key proinflammatory cytokine, TNF-α, 7 days after bleomycin treatment, and the investigators suggest that this increase contributes to the enhanced disease observed in the COX-$2^{-/-}$ mice. However, we did not measure a significant increase in TNF-α in the $IP^{-/-}$ mice compared to the wild-type mice 7 days after bleomycin treatment. In addition, our studies demonstrated enhanced neutrophil recruitment in the COX-$2^{-/-}$ mice 7 days after bleomycin treatment while the $IP^{-/-}$ mice had enhanced neutrophil recruitment 3 days after treatment. These variations raise the question whether the enhanced disease in the COX-$2^{-/-}$ mice and the $IP^{-/-}$ mice is through the same mechanism. One possible explanation is that the background of these mice is different and could be causing the slight alterations in the temporal regulation of these pathways. However, further experimentation is necessary to determine the mechanisms of cell recruitment and cell death to truly answer whether the COX-$2^{-/-}$ and the $IP^{-/-}$ mice respond similarily to bleomycin-induced lung injury.

REFERENCES

1. Atkinson JJ and Senior RM. Matrix metalloproteinase-9 in lung remodeling. *Am J Respir Cell Mol Biol* 28: 12-24, 2003.

2. Bonner JC, Rice AB, Ingram JL, Moomaw CR, Nyska A, Bradbury A, Sessoms AR, Chulada PC, Morgan DL, Zeldin DC, and Langenbach R. Susceptibility of cyclooxygenase-2-deficient mice to pulmonary fibrogenesis. *Am J Pathol* 161: 459-470, 2002.

3. Borregaard N, Lollike K, Kjeldsen L, Sengelov H, Bastholm L, Nielsen MH, and Bainton DF. Human neutrophil granules and secretory vesicles. *Eur J Haematol* 51: 187-198, 1993.

4. Chaudhary NI, Schnapp A, and Park JE. Pharmacologic differentiation of inflammation and fibrosis in the rat bleomycin model. *Am J Respir Crit Care Med* 173: 769-776, 2006.

5. Cheng Y, Austin SC, Rocca B, Koller BH, Coffman TM, Grosser T, Lawson JA, and FitzGerald GA. Role of prostacyclin in the cardiovascular response to thromboxane A2. *Science* 296: 539-541, 2002.

6. Cruz-Gervis R, Stecenko AA, Dworski R, Lane KB, Loyd JE, Pierson R, King G, and Brigham KL. Altered prostanoid production by fibroblasts cultured from the lungs of human subjects with idiopathic pulmonary fibrosis. *Respir Res* 3: 17, 2002.

7. Francois H, Athirakul K, Howell D, Dash R, Mao L, Kim HS, Rockman HA, Fitzgerald GA, Koller BH, and Coffman TM. Prostacyclin protects against elevated blood pressure and cardiac fibrosis. *Cell Metab* 2: 201-207, 2005.

8. Fukuda Y, Ishizaki M, Kudoh S, Kitaichi M, and Yamanaka N. Localization of matrix metalloproteinases-1, -2, and -9 and tissue inhibitor of metalloproteinase-2 in interstitial lung diseases. *Lab Invest* 78: 687-698, 1998.

9. Kohyama T, Liu X, Kim HJ, Kobayashi T, Ertl RF, Wen FQ, Takizawa H, and Rennard SI. Prostacyclin analogs inhibit fibroblast migration. *Am J Physiol Lung Cell Mol Physiol* 283: L428-432, 2002.

10. Moore BB, Coffey MJ, Christensen P, Sitterding S, Ngan R, Wilke CA, McDonald R, Phare SM, Peters-Golden M, Paine R, 3rd, and Toews GB. GM-CSF regulates bleomycin-induced pulmonary fibrosis via a prostaglandin-dependent mechanism. *J Immunol* 165: 4032-4039, 2000.

11. Murakami S, Nagaya N, Itoh T, Kataoka M, Iwase T, Horio T, Miyahara Y, Sakai Y, Kangawa K, and Kimura H. Prostacyclin agonist with thromboxane synthase inhibitory

activity (ONO-1301) attenuates bleomycin-induced pulmonary fibrosis in mice. *Am J Physiol Lung Cell Mol Physiol* 290: L59-65, 2006.

12. Murota SI, Morita I, and Abe M. The effects of thromboxane B2 and 6-ketoprostaglandin F1alpha on cultured fibroblasts. *Biochim Biophys Acta* 479: 122-125, 1977.

13. Narumiya S, Sugimoto Y, and Ushikubi F. Prostanoid receptors: structures, properties, and functions. *Physiol Rev* 79: 1193-1226, 1999.

14. Obayashi Y, Yamadori I, Fujita J, Yoshinouchi T, Ueda N, and Takahara J. The role of neutrophils in the pathogenesis of idiopathic pulmonary fibrosis. *Chest* 112: 1338-1343, 1997.

15. Palmgren MS, deShazo RD, Carter RM, Zimny ML, and Shah SV. Mechanisms of neutrophil damage to human alveolar extracellular matrix: the role of serine and metalloproteases. *J Allergy Clin Immunol* 89: 905-915, 1992.

16. Pardo A, Ruiz V, Arreola JL, Ramirez R, Cisneros-Lira J, Gaxiola M, Barrios R, Kala SV, Lieberman MW, and Selman M. Bleomycin-induced pulmonary fibrosis is attenuated in gamma-glutamyl transpeptidase-deficient mice. *Am J Respir Crit Care Med* 167: 925-932, 2003.

17. Selman M, Ruiz V, Cabrera S, Segura L, Ramirez R, Barrios R, and Pardo A. TIMP-1, -2, -3, and -4 in idiopathic pulmonary fibrosis. A prevailing nondegradative lung microenvironment? *Am J Physiol Lung Cell Mol Physiol* 279: L562-574, 2000.

18. Serrao KL, Fortenberry JD, Owens ML, Harris FL, and Brown LA. Neutrophils induce apoptosis of lung epithelial cells via release of soluble Fas ligand. *Am J Physiol Lung Cell Mol Physiol* 280: L298-305, 2001.

19. Shen AS, Haslett C, Feldsien DC, Henson PM, and Cherniack RM. The intensity of chronic lung inflammation and fibrosis after bleomycin is directly related to the severity of acute injury. *Am Rev Respir Dis* 137: 564-571, 1988.

20. Stratton R, Rajkumar V, Ponticos M, Nichols B, Shiwen X, Black CM, Abraham DJ, and Leask A. Prostacyclin derivatives prevent the fibrotic response to TGF-beta by inhibiting the Ras/MEK/ERK pathway. *Faseb J* 16: 1949-1951, 2002.

21. Stratton R, Shiwen X, Martini G, Holmes A, Leask A, Haberberger T, Martin GR, Black CM, and Abraham D. Iloprost suppresses connective tissue growth factor production in fibroblasts and in the skin of scleroderma patients. *J Clin Invest* 108: 241-250, 2001.

22. Taooka Y, Maeda A, Hiyama K, Ishioka S, and Yamakido M. Effects of neutrophil elastase inhibitor on bleomycin-induced pulmonary fibrosis in mice. *Am J Respir Crit Care Med* 156: 260-265, 1997.

23. Thomas DW, Mannon RB, Mannon PJ, Latour A, Oliver JA, Hoffman M, Smithies O, Koller BH, and Coffman TM. Coagulation defects and altered hemodynamic responses in mice lacking receptors for thromboxane A2. *J Clin Invest* 102: 1994-2001, 1998.

24. Travis J. Structure, function, and control of neutrophil proteinases. *Am J Med* 84: 37-42, 1988.

25. Wise H, Qian YM, and Jones RL. A study of prostacyclin mimetics distinguishes neuronal from neutrophil IP receptors. *Eur J Pharmacol* 278: 265-269, 1995.

26. Yu H, Gallagher AM, Garfin PM, and Printz MP. Prostacyclin release by rat cardiac fibroblasts: inhibition of collagen expression. *Hypertension* 30: 1047-1053, 1997.

CHAPTER 5

CONCLUSIONS

Idiopathic pulmonary fibrosis is a deadly disease that currently has no therapies available to improve life expectancy or the quality of life for patients suffering from this progressive disease. The traditional anti-inflammatory treatment of corticosteroids has not proven beneficial. Recently, research has emphasized the importance of profibrotic mediators and alterations in epithelial and mesenchymal cell characteristics in disease pathogenesis. Thus, novel therapeutic agents that target these mediators and cell types warrant investigation. Prostanoids are lipid mediators that are both anti-inflammatory/antifibrotic as well as proinflammatory/profibrotic. The data presented here advances our understanding of the role that prostanoids play in the development of pulmonary fibrosis and suggests potential therapeutic targets.

Prostaglandin E_2 (PGE_2) is a prostanoid that has received the most attention for being an antifibrotic mediator of this disease and having a protective role through its G_s-coupled receptor, EP2. Patients with IPF have decreased PGE_2 levels in BALF, and fibroblasts from these patients are defective in PGE_2 production (3, 13). PGE_2 also alters the activity and gene expression of fibroblasts (2, 4, 7). In a number of different studies, alterations in PGE_2 levels are suggested to be responsible for changes in disease susceptibility and fibrotic phenotypes (8, 11). However, often times, the analysis of other prostanoids is omitted. Our data suggests that other prostanoids, aside from PGE_2, play an important role in disease development and should not be overlooked.

We used genetically modified mice to determine if alterations in PGE_2 levels or loss of the PGE_2 G_s-coupled receptors can alter disease susceptibility to bleomycin-induced lung fibrosis. We show that, although loss of the PGE_2 synthase, mPGES1, significantly reduces lung PGE_2 levels, it does not cause enhanced disease. Consistent with this, loss of signaling

through the PGE_2 G_s-coupled receptors also does not cause enhanced disease. In addition, enhanced PGE_2 levels due to loss of the catabolic enzyme PGDH does not protect against development of pulmonary fibrosis. Surprisingly, our studies demonstrate that increased disease susceptibility in mice lacking COX-2 is due to specific loss of prostacyclin, which signals through a G_s-coupled receptor also capable of increasing intracellular cAMP. Our study provides evidence for a protective role for COX-2-derived prostacyclin in the development of pulmonary fibrosis.

The importance of prostacyclin in regulating cardiovascular homeostasis is a more traditional and well-established role for this lipid mediator. Our data, along with other studies, demonstrates a new role for prostacyclin in the complex regulation of inflammation and fibrosis. Although studies have begun to demonstrate a role for prostacyclin in fibroblast proliferation and collagen deposition, most studies still neglect this underappreciated lipid mediator in favor of PGE_2. Our data challenges the current concept that PGE_2 is the protective COX-2-derived prostanoid in pulmonary fibrosis and suggests a possible anti-proliferative and anti-inflammatory role for prostacyclin.

We evaluated the development of lung disease in the various mouse lines using traditional histological and biochemical methods. However, in addition to this, we evaluated the change in mouse lung mechanics after exposure to bleomycin. We show that bleomycin-induced fibrosis results in a decrease in static compliance and an increase in tissue elastance. We believe that this is the first demonstration of the use of these methods for evaluation of the impact of genetic alterations on the development of fibrotic lung disease in this model. Therefore, this data not only challenges the current concepts of the role of prostanoids in lung diseases but also demonstates a highly sensitive and novel method for analyzing disease

susceptibility that is physiologically based and more relevant to measurements acquired from patients with this disease.

The data presented here suggests that prostacyclin may play a protective role in the development of pulmonary fibrosis. Enhancing signaling through the IP receptor may be a novel therapeutic treatment for pulmonary fibrosis. Prostacyclin analogues, such as iloprost, increase intracellular cAMP levels through the IP receptor and are common for the treatment of pulmonary hypertension. Since these compounds are already in clinical use, our data supports the testing of these compounds in trials for treatment of IPF and other fibrotic lung disorders. As an additional treatment option, combining prostacyclin analogues with phosphodiesterase inhibitors may further enhance this signaling cascade. Phosphodiesterase inhibitors prevent the inactivation of cAMP and may help prolong the effect of the prostacyclin analogues. This would also elevate signaling through the EP2 and EP4 receptors and take advantage of any possible role for PGE_2 in disease development. Although we were unable to define a role for PGE_2 in bleomycin-induced fibrosis, we can not completely exclude a possible role for PGE_2 in human IPF and other fibrotic lung diseases due to differences between the mouse model and human disease pathogenesis.

The importance of prostacyclin in inflammation and tissue repair demonstrated by these experiments enhances the understanding of other diseases with similar pathological mechanisms. An enhanced neutrophilic infiltration in the IP-deficient mice suggests an inhibitory role for prostacyclin in early inflammatory responses. Although the role of inflammation in IPF is controversial, the pathogenesis of other interstitial lung diseases is more dependent on inflammation. Thus, the data from these chapters may support a role for prostacyclin in other interstitial lung diseases. Many other human diseases can be classified

as remodeling diseases due to basic pathogenic mechanisms including epithelial cell injury, chronic inflammation, and mesenchymal cell activation. Airway remodeling in asthma and vascular remodeling in atherosclerosis are examples of diseases that have similar underlying mechanisms. In this regard, prostacyclin receptor deficient mice were also more susceptible to airway remodeling, as well as inflammatory cell infiltration, in a model of allergic asthma (9). This report strengthens our conclusions that prostacyclin is involved in inflammation and tissue repair and demonstrates the importance of prostacyclin in the underlying mechanisms of remodeling diseases.

Interestingly, these studies also indicate that current therapeutics for IPF and other diseases may have effects that have not been previously considered. For example, along with increasing the probability of thrombotic events, the selective COX-2 inhibitors may also promote fibrosis in susceptible patients since they alter the delicate prostacyclin/thromboxane balance. As discussed earlier, glucocorticoids are the traditional treatment for patients with IPF due to their anti-inflammatory properties. However, as discussed in chapters 1 and 2, inhibition of COX-2 expression is one of the mechanisms that account for the anti-inflammatory actions of glucocorticoids. Thus, glucocorticoids could be limiting the production of the protective COX-2 metabolite prostacyclin, and as our data suggests, this can have severe negative effects on the inflammatory and fibrotic response. This demonstrates the importance of understanding the mechanisms behind the actions of glucocorticoids since these are the most widely prescribed drugs in the United States.

In Chapter 2, we actually explored the complex interactions between the glucocorticoid receptor and prostanoid metabolism. We were interested in determining the *in vivo* role of the putative PGE_2 synthase, cPGES, and how it effects the progression of

fibrosis, so we created a mouse line lacking cPGES/p23. Through analysis of embryonic tissues and fibroblasts from these mice, we were unable to establish a role for cPGES/p23 in the direct production of PGE_2 from COX-derived PGH_2. However, we demonstrated that cPGES/p23 is an important co-chaperone for the Hsp90/GR complex and is required for both DNA-binding-dependent and -independent mechanisms of GR signaling. Thus, an indirect mechanism exists in which overexpression or loss of cPGES/p23 may effect prostaglandin production through glucocorticoid signaling. However, further experimentation is necessary to establish whether cPGES/p23 may also effect prostanoid production through an independent mechanism yet to be established. An independent role for cPGES/p23 in growth and proliferation was suggested by our data. This is consistent with the recent findings that cPGES/p23 is upregulated in cancer tissues and increases proportionately according to tumor grade in breast cancer cell lines (10). Further exploration of the cPGES/p23-null mice and the primary cell lines established from these mice has the potential to unravel the mystery behind cPGES/p23 in cancer and tumor growth. In addition, elucidating the role for cPGES/p23 in proliferation could shed light on a basic mechanism behind enhanced fibroblast proliferation in the setting of lung fibrosis.

Interestingly, other novel roles for p23 have recently been demonstrated that involve basic mechanisms important in pulmonary fibrosis. cPGES/p23 has been shown to associate with human telomerase reverse transcriptase (hTERT) and aid in proper active telomerase complex assembly (5). Another study showed that the p23 yeast homologue, Sba1, is required for telomere length maintenance in a telomerase DNA-binding-dependent manner (12). Recently, a few studies have implicated telomerase in the pathogenesis of pulmonary fibrosis. Mutations in hTERT have been demonstrated in familial cases of idiopathic

pulmonary fibrosis (1). Also, loss of telomerase expression causes enhanced fibroblast to myofibroblast transition (6). Future research is still necessary to elucidate the role of telomerase in idiopathic pulmonary fibrosis, as well as, the role of cPGES/p23 in telomerase function. However, it is interesting to speculate that cPGES/p23 may play a role in the progression of pulmonary fibrosis. A loss of cPGES/p23 expression may cause a loss of telomerase expression and enhance the fibrotic response through increased fibroblast to myofibroblast transition, and, as discussed above, upregulation of cPGES/p23 may lead to enhanced fibroblast proliferation through an independent mechanism.

We originally began investigating the role of cPGES/p23 to better understand its role as a PGE_2 synthase and how loss of this protein may effect PGE_2 production and subsequent fibrosis. We, however, did not find a role for cPGES/p23 in direct PGE_2 synthesis. Fortuitously, we discovered a role for cPGES/p23 in growth and proliferation as well as glucocorticoid receptor function, and other studies have suggested a role for cPGES/p23 in telomerase complex formation. Altered expression of cPGES may effect the pathogenesis of fibrotic lung disease through any one of these different pathways. Thus, cPGES/p23 may still turn out to be an important therapeutic target for idiopathic pulmonary fibrosis.

REFERENCES

1. Armanios MY, Chen JJ, Cogan JD, Alder JK, Ingersoll RG, Markin C, Lawson WE, Xie M, Vulto I, Phillips JA, 3rd, Lansdorp PM, Greider CW, and Loyd JE. Telomerase mutations in families with idiopathic pulmonary fibrosis. *N Engl J Med* 356: 1317-1326, 2007.

2. Bitterman PB, Wewers MD, Rennard SI, Adelberg S, and Crystal RG. Modulation of alveolar macrophage-driven fibroblast proliferation by alternative macrophage mediators. *J Clin Invest* 77: 700-708, 1986.

3. Borok Z, Gillissen A, Buhl R, Hoyt RF, Hubbard RC, Ozaki T, Rennard SI, and Crystal RG. Augmentation of functional prostaglandin E levels on the respiratory epithelial surface by aerosol administration of prostaglandin E. *Am Rev Respir Dis* 144: 1080-1084, 1991.

4. Clark JG, Kostal KM, and Marino BA. Modulation of collagen production following bleomycin-induced pulmonary fibrosis in hamsters. Presence of a factor in lung that increases fibroblast prostaglandin E2 and cAMP and suppresses fibroblast proliferation and collagen production. *J Biol Chem* 257: 8098-8105, 1982.

5. Holt SE, Aisner DL, Baur J, Tesmer VM, Dy M, Ouellette M, Trager JB, Morin GB, Toft DO, Shay JW, Wright WE, and White MA. Functional requirement of p23 and Hsp90 in telomerase complexes. *Genes Dev* 13: 817-826, 1999.

6. Liu T, Hu B, Chung MJ, Ullenbruch M, Jin H, and Phan SH. Telomerase regulation of myofibroblast differentiation. *Am J Respir Cell Mol Biol* 34: 625-633, 2006.

7. McAnulty RJ, Hernandez-Rodriguez NA, Mutsaers SE, Coker RK, and Laurent GJ. Indomethacin suppresses the anti-proliferative effects of transforming growth factor-beta isoforms on fibroblast cell cultures. *Biochem J* 321 (Pt 3): 639-643, 1997.

8. Moore BB, Coffey MJ, Christensen P, Sitterding S, Ngan R, Wilke CA, McDonald R, Phare SM, Peters-Golden M, Paine R, 3rd, and Toews GB. GM-CSF regulates bleomycin-induced pulmonary fibrosis via a prostaglandin-dependent mechanism. *J Immunol* 165: 4032-4039, 2000.

9. Nagao K, Tanaka H, Komai M, Masuda T, Narumiya S, and Nagai H. Role of prostaglandin I2 in airway remodeling induced by repeated allergen challenge in mice. *Am J Respir Cell Mol Biol* 29: 314-320, 2003.

10. Oxelmark E, Roth JM, Brooks PC, Braunstein SE, Schneider RJ, and Garabedian MJ. The cochaperone p23 differentially regulates estrogen receptor target genes and promotes tumor cell adhesion and invasion. *Mol Cell Biol* 26: 5205-5213, 2006.

11. Peters-Golden M, Bailie M, Marshall T, Wilke C, Phan SH, Toews GB, and Moore BB. Protection from pulmonary fibrosis in leukotriene-deficient mice. *Am J Respir Crit Care Med* 165: 229-235, 2002.

12. Toogun OA, Zeiger W, and Freeman BC. The p23 molecular chaperone promotes functional telomerase complexes through DNA dissociation. *Proc Natl Acad Sci U S A* 104: 5765-5770, 2007.

13. Wilborn J, Crofford LJ, Burdick MD, Kunkel SL, Strieter RM, and Peters-Golden M. Cultured lung fibroblasts isolated from patients with idiopathic pulmonary fibrosis have a diminished capacity to synthesize prostaglandin E2 and to express cyclooxygenase-2. *J Clin Invest* 95: 1861-1868, 1995.